Cytoplasmic cyclin D1 roles in neurons: effects on neuritogenesis and type A GABA receptors

Maria Ventura Monserrat Monserrat

Universitat de Lleida

TESI DOCTORAL

Cytoplasmic cyclin D1 roles in neurons: effects on neuritogenesis and type A GABA receptors

Maria Ventura Monserrat Monserrat

Memòria presentada per optar al grau de Doctor per la Universitat de Lleida
Programa de Doctorat en Salut

Director/a
Neus Pedraza González
Francisco Ferrezuelo Muñoz

Tutor/a
Eloi Garí Marsol

2019

Ses nostres neurones funcionen com una bicicleta. Ben engranades, ens permeten viatjar cap a on vulguem.

A tu, padrí ***Mateu***

A tu, padrina ***Ventura***

A vosaltres, que ***hi sou*** *sense ser-hi.*

AGRAÏMENTS

Ja començo a veure les pancartes dels últims kilòmetres i visualitzo com serà l'esprint final. Mentre vaig planejant com serà l'atac a meta, no puc evitar fer memòria de tots i totes els que m'han acompanyat durant aquesta llarga i dura cursa que, si tot acaba com he calculat, em portarà als Camps Elisis.

Primerament, voldria agrair als meus directors de tesi la seva feina i dedicació. I és que una no pot arribar exitosament al final sense un bon director de files. Per això, gràcies Neus, gràcies Paco i gràcies Eloi per l'oportunitat i per fer-me créixer científicament.

Tampoc podria deixar d'agrair als meus companys d'equip la seva feina. No és possible arribar lluny si no tens bons companys. Així, vull agrair a tots els qui heu fet que la meva etapa aquí fos tan profitosa tant a nivell personal com professional.

En aquest gran Tour m'he trobat amb participants que tot i vestir mallots de diferent equip m'han ajudat a superar ports de primera categoria i hem gaudit de les millors baixades convertint-se en gent que mai no oblidaré.

Sense dubte, l'etapa reina de la cursa ha estat la de Madrid. De estas intensas y de sudar. La victoria en esa etapa no habría sido posible sin la colaboración de Jose Antonio Esteban y la inestimable ayuda de quienes fueron mis compañeros de equipo. A todos vosotros, ¡Muchas Gracias!

Però pedalejar i pedalejar sense decaure no sempre és fàcil. I és en aquells moments de dificultats on te n'adones de tots aquells "supporters" que arrossegues en cada una de les teves etapes. Hem van passant les cares de tots aquells que m'han fet costat d'una manera o una altra.... Sa teva moc, durant totes ses nostres vivències dins i fora de pista; dins i fora de Gabriel Alomar! Sa del meu cosí Guillem, es dia de decidir que fèiem bioquímica o quan a sa facultat ens rèiem dels qui volien fer un doctorat. Sa de la meva cosina Kate i es seu lloro. Sa des patró i sa tia dins en Teo a Cala Entugores i sa de tota sa família fent matances a Son Cosme. Sa de tota sa família de Cas Concos perquè amb vosaltres és impossible no riure. M'agafes? Sa de la meva madrina i es meu padrino per ser-hi sempre i per tot. A tots els que feis que sempre senti que tornar a casa és la millor part de l'aventura.

Les passades en ruta per Aragó m'han fet sentir benvinguda i estimada. Por todo vuestro apoyo y por hacerme sentir como en casa, muchísimas gracias Yolanda, Eduardo y Diego. Sin olvidarme, por supuesto, de la yaya. ¡Que se joda el cuerpo!, pienso muy a menudo en este mundillo...

A més, si hi ha una cosa important durant aquestes llargues etapes, és la nutrició... i en això sempre he tingut a la millor per als avituallaments. Gràcies padrina per tots els teus consells, el teu suport i la teva comprensió.

El preparador que he tingut per afrontar la cursa, no ha quedat enrere i ha fet una gran feina. Tu has estat, pare, qui m'ha enllestit per fer possible un somni. Esforç, sacrifici, i petites dosis de satisfacció.

He d'admetre però, que m'he dopat. Que cada vegada que anava a sa roqueta visitava un lloc especial prop de sa Serra que me feia volar. Allà em cuidaven, em portaven a cercar bolets i anava al parc. En aquest petit bocí de paradís hi ha en Tomeu, sa mamà, i els dos motius més bonics per anar a sa lluna i tornar. Tomi, gràcies per tot, sobretot per torrar sa carn. Gràcies mami per haver estat i ser el pilar i el mirall. Per demostrar-me com es lluita i per ser la papallona que vola més amunt. A tu Guillem, infinit amor que mai canviarà. Ho saps. I a tu príncep, gràcies per arribar i donar-nos aquesta vida extra. T'estim, ho sabràs.

Finalment, i per això molt important, he d'agrair als imprescindibles. Tramuntana i Zetuki, els millors psicòlegs i terapeutes que es poden tenir. Per abstreure'm dels mals moments, per animar-me, per jugar amb mi quan m'avorria d'escriure i per ser tan incondicionalment genials. I a tu Irene, per fer que aquesta cursa pogués arribar a bon port, sense importar si punxava pel camí o si trencava cadena, tu sempre ho repares i em fas tirar endavant. No hi ha millor mecànic de sentiments. Amb la teva ajuda es podrien creuar els Andes en monocicle. Gràcies als tres per ser el motiu de la victòria!

ABSTRACT

Cyclin D1 and its kinase partner Cdk4 form a complex which is well known for its nuclear role regulating the cell cycle. In addition, non-canonical functions of cyclin D1 are related to transcription, DNA damage repair, differentiation and metabolism. Also, our group has demonstrated a cytoplasmic role of cyclin D1 in cell invasion and metastasis through the phosphorylation of paxillin. Cyclin D1 knockout mice show neurological deficiencies. Cyclin D1 has been found at the cytoplasm of differentiated neurons, and is required for NGF-induced neurite outgrowth in PC12 cells. Hence, we have aimed to explore cyclin D1 cytoplasmic functions in neurons. Here we show that cytoplasmic cyclin D1-Cdk complexes are important for early neurite outgrowth in embryonic cortical neurons. Overexpression of cytoplasmic cyclin D1 or Cdk4 promotes axon and neurite outgrowth, while downregulation of endogenous cyclin D1 inhibits neuritogenesis in cultured cortical neurons. Our data point to paxillin as a downstream effector of cyclin D1 in this process since a non-phosphorylatable mutant of paxillin results in a decrease in axon and neurite lengths.

We have also focused on the regulation of type A GABA receptors by cyclin D1. GABA is the main inhibitory neurotransmitter in the mammalian brain, exerting its actions by binding and activating the so-called GABA receptors. Ionotropic $GABA_AR$ function and abundance are often regulated by phosphorylation at the intracellular loop of its subunits. Here we describe that cyclin D1 directly interacts with the α4 and β3 subunits of $GABA_A$ receptors, and co-immunoprecipitates and colocalizes with the α4 subunit at the hippocampus of adult mice. Moreover, we prove that the cyclin D1-Cdk4 complex phosphorylates α4 at residues T423 and S431, and that cyclin D1 or a phosphomimetic allele of α4 prevent $GABA_AR$ run-down in HEK tsA201. Finally, the inhibition of cyclin D-Cdk4/6 complexes by Palbociclib reveals that these complexes are necessary for maintaining GABA-tonic currents and miniature inhibitory postsynaptic currents in hippocampal slices.

Taken together, our results strongly suggest new roles for cytoplasmic cyclin D1 in the central nervous system, regulating early neuritogenesis and neuronal activity through $GABA_A$ receptors. This may shed light on the neurological phenotype of the cyclin D1 knockout mice and be relevant for several mental disorders wherein dysregulation of GABA inhibitory functions may be a determining factor.

RESUMEN

Ciclina D1 y la quinasa Cdk4 forman un complejo con una función nuclear bien definida, regulando el ciclo celular. Por otro lado, ciclina D1 ejerce funciones no canónicas relacionadas con la transcripción, la reparación del ADN, la diferenciación y el metabolismo. En nuestro grupo hemos demostrado que ciclina D1 en el citoplasma regula la invasión celular y la metástasis a través de la fosforilación de paxilina. Los ratones *knockout* de ciclina D1 presentan deficiencias neurológicas. Ciclina D1 se ha encontrado en el citoplasma de neuronas diferenciadas y es necesaria para el crecimiento de neuritas inducido por NGF en células PC12. Así pues, nos hemos propuesto explorar las funciones de ciclina D1 citoplasmática en neuronas. Aquí mostramos que los complejos ciclina D1-Cdk son importantes para el crecimiento inicial de neuritas en neuronas corticales embrionarias. La sobreexpressión de ciclina D1 o Cdk4 promueve el crecimiento del axón y las neuritas, mientras que una disminución de los niveles de ciclina D1 endógena inhibe la neuritogénesis en neuronas corticales en cultivo. Nuestros resultados apuntan a paxilina como efector *downstream* de ciclina D1 en este proceso, puesto que el mutante no fosforilable de paxilina produce una disminución de la longitud del axón y de las neuritas.

También, nos hemos centrado en la regulación de los receptores de GABA tipo A por parte de ciclina D1. GABA es el principal neurotransmisor inhibitorio del cerebro de los mamíferos, ejerciendo su acción a través de su unión a los receptores de GABA. Tanto la función como la abundancia de los receptores $GABA_A$ ionotrópicos a menudo son reguladas por la fosforilación del bucle intracelular de sus subunidades. Aquí describimos que ciclina D1 interacciona directamente con las subunidades α4 y β3 de los $GABA_A$Rs, y que colocaliza y co-inmunoprecipita con la subunidad α4 en el hipocampo de ratón adulto. Además, hemos demostrado que el complejo ciclina D1-Cdk4 fosforila α4 en los residuos T423 y S431 y que tanto ciclina D1 como un alelo fosfomimético de α4 previenen la pérdida de funcionalidad (*run-down*) de los $GABA_A$R en células HEK tsA201. Finalmente, la inhibición de los complejos ciclina D-Cdk4/6 mediante Palbociclib revela que estos complejos son necesarios para mantener las corrientes tónicas de GABA así como las corrientes postsinápticas miniatura en el hipocampo. Globalmente, nuestros resultados sugieren nuevos roles de ciclina D1 citoplasmática en el sistema nervioso central, regulando la neuritogénesis y la actividad neuronal a través de los receptores tipo A de GABA. Esto podría esclarecer el fenotipo del ratón carente de ciclina D1 y ser relevante para comprender diferentes trastornos mentales en los que la desregulación de la inhibición GABAérgica es un factor determinante.

RESUM

Ciclina D1 i la quinasa Cdk4 formen un complex que és regularment conegut pel seu paper dintre del nucli regulant el cicle cel·lular. D'altra banda, ciclina D1 exerceix funcions no canòniques relacionades amb la transcripció, la reparació de l'ADN, la diferenciació i el metabolisme. En el nostre grup hem demostrat que ciclina D1 en el citoplasma regula la invasió cel·lular i la metàstasi a través de la fosforilació de paxilina. Els ratolins *knockout* de ciclina D1 presenten deficiències neurològiques. Ciclina D1 s'ha trobat al citoplasma de neurones diferenciades i és necessària per al creixement de neurites induït per NGF en cèl·lules PC12. Així doncs, ens hem proposat explorar les funcions de ciclina D1 citoplasmàtica en neurones. Aquí demostrem que els complexos ciclina D1-Cdk són importants per al creixement inicial de neurites en neurones corticals embrionàries. La sobreexpressió de ciclina D1 o Cdk4 promou el creixement de l'axó i les neurites, mentre que una disminució dels nivells de ciclina D1 endògena inhibeix la neuritogènesi en neurones corticals en cultiu. Els nostres resultats assenyalen paxilina com a efector *downstream* de ciclina D1 en aquest procés ja que el mutant no fosforilable de paxilina comporta una disminució de les longituds de l'axó i les neurites.

També ens hem centrat en la regulació dels receptors de GABA tipus A per part de ciclina D1. GABA és el principal neurotransmissor inhibitori del cervell dels mamífers, exercint les seves accions a través de la seva unió als receptors de GABA. Tant la funció com l'abundància dels receptors ionotròpics $GABA_A$ sovint són regulades per la fosforilació del bucle intracel·lular de les seves subunitats. Aquí descrivim que ciclina D1 interacciona directament amb les subunitats α4 i β3 dels $GABA_A$Rs, i que colocalitza i coimmunoprecipita amb la subunitat α4 a l'hipocamp de ratolí adult. A més, hem demostrat que el complex ciclina D1-Cdk4 fosforila α4 en els residus T423 i S431, i que, tant ciclina D1 com un al·lel fosfomimètic d'α4 prevenen la pèrdua de funcionalitat (*run-down*) dels $GABA_A$R en cèl·lules HEK tsA201. Finalment, la inhibició dels complexos ciclina D1-Cdk4/6 mitjançant Palbociclib revela que aquests complexos són necessaris per a mantenir els corrents tònics de GABA així com els corrents postsinàptics miniatura en l'hipocamp.

Globalment, els nostres resultats suggereixen nous papers de ciclina D1 citoplasmàtica en el sistema nerviós central, regulant la neuritogènesi i l'activitat neuronal a través dels receptors tipus A de GABA. Això podria aclarir el fenotip del ratolí mancat de ciclina D1 i ser rellevant per a comprendre diferents trastorns mentals en els que la desregulació de la inhibició GABAèrgica n'és un factor determinant.

TABLE OF CONTENTS

TABLE OF CONTENTS

ABBREVIATIONS

1. INTRODUCTION 1

1.1 CYCLINS AND CYCLIN DEPENDENT KINASES 1

1.1.1. D-type cyclins are essential 1

1.1.2. Canonical function of cyclin D1 2

1.1.3. Non-canonical functions of cyclin D1 3

1.1.4. Regulation of cyclin D1 expression 5

1.1.5. Phenotype of cyclin D1 knockout mice 6

1.1.6. Cyclin D1 in neurons 6

1.2 PAXILLIN 7

1.2.1. Paxillin regulation by phosphorylation 8

1.2.2. Focal adhesions 8

1.2.3. Paxillin in the central nervous system 9

1.2.4. Rho GTPases 11

1.3 GABAERGIC NEUROTRANSMISSION 11

1.3.1. GABA synthesis, reuptake and degradation 12

1.3.2. GABA receptor types 12

1.3.3. $GABA_A$ receptor subunits 14

1.3.4. $GABA_A$ receptors, structure and composition 15

1.3.5. Cellular and subcellular localization of $GABA_A$ receptors 16

1.3.6. Assembly and trafficking of $GABA_A$ receptors 17

1.3.7. $GABA_A$ receptor function 21

1.3.8. Regulation of the $GABA_A$ receptors and their relation to diseases 24

1.3.9. Regulation of $GABA_AR$ activity through phosphorylation 27

2. HYPOTHESIS AND OBJECTIVES 33

2.1 HYPOTHESIS 33

2.2 OBJECTIVES 34

3. MATERIALS AND METHODS 37

3.1 MOLECULAR BIOLOGY TECHNIQUES 37

3.1.1. Plasmid constructions 37

3.1.2. RNA extraction and RT-qPCR 40

3.2 CELLULAR BIOLOGY TECHNIQUES 41

3.2.1. Growing and harvesting cells 41

3.2.2. Primary culture of cortical neurons 42

3.2.3. Organotypic hippocampal slices preparation *45*
3.2.4. Cell transfection *45*
3.2.5. Competent cells transformation *47*
3.3 MICROSCOPY TECHNIQUES 48
3.3.1. Immunofluorescence *48*
3.4 BIOCHEMICAL ANALYSES 48
3.4.1. Antibodies *48*
3.4.2. Protein extraction and immunodetection by western blot *50*
3.4.3. Electrophoresis (SDS-PAGE) *50*
3.4.4. Electroblotting *50*
3.4.5. Membrane blocking *51*
3.4.6. Immunodetection *51*
3.4.7. Chemiluminescent detection and data analysis *51*
3.5 PROTEIN INTERACTION ASSAYS 52
3.5.1. Immunoprecipitation using anti FLAG M2 agarose beads *52*
3.5.2. Immunoprecipitation of endogenous cyclin D1 in adult hippocampus *52*
3.5.3. Affinity purification of GST-α4 ..... *53*
3.5.4. In vitro protein interaction assay *54*
3.6 KINASE REACTION ASSAYS 54
3.6.1. In vitro kinase assay *54*
3.6.2. Mass spectrometry (HPLC-MSMS) *54*
3.7 ELECTROPHYSIOLOGY 55
3.7.1. Whole-cell currents measurements in tsA201 cells *55*
3.7.2. Whole-cell recordings in organotypic hippocampal slices *56*
3.8 SURFACE BIOTINYLATION ASSAY 57
3.8.1. Biotin labeling of membrane proteins *57*
3.8.2. Receptor internalization assay using biotin labeling *58*
3.8.3. Assessment of receptor insertion into the membrane by biotin labeling *58*
3.9 STATISTICAL ANALYSIS 59
3.10 ETHICAL CONSIDERATIONS 59

4. RESULTS 63

4.1 ROLE OF CYTOPLASMIC CYCLIN D1 IN NEURITOGENESIS 63
4.2 EFFECT OF PAXILLIN PHOSPHORYLATION AT S83 AND S178 IN NEURITOGENESIS 68
4.3 CYCLIN D1 EFFECTS ON $GABA_A$ RECEPTORS 70
4.3.1. Interaction between cyclin D1 and α4 subunit of the $GABA_A$ receptor *70*
4.3.2. The alpha 4 subunit of the $GABA_A$ receptor as a phosphorylation target for cyclin D1-Cdk4 complex *75*
4.3.3. Functional effects of the α4 phosphorylation by cytoplasmic Ccnd1-Cdk4 complex by whole-cell patch clamp in HEK tsA201 cells *78*

4.3.4. Cyclin D-Cdk4/6 complex effect on the functionality of $GABA_A$ receptors in rat hippocampal slices. *80*
4.3.5. Cyclin D1-Cdk4/6 complex inhibition with Palbociclib *80*
4.3.6. Cdk4/6 role in GABA tonic currents *82*
4.3.7. Cdk4/6 role in GABA mIPSC *82*
4.4 CYTOPLASMIC CYCLIN D1 ROLE IN THE ASSEMBLY OF α4β3 CONTAINING $GABA_A$ RECEPTORS. 84
4.4.1. Cyclin D1 interaction with β3 subunit of the $GABA_A$ receptor *84*
4.4.2. Cytoplasmic cyclin D1 effect on α4 and β3 surface levels *87*

5. DISCUSSION 95

5.1 CYTOPLASMIC CYCLIN D1-CDK4/6 COMPLEXES INDUCE NEURITOGENESIS IN CORTICAL NEURONS 95
5.2 PAXILLIN PHOSPHORYLATION AT S83, S178 AND S244 PROMOTES NEURITE OUTGROWTH 96
5.3 CYTOPLASMIC CYCLIN D1 INTERACTS WITH AND PHOSPHORYLATES THE α4 SUBUNIT OF $GABA_A$ RECEPTORS PREVENTING THEIR RUN-DOWN 98
5.4 CYCLIN D-CDK4/6 COMPLEX MODULATES GABA TONIC CURRENTS AND MIPSCS IN HIPPOCAMPAL SLICES 100
5.5 CYTOPLASMIC CYCLIN D1 REGULATES α4β3-CONTAINING $GABA_AR$ EXPRESSION AT THE CELL SURFACE 102

6. CONCLUSIONS 109

7. BIBLIOGRAPHY 113

TABLE OF FIGURES

Figure 1: Multiple roles of cyclin D1…… 2

Figure 2: Focal adhesions serve as a link between the ECM and the actin cytoskeleton…9

Figure 3: Synaptic and extrasynaptic $GABA_AR$ neuronal localization……..13

Figure 4: Schematic representation of $GABA_AR$ structure……..14

Figure 5: Modulation of $GABA_ARs$ trafficking by phosphorylation……..19

Figure 6: Scheme of the conditions used for qPCR……..40

Figure 7: Disruption of CCND1 gene……..44

Figure 8: Scheme of the workflow followed for hippocampal slice preparation……..45

Figure 9: Representative examples of recordings of GABA tonic currents……..57

Figure 10. Cytoplasmic localization of cyclin D1 avoids apoptotic neuronal death……63

Figure 11: Cytoplasmic cyclin D1 induces neuritogenesis in cortical neurons at 4 DIV..64

Figure 12: Cytoplasmic Cdk4 induced neuritogenesis in cortical neurons at 4 DIV……65

Figure 13: Cyclin D1 mRNA level drops at 1 DIV and continues to decrease at 3 DIV…66

Figure 14: Downregulation of cyclin D1 affects neuritogenesis in cortical neurons at early stages of differentiation…… 67

Figure 15: Cyclin D1 deficient cortical neurons have shorter axons and neurites at 1 DIV……..68

Figure 16: Paxillin phosphorylation at serines 83 and 178 is lower at 4 DIV in comparison to 1DIV……..69

Figure 17: Phosphorylation of paxillin at serines 83, 178 and S244 is involved in early neuritogenesis control……..70

Figure 18: Ccnd1 interacts in vitro with the C-terminus of the α4 subunit of the GABAA receptor……..71

Figure 19: Heterologous Ccnd1 interacts with the C-terminus of α4 subunit of GABA receptor……..72

Figure 20: Cyclin D1-CAAX and α4 co-localize in HEK293T transfected cells……..72

Figure 21: Heterologous α4 and Ccnd1 co-localize in primary cortical neurons……..73

Figure 22: α4 subunit and CCND1 mRNA expression patterns in mouse adult brain…..74

Figure 23: Endogenous Ccnd1 and α4 interact in adult hippocampus……74

Figure 24: Mus musculus $GABA_A$ receptor α4 subunit amino acidic sequence……..75

Figure 25: α4 is phosphorylated in vitro by the Ccnd1-Cdk4 complex……76

Figure 26: α4 T423A-S431A mutant has reduced phosphorylation by Ccnd1-Cdk4 complex……..76

Figure 27: Residues T423 and S431 in α4 are phosphorylated by Ccnd1-Cdk4 complex……..77

Figure 28: Cytoplasmic cyclin D1 or mimicking phosphorylation of the alpha 4 subunit of GABAA receptor prevent GABA receptor's run-down……79

Figure 29: Inhibition of Cyclin D-Cdk4/6 complexes by 2.5 μM Palbociclib significantly reduces the phosphorylation state of paxillin at serine 83 in hippocampal slices……81

Figure 30: Cyclin D-Cdk4/6 inhibition with Palbociclib significantly reduces GABA tonic currents in hippocampal slices……83

Figure 31: Palbociclib treatment decreases both mIPSC amplitude and frequency in organotypic hippocampal slices……84

Figure 32: Cyclin D1 interacts with β3 in vitro……85

Figure 33: Heterologous HA-Ccnd1-CAAX interacts with β3-FLAG……85

Figure 34: Human $GABA_A$ receptor β3 subunit amino acidic sequence……86

Figure 35: β3 is not an in vitro substrate of Cyclin D1-Cdk4 complex……86

Figure 36: Cyclin D1-CAAX presence diminishes surface levels of β3, but not α4, subunit……88

Figure 37: Endocytosis process of the α4 and β3 subunits is not affected by cytoplasmic cyclin D1 in HEK293 cells……89

Figure 38: Cytoplasmic cyclin D1 decreases the insertion of β3 to the cell surface in HEK293…… 90

Figure 39: Cyclin D1-CAAX promotes ubiquitination of β3 in HEK293……91

Figure 40: Proposed model whereby Ccnd1 promotes neurite outgrowth……97

Figure 41: Model of the mechanism whereby Ccnd1 controls $GABA_A$ receptor expression and function proposed based on the results obtained in this thesis……105

ABBREVIATIONS

ABBREVIATIONS

α4: alpha 4 subunit of the $GABA_A$ receptor

ATF2: activating transcription factor 2

AP: action potential

AP-V: ((2R)-amino-5-phosphonovaleric acid; (2R)-amino-5-phosphonopentanoate)

β3: beta 3 subunit of the $GABA_A$ receptor

BSA: bovine serum albumine

CBP: CREB-binding protein

CDK: cyclin dependent kinase

Ccnd1: cyclin D1

Cip: CDK interacting protein

CKI: CDKs inhibitor

CNQX: cyanquizaline (6-cyano-7-nitroquinoxaline-2,3-dione)

CNS: central nervous system

DIV: days *in vitro*

ECD: extracelular domain

ECM: extracellular matrix

EGF: epidermal growth factor

ERK: extracellular signal-regulated kinase

FA: focal adhesion

FAK: focal adhesion kinase

FBS: fetal bovine serum

FOXM1: forkhead protein M1

GABA: gamma-aminobutyric acid

$GABA_AR$: type A GABA receptor

GAD: glutamate decarboxylase

GAP: GTPase-activating protein

ABBREVIATIONS

GAPDH: glyceraldehyde 3-phosphate dehydrogenase

GDI: GDP-dissociation inhibitor

GEF: guanine nucleotide exchange factor

GFP: green fluorescent protein

GSK3β: glycogen synthase kinase 3 beta

HBSS: Hank's balanced salt solution

JNK: JUN N-terminal kinase

Kip: kinase inhibitory protein

KO: knockout

LTD: long-term depression

LTP: long-term potentiation

MAP1B: microtubule-associated protein-1B

MEFs: mouse embryonic fibroblasts

MEK: MAPK and extracellular signal-regulated kinase

mIPSC: miniature inhibitory postsynaptic current

NGF: nerve growth factor

NRF1: nuclear respiratory factor 1

OL: oligodendrocyte

PAK: p21-activated kinase

PBS: Phosphate-buffered saline

PEI: polyethylenimine

PFA: paraformaldehide

PKC: protein kinase C

PKA: protein kinase A

PPARγ: peroxisome proliferator-activated receptor-γ

PSA: ammonium persulfate

Pxn: paxillin

P/S: penicillin-streptomycin

RB: retinoblastoma protein

ROCK: RHO kinase

SE: status epilepticus

TEMED: N,N,N’,N’-tetramethylethylenediamine

TLE: temporal lobe epilepsy

TTX: tetrodotoxin

WB: western Blot

WT: wild type

INTRODUCTION

1. INTRODUCTION

1.1 Cyclins and cyclin dependent kinases

Cyclins are a family of proteins that regulate the progression through the different stages of the cell cycle by forming complexes with catalytic subunits, termed cyclin dependent kinases (CDKs), which are serine/threonine kinases. In the cell cycle, the function of these cyclin-CDK complexes is to ensure the proper control of both DNA replication and chromosomal segregation (*Bendris et al. 2015*). For instance, the formation of heterodimeric cyclin D-Cdk4/6 complexes regulate the entrance to the cell cycle that activates cyclin E-Cdk2 (or Cdk1 to a lesser extend) and cyclin A which promote the phosphorylation of various targets that contribute to the cell cycle progression. Alternatively, cyclin C-Cdk3 participate in the transition from G0 to G1. To date, 29 cyclins and 20 CDKs have been described in humans, although not all of them are involved in cell cycle control (*Malumbres 2011)*, and there is some degree of redundancy among cyclins and among CDKs. Actually, in mammals, the only CDK that seems to be essential is Cdk1 (*Hochegger et al. 2008*). The activity of CDKs varies during the cell cycle due to activating phosphorylation and the transient interactions with specific cofactors such as cyclins and CDKs inhibitors (CKIs). In this sense, cyclins play a role in activating CDKs while CKIs inhibit them (*Bendris et al. 2015*).

1.1.1. D-type cyclins are essential

The progression through the cell cycle in mammals is orchestrated by D-type cyclins. This family of homologous proteins (D1, D2 and D3) (*Charles J. Sherr 1995*) associate with Cdk4 or Cdk6 (Cdk4/6) to form a complex that phosphorylates target proteins (*Paternot et al. 2006*). D-type cyclin expression is tissue specific (*Matsushime et al. 1991*) and for this reason, the ablation of each cyclin D produces deficits in a tissue specific manner. For instance, CCND1 knockout (KO) mice are smaller than wild type (WT) mice and also they develop retina and mammary gland abnormalities during gestation and are born with neurological deficiencies (*Fantl et al. 1995*; *Sicinski et al. 1995*), while CCND2 KO mice show female sterility as well as cerebral and lymphocyte proliferation deficiencies (*Sicinski et al. 1996*; *Huard et al. 1999*; *Lam et al. 2000*), and mice lacking CCND3 present defects in T lymphocytes maturation (*Sicinska et al. 2003*). Mice lacking all three D-type cyclins developed normally until half gestation with all organs developed as in WT, demonstrating that D-type cyclin deficit does not affect cellular proliferation. Nevertheless, these mice die before birth due to anemia and coronary deficits because of the essential role of cyclins D in the expansion of hematopoietic stem cells (*Kozar et al. 2004*).

Reassuringly, the CDK4/6 KO mouse presents a similar phenotype (*Malumbres et al. 2004*). Thus, D-type cyclins display some degree of redundancy in specific functions that are essential during development, but there are also cell types able to proliferate almost normally in the absence of these cyclins. For instance, fibroblasts of mice lacking cyclins D proliferate similar to WT even though they need more mitogenic signals to reenter the cell cycle (*Kozar et al. 2004*).

1.1.2. Canonical function of cyclin D1

The most studied D-type cyclin is cyclin D1 (Ccnd1) since it is amplified in many tumors of different types and origin (*Beroukhim et al. 2010*). Ccnd1, together with Cdk4/6, controls the transition from G1 to S phase in the cell cycle, establishing a point of no return called the Restriction point, where cells commit to a new round of cell division (Figure 1). Under mitogenic signals and nutrient availability, Ccnd1 expression is induced and Ccnd1-Cdk4/6 complexes are activated and phosphorylate the retinoblastoma protein (Rb). The classical view of how cell cycle entry takes place assumes that Ccnd1-Cdk4 inactivates Rb by progressive multiphosphorylation.

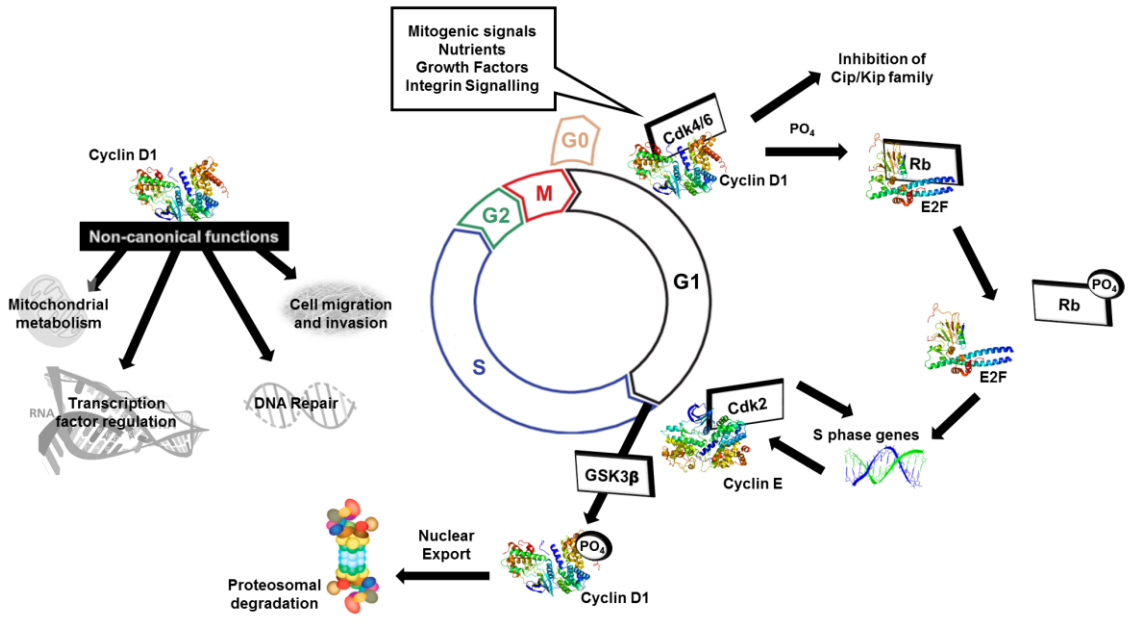

Figure 1: Multiple roles of cyclin D1. Cyclin D1 acts at the Restriction point of the cell cycle. Under mitogenic stimuli, Ccnd1 forms a heterodimer with Cdk4/6 that is able to initiate the phosphorylation of the retinoblastoma protein (Rb) that was retaining E2F transcription factor. Once released, E2F is able to trigger the transcription of genes necessaries for S phase such as cyclin E. The activation of cyclinE-Cdk2 complex gives rise to a positive feedback. Ccnd1-Cdk4/6 complex also contributes to the cell cycle progression by retaining Cip/kip, which are Cdk inhibitors. Non-canonical functions of Ccnd1 include: inhibition of mitochondrial metabolism, regulation of transcription factor activity, enhancement of DNA repair and induction of cell migration and invasion. At late G1 phase, Ccnd1 is phosphorylated by GSK3β, exported to the cytoplasm and degraded in the proteasome. Adapted from: Sherr 1999.

Hypophosphorylated Rb still interacts with the E2F transcription factor and prevents the expression of many genes necessary for cell cycle entry. Eventually, when Ccnd1-Cdk4-induced phosphorylation of Rb reaches a threshold, E2F is partially released from its inhibition and some E2F target genes get expressed, at least to some extent. One of these genes is cyclin E, which together with Cdk2 completes the phosphorylation of Rb at late G1 phase to produce an inactive hyperphosphorylated Rb, thereby allowing the full expression of a transcriptional program driven by E2F that leads to DNA replication (S phase) (*Dulić et al. 1992*; *Kato et al. 1993*). Although this constitutes a widely accepted model of G1 cell cycle progression in mammals, it has been brought into question by recent studies (*Narasimha et al. 2014*; *Sanidas et al. 2019*) that demonstrate that Ccnd1-Cdk4 can only monophosphorylate Rb at any of 14 residues, giving rise to 14 different monophosphorylated forms of the protein.

Moreover, Ccnd–Cdk4/6 complexes also contribute to the progression to S phase by sequestering members of the Cip/Kip (CDK interacting protein/Kinase inhibitory protein) family of CKIs (*Sherr and Roberts 1999*). These inhibitors do not inhibit Ccnd-Cdk4/6 complexes –in fact they are required for their proper functionality- but do inhibit cyclin E and cyclin A in complex with Cdk2.

1.1.3. Non-canonical functions of cyclin D1

Besides its well-known function as a cell cycle regulator, Ccnd1 has been involved in some other processes such as the induction of cell migration and invasion, inhibition of mitochondrial metabolism, regulation of transcription factor activity, and enhancement of DNA repair (*Hydbring et al. 2016*). Concerning the function of Ccnd1 as a regulator of transcription factor activity, both kinase-dependent and -independent roles have been described. Ccnd-Cdk4/6 complexes activate the forkhead transcription factor protein (FOXM1) which further regulates the transcription of several cell cycle regulators. Also, Ccnd1–Cdk4 complexes phosphorylate the methylosome protein 50, thus increasing the activity of the chromatin modifier PRMT5 (protein Arg N-methyltransferase 5), involved in neoplastic growth. Besides, Ccnd1 has direct roles in transcription that do not implicate kinase activity of Cdks. For instance, Ccnd1 can directly bind to and inhibit histone acetyltransferases like CREB-binding protein (CBP) avoiding their binding to promoters of target genes such as the peroxisome proliferator-activated receptor-γ (PPARγ). Moreover, Ccnd1 is involved in the process of DNA repair, even though Ccnd1 is degraded as a consequence of DNA damage. Specifically, Ccnd1 recruits RAD51 thus stimulating homologous recombination. Ccnd1 also regulates mitochondrial metabolism. Studies done in transgenic CCND1 KO mice showed an important role of Ccnd1 as an inhibitor of mitochondrial biogenesis and activity since it phosphorylates and inhibits the nuclear respiratory factor 1 (NRF1) which is an inducer of the expression of nuclear-encoded mitochondrial genes (*Wang et al. 2006*). Also,

Sakamaki and co-workers demonstrated in Ccnd1-induced mammary tumors that Ccnd1 overexpression promotes inhibition of mitochondrial activity while the silencing of Ccnd1 promotes mitochondrial metabolism (*Sakamaki et al. 2006*).

One of the non-canonical functions of Ccnd1, particularly relevant to this work, is its role in cell migration (reviewed in *Pestell 2013*; *Hydbring et al. 2016*). It has been postulated that Ccnd1 governs cell adhesion and migration in different cells, including bone-marrow derived macrophages, fibroblasts and mammary gland epithelial cells. Indeed, Ccnd1 ablation in both fibroblasts and macrophages leads to defects in cell motility and invasion as well as cell matrix adhesion (*Neumeister 2003*; *Li et al. 2006b*). Genetic complementation experiments showed that Ccnd1 rescued the cell migration phenotype of CCND1 KO cells only when a productive complex with Cdk4 formed (*Li et al. 2006a*, *c*). These authors showed that Ccnd1 promotes fibroblasts migration through the inhibition of the thrombospondin 1 and RHO kinase (ROCK) signaling pathways (*Li et al. 2006b*). Besides, Ccnd1 negatively regulates the transcription of E3 ubiquitin ligase factor SKP2 (S-phase kinase-associated protein 2) to enhance cell migration (*Li et al. 2006a*). Put together, these results suggest that cyclin D1 mediates cell adherence and migration through its function in the nucleus as a transcriptional regulator of genes involved in controlling those processes.

Yet, because Ccnd1 interacts with different substrates in the cytoplasm such as filamin A, PACSIN2, RhoA, Ral GTPases and paxillin (Pxn), it is thought to play an active role in this compartment regulating cell migration and adhesion (*Alhaja et al. 2004*; *Zhong et al. 2010*; *Fernández et al. 2011*; *Meng et al. 2011*; *Li et al. 2014*; *Fusté et al. 2016*). For instance, Ccnd1 can bind to and promote the phosphorylation of filamin A, which is a member of the actin-binding filamin protein family favoring cell migration (*Zhong et al. 2010*). Also, Ccnd1 negatively regulates RhoA function to promote cell migration in a manner that in cells lacking CCND1 there is an increase in RhoA activity that eventually leads to diminished cellular motility. Besides, during keratinocyte differentiation, Ccnd1 interacts with exocyst proteins such as SEC6, β1 integrin and RALA. The overexpression of Ccnd1 in keratinocytes results in a reduction of β1 integrin in the membrane and loss of cell adhesion to the matrix.

Moreover, Fusté et al demonstrated that Ccnd1 controls not only cell adhesion and migration but also metastases, by way of activated Ccnd1-Cdk4/6 – Pxn – Rac1 axis (*Fusté et al. 2016*) since Ccnd1 knockdown cells show both reduced phosphorylated Pxn at serine 83 and reduced Rac1 activation in the membrane thus leading to diminished cell metastatic potential. By contrast, phospho-pxn expression in Ccnd1-deficient cells restores metastases.

1.1.4. Regulation of cyclin D1 expression

Because of the relevant role of Ccnd1 in cell cycle regulation, a stringent modulation of its function is mandatory (*Charles J. Sherr 1995*; *Sherr 1996*; *Sherr et al. 2004*). On the one hand, Ccnd1 expression is induced by mitogenic signals, both from soluble growth factors and from interactions with the extracellular matrix (ECM) (*Assoian and Klein 2008*). On the other hand, anti-proliferative stimuli repress Ccnd1 expression. For instance, growth factors modulate both the activity and localization of GSK3β through Ras/PI3K/Akt pathway in a manner that when growth factors are present, Akt phosphorylates and inhibits GSK3β (*Cross et al. 1995*; *Dudek et al. 1997*). This is important because GSK3β phosphorylates Ccnd1 at threonine T286 in the C-terminus of the protein (*Diehl et al. 1998*), allowing Ccnd1 nuclear export, its polyubiquitination and degradation. During G1 phase, GSK3β mostly cytoplasmic but during G1/S transition, GSK3β is translocated to the nucleus, where it phosphorylates Ccnd1 allowing its export to the cytoplasm by the nuclear exportin CRM1 (*Alt et al. 2000*). Accordingly, the non-phosphorylatable mutant T286A as well as Ccnd1b (an alternative splicing mutant lacking the last 33 amino acids of the C-terminus) (*Knudsen 2006*) are more stable and they localize at the nucleus since they cannot be phosphorylated by GSK3β (*Diehl et al. 1997*) nor exported by CRM1 (*Alt et al. 2000*). Once at the cytoplasm, Ccnd1 is polyubiquinated and recognized for degradation by the 26S proteasome. Alt and co-workers showed the relevance of the correct Ccnd1 nuclear exportat since the constitutive overexpression of the Ccnd1 T286A mutant in mouse fibroblasts produces cellular transformation and has markedly enhanced oncogenic potential in immunodeficient mice (*Alt et al. 2000*). Besides, some studies found somatic mutations of this residue in endometrial and esophageal cancers (*Moreno-Bueno et al. 2003*; *Benzeno et al. 2006*)

CCND1 gene expression however, is tightly regulated by multiple transcription factors (reviewed in *Klein and Assoian 2008*). CCND1 transcription is enhanced by mitogenic growth factors since CCND1 promoter contains binding sites for AP-1, which is regulated by Fos and Jun which in turn are activated by the canonical Ras-Raf-MEK-ERK pathway under mitogenic signaling. In addition, Ras activation by growth factors induces Sp-1 mediated CCND1 gene expression. Similarly, Rac and NF-κB stimulated by mitogenic signals are also strong enhancers of CCND1 expression, and cytokines are also capable of inducing CCND1 gene expression via the JAK-STAT pathway. Importantly, proteins of the ECM such as collagen, fibronectin and vitronectin can trigger focal adhesion kinase (FAK) upon integrin clustering and further promote CCND1 expression through different transcription factors.

On the other hand, CCND1 expression is inhibited by several transcription factors in a process that is of high relevance for cell differentiation in certain cell lineages. Actually, Ccnd1

transcriptional repressors are cell-type-specific. For example, jumonji (Jmj; JARID2) repression of CCND1 is necessary for neurogenesis in the mouse hindbrain and cardiac morphogenesis while in epithelial cells SIP1 downregulates CCND1 inducing an epithelial-mesenchymal transition. Apart from controlling cell differentiation, the repression of CCND1 is very important to avoid unwanted cell proliferation.

1.1.5. Phenotype of cyclin D1 knockout mice

The phenotype of mice lacking CCND1 was studied parallelly by Fantl and Sicinski (*Fantl et al. 1995*; *Sicinski et al. 1995*). Sicinski and co-workers did not observe embryonic lethality while Fantl and co-workers saw a modest but statistically significant reduction in the number of Ccnd1 KO animals born as compared to the expected value (18% vs 25%), suggesting some degree of embryonic lethality. This difference may be attributed to the different genetic backgrounds used. Both studies reported that lack of Ccnd1 gave rise to smaller than normal animals, produced severe developmental defects in the retina, and a failure to undergo the massive proliferation of the mammary epithelium that takes place during pregnancy. Interestingly, Sicinski and co-workers also observed an abnormal limb reflex phenotype in Ccnd1 KO mice, indicative of a neurological impairment.

1.1.6. Cyclin D1 in neurons

Neurons are generated from cells of the neural tube in a process known as neurogenesis. In the central nervous system (CNS), progenitor cells may undergo two different divisions: proliferative and differentiative. In the symmetric proliferative division, a progenitor cell divides generating two progenitors that maintain cycling capacity. By contrast, in the differentiative division at least one daughter cell stops dividing and differentiates into a neuron (*Dehay and Kennedy 2007*; *Knoblich 2008*). It is ill-defined what makes a cell to follow one of these alternatives, but there appears to be a correlation between the length of G1 phase and the final output. Thus, regulators of G1 phase such as cyclins D may play an important role in neurogenesis (*Lange et al. 2009*; *Pilaz et al. 2009*; *Najas et al. 2015*). Once generated, neurons must undergo specialization according to its final location and function. A morphological characteristic of neuronal differentiation is the growth of prolongations (neuritogenesis) from the main cell body (soma), the neurites and the axon, that will allow the neuron to communicate with other cells. Proper generation and extension of neurites and axons in time and orientation is critical for neuronal connectivity and, as a consequence, for brain function (see below). Interestingly, a role for Ccnd1 in neuritogenesis has been reported as its downregulation by shRNA prevents the NGF-induced neuritogenesis in PC12 cells (*Marampon et al. 2008*).

Cytoplasmic sequestration of Ccnd1 in neurons has been proposed as a survival mechanism for differentiated cells (*Sumrejkanchanakij et al. 2003*). In this case, it is the inhibition of Ccnd1 nuclear import, rather than the acceleration of nuclear export, what prevents the nuclear accumulation of Ccnd1 and, in this manner, prevents neuronal death. Importantly, both mRNA and protein levels of Ccnd1 are increased after exposure to stress conditions in *in vitro* and *in vivo* models of neurodegeneration (*Osuga et al. 2000*; *Di Giovanni et al. 2005*; *Byrnes et al. 2007*). Similarly, Ccnd1 expression levels are elevated subsequent to glutamate- or kainate- induced neurotoxicity (*Koeller et al. 2008*; *Negis and Karabay 2016*). Actually, hippocampal neurons from Ccnd1$^{+/-}$ mice presented reduced cytotoxicity after kainate exposure compared to those from WT mice (*Koeller et al. 2008*). In addition, overexpression of cytoplasmic Ccnd1 in *in utero* electroporated cells resulted in an increase in migration (*Rocandio 2018*). Besides, cytoplasmic Ccnd1 has been detected in important adhesion sites of the radial glia fiber, suggesting that it plays a role in brain development (*Rocandio 2018*). In fact, Ccnd1 deficiency during radial migration leads to defects in the organization of layer V at postnatal ages that could be responsible for the abnormal limb reflex and leg clasping movements present in Ccnd1 KO mice (*Urbánek et al. 1994*; *Sicinski et al. 1995*; *Rocandio 2018*).

1.2 Paxillin

Paxillin is a 68 kDa protein with multiple domains that is a structural and regulatory component of focal adhesions (FAs), the macromolecular structures connecting the cytoskeleton and the extracellular matrix (ECM). Pxn actively mediates cell signaling and participates in FA assembly (*Brown and Turner 2004*) functioning as an adaptor protein that facilitates the interaction between different molecules such as kinases, other adaptor proteins, nucleotide exchange factors and cytoskeleton proteins (*Brown et al. 1996*). Notably, Pxn interacts with several proteins involved in the regulation of various processes such as cell motility, cell survival, actin cytoskeleton organization, cell proliferation, embryonic development, wound healing and immunity (*Schaller 2001*).

Paxillin knockout mouse is embryonic lethal, and *in vitro* cultured Pxn-deficient MEFs has altered processes of fibronectin signaling such as inadequate FA formation and an inefficient distribution of focal adhesion kinase (FAK), a cytoplasmic tyrosine kinase that is a key mediator of integrin signaling. The shortage of phosphorylation by FAK leads to reduced spreading capacity, loss of lamellipodia and decreased rates of cell migration (*Hagel et al. 2002*).

1.2.1. Paxillin regulation by phosphorylation

Paxillin contains multiple phosphorylation sites that are critical for its localization and functions, and that are the targets of a wide variety of kinases and phosphatases. Even though tyrosines 31 and 118 are the main phosphorylation sites, several serine/threonine kinases phosphorylate residues at the N-terminal half of the protein during cell migration, thus controlling its function and also proteasomal degradation. Amongst these kinases, JNK (JUN N-terminal kinase) phosphorylates Pxn at Ser178, a critical step in cell migration (*Zeid et al. 2006*; *Huang et al. 2008*). Phosphorylation at Ser273 by the p21-activated kinase (PAK) participates in the regulation of cell adhesion through Rac activation (Nayal et al. 2006). Also, Pxn has been shown to be phosphorylated by GSK3β at Ser130 and by Raf/MEK/ERK at Ser126 (*Woodrow et al. 2003*). By contrast, phosphorylation at serine residues in the C-terminal domains of the protein has been suggested to govern Pxn localization at FAs. For instance, phosphorylation at Ser272 blocks the nuclear export of Pxn, leading to its accumulation in the nucleus where it enhances androgen receptor and ERK-mediated transcription (*Dong et al. 2009*; *Ma and Hammes 2018*).

1.2.2. Focal adhesions

Adhesion of cells to the ECM is a key step in processes such as cell migration through tissues, cell differentiation and proliferation, embryonic development, immunology and tissue repair (*Gumbiner 1996*). The attachment of cells to ECM components is mediated by cell-surface proteins called integrins, which are transmembrane proteins formed by a heterodimer of an α and a β subunit, with a large extracellular domain and a cytoplasmic portion. Although integrins lack intrinsic enzymatic activity in their cytoplasmic domain, interaction with the ECM promotes their dimerization and the recruitment of structural and regulatory proteins to the FA (Figure 2). At present, 24 distinct heterodimers have been characterized in mammals from the combination of 18 different α subunits and 8 β subunits (*Van der Flier and Sonnenberg 2001*; *Hynes 2002*; *Luo et al. 2007*). Each integrin is capable of recognizing a distinct ligand of the ECM. As such, integrins on the surface of a cell act as sensors for the ECM environment (*Hynes 2002*). The adaptor/scaffold proteins in FAs mediate the interaction with the actin cytoskeleton thereby connecting cells firmly to the ECM. On the other hand, signaling proteins in FAs mediate cytoskeleton dynamics, FA formation and cell contraction through the actin-myosin filaments (*Burridge et al. 1992*; *Geiger et al. 2001*; *Zaidel-Bar et al. 2006*). This generates enough force to alter cell morphology and to move the cell body during migration. Upwards of 125 proteins have been reported to take part in FAs (*Turner 2000*; *Zaidel-Bar et al. 2007*), and among them Pxn serves as a scaffold protein to facilitate the functional integration of multifold components of the complex (*Deakin and Turner 2008*).

A correct FA assembly and recycling is crucial for cell adherence and motility (*Geiger et al. 2001*; *Parsons et al. 2010*). The activity of these complexes is often regulated by the phosphorylation of the clustered proteins forming the FA such as Pxn, Src and FAK (*Webb et al. 2004*; *Li et al. 2005*). FA dynamics is believed to be controlled by small GTPases like Rac and Rho, one controlling the early formation of FA and the other the maturation of the complex, respectively (*Wozniak et al. 2004*). The dysregulation of FAs can lead to pathological conditions. For instance, Pxn is upregulated at both RNA and protein levels in many human cancers, thus acting as an oncogene in malignancy progression (*Jagadeeswaran et al. 2008*; *Kim et al. 2012*; *Sen et al. 2012*; *Chen et al. 2013*; *Wu et al. 2014*; *Huang et al. 2015*; *Li et al. 2015*).

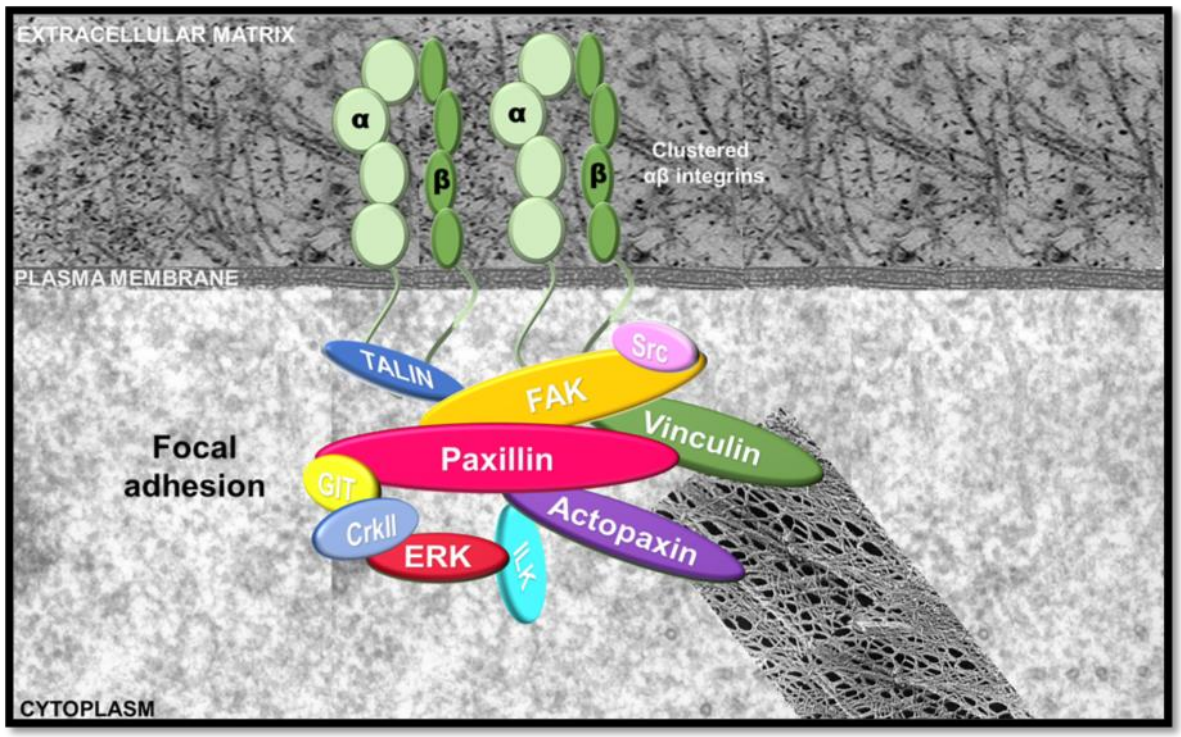

Figure 2: Focal adhesions serve as a link between the ECM and the actin cytoskeleton. Cells adhere to the ECM through αβ-integrin heterodimers, which result activated and recruit cytoplasmic proteins, including Pxn, to the plasma membrane. In this structure, Pxn acts as scaffold protein. Adapted from: Deakin and Turner 2008.

1.2.3. Paxillin in the central nervous system

The generation of neurites or neuritogenesis is a process common to all neurons. It begins with the formation of an initial budding in the neuronal sphere, followed by the sprouting of cell projections (neurites) from this and other buds on the cell surface, and the polarized growth of these cell extensions to become axons or dendrites (*Da Silva and Dotti 2002*). Polarized growth takes place at the distant tip of the neurite, a region called the growth cone. It is the interaction between membrane proteins and the ECM during cell adhesion that makes possible the formation

of lamellipodia adjacent to the leading edge of the growth cone (*Da Silva and Dotti 2002*; *Thoumine 2008*). The progression of this growth cone is based on two processes. First, there is a retrograde flow of actin generated by actin polymerization at the leading extremity combined with actin depolymerization in the central region and myosin rending on actin filaments in lamellipodia (*Diefenbach et al. 2002*). This results in a mechanical tension that will drive neurite outgrowth (*Schaefer et al. 2008*). Second, cell adhesion molecules contact with the ECM and adjacent cells and coordinate migration speed. FA proteins facilitate the signaling across the membrane and lead to cell migration and neuritogenesis (*Milner and Campbell 2002*). In fact, integrin-mediated adhesions are essential for neurite outgrowth (*Rhee et al. 2000*; *Ivankovic-Dikic et al. 2000*) and inhibition of Pyk2/FAK is sufficient to block neuritogenesis induced by ECM (*Ivankovic-Dikic et al. 2000*). Mechanisms controlling neuronal migration and neurite extension must be well coordinated since the final morphology, functionality and connectivity of the neuron will depend on this (*Hatten 2002*; *Solecki et al. 2006*). Consequently, defects on these processes may cause several pathologies such as mental retardation, epilepsy or learning deficiencies (*Marin and Rubenstein 2003*).

Although the CNS is the tissue with lower Pxn expression levels, Pxn plays a critical role in neuritogenesis. In particular, Pxn acts both by linking extracellular receptors to the actin cytoskeleton and also by regulating Rho-GTPase signaling (*Brown and Turner 2004*). Pxn phosphorylation is necessary for cell spreading and neurite formation, both characteristics of the morphological phenotype of a differentiated neuron, and Pxn levels are increased in differentiated neurons in comparison with undifferentiated cells (*Leventhal and Feldman 1996*). Importantly, Pxn deficiency disrupts neuronal positioning and neuronal migration in post-mitotic neurons (*Rashid et al. 2017*). Several studies implicate Pxn phosphorylation in neurite outgrowth in different cell types. For instance, laminin-induced neurite outgrowth depends on the phosphorylation of both FAK and Pxn mediated by the AKT/GSK3β pathway (*Chen et al. 2009*). Besides, Pxn plays a key role in cell migration in the central and peripheral nervous system during development. Phosphorylation of Pxn at S178 by JNK regulates Schwann cell migration (*Miyamoto et al. 2012*). In oligodendrocytes (OLs), S244 phosphorylation by Cdk5 following induction of OLs differentiation suggests that Pxn may also be involved in OL differentiation and myelination through Cdk5 phosphorylation (*Miyamoto et al. 2007*). *In vitro* studies in PC12 cells show that Pxn promotes neurite outgrowth induced by NGF and EGF. In particular, mutation of S85 in Pxn, a known phosphorylation target of p38MAPK, dramatically reduces NGF-induced neuritogenesis (*Huang et al. 2004*). Additionally, Nemo-like kinase phosphorylation of Pxn S126 and microtubule-associated protein-1B (MAP1B) have been proposed as a downstream mechanism of NGF control of cytoskeleton dynamics and neurite extension (*Ishitani et al. 2009*).

1.2.4. Rho GTPases

The Rho family of small GTPases is a subfamily of the superfamily of Ras GTPases that in mammals is composed by some 20 members, among which Cdc42, Rac1 and RhoA are the best characterized. These GTPases are involved in the control of different processes such as the actin cytoskeleton and FA organization, cell motility, gene transcription and cell cycle progression (*Ridley 2015*). Some members of this family are necessary for the metastatic potential of tumor cells *in vivo (Burbelo et al. 2004)*. The activity of Rho GTPases is tightly regulated by nucleotide exchange, with an inactive form bound to GDP, and an active one bound to GTP. The alternation between these two states is controlled by guanine nucleotide exchange factors (GEFs), GTPase-activating proteins (GAPs), and GDP-dissociation inhibitors (GDIs). GEFs activate GTPases by facilitating the exchange of GDP for GTP. GAPs stimulate GTPase activity, promoting GTP hydrolysis into GDP, thus inactivating the GTPase, and GDIs inhibit the dissociation of GDP from the protein, avoiding its exchange for GTP *(Hoffman and Cerione 2002*). These GTPases can be activated by extracellular signals like EGF or insulin, which control Rac activity and generate lamellipodia and membrane ruffles. On the other hand, Cdc42 activation leads to the formation of filopodia while RhoA promotes cell migration by regulating the adhesion of the cell *(Ridley 2001a, b; Raftopoulou and Hall 2004)*.

1.3 GABAergic neurotransmission

Gamma-Aminobutyric acid (GABA) is the principal inhibitory neurotransmitter in the CNS. GABA is released by up to 40% of neurons to activate chloride channels generally leading to the inhibition of firing (*Bowery and Smart 2006*). GABAergic neurons are found all through the brain, especially in the hippocampus, thalamus, cerebral cortex, substantia nigra, striatum and cerebellum (*Fritschy and Brünig 2003*). Since it is present in large amounts in the brain and distributed in a cellular-specific manner, GABA has multiple roles in the CNS. For example, GABA is involved in physiological mechanisms like feeding and sexual behavior, mood, aggression, locomotor activity, pain sensitivity, cardiovascular regulation and thermoregulation (*Matsumoto 1989*). The abnormal function of the GABAergic neurotransmission can lead to several disorders such as epilepsy, anesthesia, anxiety, stress, schizophrenia, neurodegenerative diseases and disorders in memory, sleep, stress and cardiovascular and neuroendocrine function (*Wong et al. 2003*). Consequently, many drugs target GABA receptors including benzodiazepines, barbiturates, ethanol, anesthetics and neuroactive steroids (*Froestl 2011*),

1.3.1. GABA synthesis, reuptake and degradation

GABA is a glutamate derivate synthetized by the enzyme glutamate decarboxylase (GAD) and found exclusively in GABAergic neurons. There are two enzyme isoforms, GAD65 and GAD67, which differ in their cerebral and cellular distribution. While GAD65 is mainly found at neuronal terminals, GAD67 is spread all through the cell and it is used as a marker for GABAergic neurons. Once synthetized, GABA is introduced in secretory vesicles by means of the vesicular transporter vGAT and further released out of the cell in a Ca^{2+} dependent manner following presynaptic neuron depolarization. The release of GABA vesicles can be modulated by autoreceptors of GABA located presynaptically, which results in a negative feedback; or by the hyperpolarization of the GABAergic neuron by another GABAergic neuron. Released GABA binds to and acts on postsynaptic receptors. Further, and as a mechanism for cessation of the GABAergic transmission, GABA is captured by Na^+/Cl^- GABA transporters (GAT1-3 and BGT1) in astrocytes or GABAergic neurons. In astrocytes, GABA is degraded by GABA transaminase while GABAergic neurons can reuse it as a neurotransmitter (*Martin and Rimvall 1993*; *Madsen et al. 2007*).

1.3.2. GABA receptor types

GABA exerts its effects activating two different types of GABA receptors. $GABA_A$ receptors ($GABA_AR$) are pentameric ligand-gated ion channels (pLGIC) whereas $GABA_B$ receptors are metabotropic (*Olsen and Sieghart 2008*). They were first distinguished and named on the basis of sensitivity to bicuculline and baclofen respectively. However, their classification has been confounded by the finding of ionotropic receptors that are insensitive to both bicuculline and baclofen. These are $GABA_c$ receptors, nowadays belonging to the $GABA_A$ receptor family. Ionotropic type A receptors are the major inhibitory receptors in the CNS and are selectively permeable to Cl^- (and HCO^{3-}). When activated by GABA binding, they commonly allow the rapid influx of anions into the cell leading to hyperpolarization of the plasmatic membrane and consequently to the inhibition of the neurotransmission (*Farrant and Kaila 2007*). On the other hand, $GABA_B$ receptors are coupled to G proteins and their mechanism of action depends on which G protein(s) it is coupled to. Finally, the structure, pharmacology and physiology of $GABA_c$ receptors is different from other $GABA_AR$ although they preserve the main functional properties such as Cl^- permeability. They are almost exclusively found in the retina (*Albrecht and Darlison 1995*).

The main action of GABA is mediated by pLGIC or type A receptors. $GABA_AR$ belongs to the Cys-loop superfamily of LGICs along with other receptors such as the nicotinic acetylcholine receptors (nAChRs) (*Corringer et al. 2000*), glycine receptors (GlyRs) (*Breitinger and Becker*

2002), type-3 5-hydroxytrypamine receptors (5-HT_3R) (*Lummis 2012*) and the Zn^{2+}-activated cation channel (ZAC) (*Davies et al. 2003*). They are called Cys-loop receptors because they contain a conserved structural motif formed by a disulphide bridge in the extracellular domain (ECD). Cys-loop receptors are heteropentameric structures that form an ion-permeable central pore. Upon agonist binding, there is a conformational change in the receptor complex with the consequent ion channel opening. In most mature neurons, this generates a net inward flow of anions and the consequent hyperpolarizing postsynaptic response known as inhibitory postsynaptic potential (IPSP). This phenomenon occurs following release of GABA from presynaptic vesicles. The high concentration of GABA briefly stimulates postsynaptic $GABA_AR$ resulting in an increase in membrane conductance which in turn underlies what is known as "phasic" inhibition (Figure 3).

However, GABA inhibition of the CNS is not only due to the activation of postsynaptic $GABA_AR$, but also due to the persistent or "tonic" stimulation of extrasynaptic $GABA_AR$ (Figure 3). Those responses are less spatially and temporally specific and are generated by low GABA concentrations in the extracellular space. Hence, extrasynaptic $GABA_AR$ present higher affinity for GABA than postsynaptic receptors. Moreover, tonic receptors remain opened for a longer time upon GABA binding (*Farrant and Nusser 2005*). Alterations in the modulation of this tonic inhibition have been linked to several disease states.

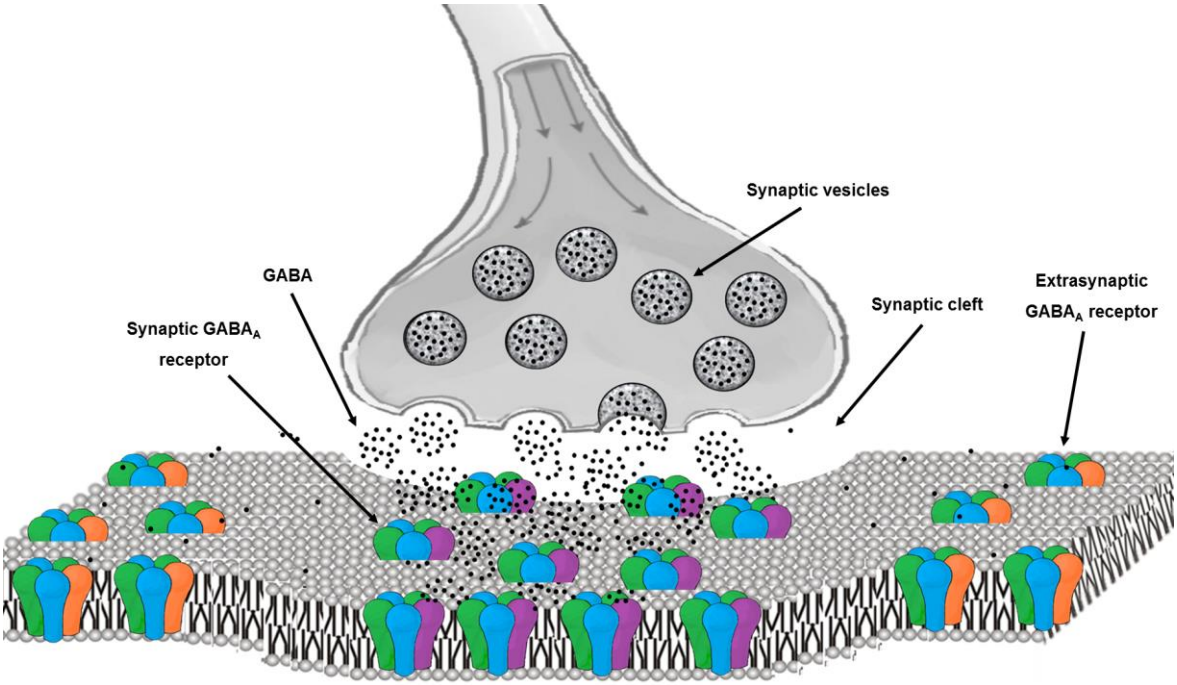

Figure 3: Synaptic and extrasynaptic $GABA_AR$ neuronal localization. $GABA_ARs$ containing α(1-3)βγ subunits are mainly located at the synapse mediating phasic inhibition, whereas α(4,6)βδ and α(5)βγ receptors are located at extrasynaptic sites modulating tonic inhibition.

1.3.3. $GABA_A$ receptor subunits

All the pLGICs show a common transmembrane topology with many residues and motifs conserved between members, which indicates their relevance in the structure and function of the receptor. Within the members of the eukaryotic Cys-loop superfamily, tertiary and quaternary structures are conserved (*Sine and Engel 2006*). Each mature subunit is approximately 450 amino acid residues in length and contains a very large hydrophilic amino (N)-terminal ECD containing agonist binding sites and the characteristic Cys-loop. Besides, they contain a transmembrane domain (TM) composed of four transmembrane alpha-helices (TM1-4) where the TM2 of each subunit forms the lining of the channel pore (Figure 4A,B).

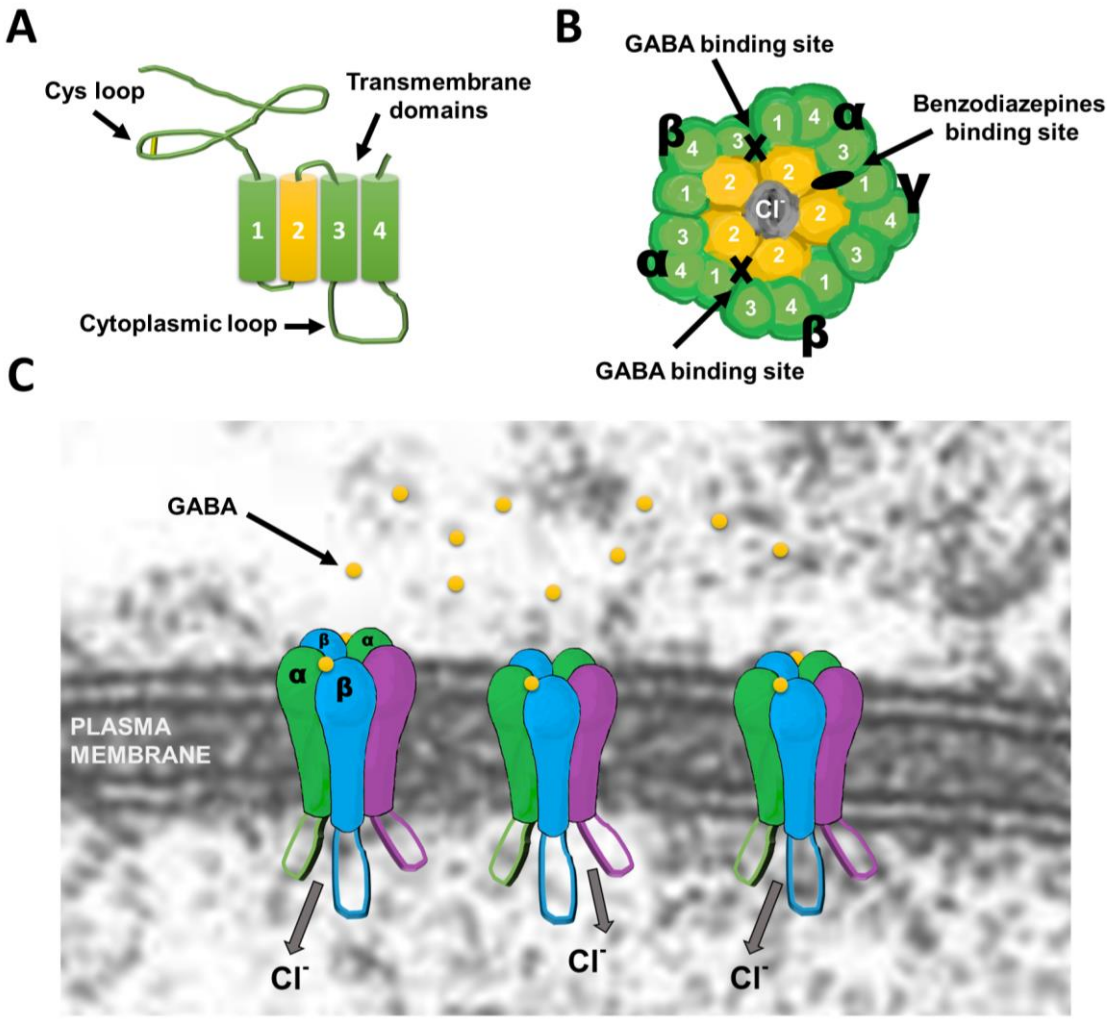

Figure 4: Schematic representation of $GABA_AR$ structure. A) Typical $GABA_AR$ subunit structure with a large extracellular N terminal, four transmembrane domains (TM1-4), one short intracellular loop between TM1-2, one short extracellular loop that links TM2-3 and one long intracellular loop between TM3-4 susceptible to phosphorylation. **B)** Top view of the pentamer showing the distribution of each subunit. TM2 of each subunit (in yellow) forms the lining of the channel pore. GABA binding site is located between α and β subunits while benzodiazepines bind at the interface between α and γ. **C)** $GABA_ARs$ are pentamers forming a channel that is permeable to chloride anion.

Between the TM3 and TM4 they contain a large intracellular loop which is susceptible to phosphorylation as a mechanism of regulation of the activity and trafficking of the receptor ($GABA_AR$ modulation via intracellular loop phosphorylation will be discussed below). Finally, $GABA_ARs$ have two binding sites for GABA located to the β/α interface. Moreover, they have an extra binding site at the α/γ subunit interface where benzodiazepines and other drugs bind (Figure 4B) (*Sigel and Steinmann 2012*).

In the human genome, 19 genes have been identified to encode for $GABA_AR$ subunits, including six α subunits, three β subunits, three γ subunits, three ρ subunits (forming $GABA_CR$), and one each of the ε, δ, θ and π subunits (*Barnard et al. 1998*; *Whiting 1999*). Additionally, some $GABA_AR$ subunits present different forms following alternative splicing. For instance, splice variants are found for the α1-3, β2, ρ1, γ 2-3 and ε subunits. The majority of genes coding for the $GABA_AR$ subunits are organized in four clusters on chromosomes 4, 5, 15 and X in the human genome (*Darlison et al. 2005*). This distribution is thought to contribute to coordinated gene expression.

In this thesis, we focus on the study of the α4 and β3 subunits. For this reason, a special mention of them will be done in each section.

1.3.4. $GABA_A$ receptors, structure and composition

As mentioned above, $GABA_ARs$ are formed by the assembly of five subunits (Figure 4C). Commonly receptors are heteropentamers formed by several types of subunits. Hence, in physiological conditions five subunits selected from 19 isoforms form a pentameric complex and surrounding a central ion channel. Furthermore, some $GABA_AR$ subunits (e.g. β3) can form homopentameric functional receptors *in vitro* (*Wooltorton 1997*). In fact human β3 subunit is able to assemble into functional homomeric channels although they have not been identified as discrete populations in the brain yet (*Miller and Aricescu 2014*). Actually, the functional properties of the receptors depend on both subunit composition (*Sigel et al. 1990*) and arrangement (*Minier and Sigel 2004*). Therefore, receptors formed by the same subunits but differently arranged will have distinct functional properties. Usually, $GABA_AR$ are made up of two α, two β and one γ or δ subunits being the most common combination in the adult brain α1β2γ2 (40-60%) (*Whiting et al. 1995*; *Barnard et al. 1998*) with the other common subunit combinations being α2β2γ2 (15-20%), α4βδ/γ2 (<5%) and α6βδ/γ2 (<5%) (*Fritschy and Mohler 1995*; *Whiting et al. 1995*; *Sieghart and Sperk 2002*). Also, $GABA_ARs$ containing other subunit stoichiometries, like binary constructs of α and β subunits have been reported (*Fritschy et al. 2012*; *Fritschy and Panzanelli 2014*). Notably, α6 subunit is nearly exclusively expressed in granule cells in the cerebellum of the adult

brain forming α6βγ receptors (*Nusser et al. 1998*). The α4βγ2 is expressed in the thalamus, dentate gyrus and caude-putamen (*Pirker et al. 2000*). The α4β2δ is expressed in the thalamic relay nuclei (*Chandra et al. 2006*), and the α4β3δ subtype is expressed in dentate granule cells of the hippocampus (*Liang et al. 2006*). Both α4β2δ and α4β3δ are found in the cerebral cortex while α4β3δ predominates in the striatum. Notably, α4 subunit can form functional receptors with βxγ2 and βxδ, both expressed in the thalamus and the dentate gyrus of the hippocampus, although they differ in their subcellular localization: being the first located synaptic and the second extrasynaptic (*Bencsits et al. 1999*). Though α4βδ receptors represent only 1% of the total subtypes (*Bencsits et al. 1999*), their role is highly important since they are involved in extrasynaptic tonic inhibition. In the cerebellum, β2/3 subunits interact with α6 and δ to form extrasynaptic receptors (*Wei et al. 2003*; *Scimemi 2005*; *Hörtnagl et al. 2013*; *Fritschy and Panzanelli 2014*). Moreover, β3 subunit can be found together with α5 and γ2/3 in hippocampal pyramidal cells (*Fritschy and Mohler 1995*).

1.3.5. Cellular and subcellular localization of $GABA_A$ receptors

The regional and subcellular localization of $GABA_A$Rs is ruled by its subunit composition and varies all over the brain throughout development (*Laurie et al. 1992*; *Wisden et al. 1992*). Most subunits are present in several regions of the CNS, although α6 subunit is exclusively expressed in granular cells in the cerebellum of the adult brain and ρ subunit is nearly restricted to retina cells (*Sieghart and Sperk 2002*). Besides, $GABA_A$Rs containing α1 subunit are mainly found on interneurons and Purkinje cells while α2 subunit-containing receptors are localized to motor neurons and pyramidal cells (*Sieghart and Sperk 2002*). Concerning α4 subunit, it is specifically located in the thalamus, dentate gyrus and striatum (*Chandra et al. 2006*) and its expression varies along the development. In immature and newborn granule cells, α4 is required for the assembly of functional $GABA_A$Rs. Expression of α4 subunit expression increases in hippocampal pyramidal neurons at puberty, which has been proposed as a mechanism for the decline in Long-Term Potentiation (LTP) observed at puberty (*Shen et al. 2010*). Finally, in the adult brain, there is a decrease in the expression of the α4 subunit (*Peng et al. 2004*). α4 deficient cells from adult hippocampus present incomplete migration and altered dendritic maturation attributed to the lack of α4-containing $GABA_A$Rs (*Duveau et al. 2011*). Regarding β3 subunit, it is expressed at different structures of the brain, including among others the cerebral cortex, hippocampus, cerebellum and the thalamus. Again, its expression varies at different stages of development and maturity. For instance, peaks are reached prenatally in the thalamus, the hippocampus and the cerebral cortex and further postnatally in the cerebellar cortex (*Laurie et al. 1992*; *Nadler et al. 1994*). After each peak of expression, rapid down-regulation takes place. Along postnatal

maturation, the cerebral cortex and, not as much, the hippocampus present lower β3 subunit levels while expression in the cerebellum does not change (*Laurie et al. 1992*; *Nadler et al. 1994*). In the end, in mature mice, the expression of the β3 subunit is higher in the cerebellum (Purkinje and granule cells), the pyriform cortex and the hippocampus (*Wisden et al. 1992*).

In the CNS, the subcellular localization of $GABA_AR$ has been studied by immunofluorescence and electron microscopy (EM). For instance, αβγ receptors are enriched at GABA-synapses of postsynaptic neurons in numerous brain regions such as the cerebellum (*Craig et al. 1994*) (*Nusser et al. 1995*), hippocampus (*Nusser et al. 1996*) and neocortex (*Farrant and Nusser 2005*). Nevertheless, so far not a single receptor has been described to be uniquely found at synapses. Thus, even the more enriched form at synapses, the α1β2/3γ2L, is also present outside the synapses (*Nusser et al. 1995*). On the other hand, δ-containing $GABA_ARs$ do not localize at the synapse and exist exclusively in extrasynaptic and perisynaptic sites in hippocampal CA1 pyramidal neurons and dentate granule cells (*Wei et al. 2003*; *Scimemi 2005*). For instance, δ subunit forms receptors with α6 and β2/3 in the cerebellum and with α4 and βX in the hippocampus (*Hörtnagl et al. 2013*; *Fritschy and Panzanelli 2014*). In summary, γ2-containing $GABA_ARs$ (co-assembled with α1-3 and β2/3 subunits) predominantly exist at inhibitory synapses mediating phasic inhibition, while receptors formed by α4-6 subunits co-assembled with δ subunit are almost exclusively found peri- and extrasynaptically and mediate tonic inhibition.

Apart from its localization at postsynaptic neurons, $GABA_AR$ have also been found at presynaptic membranes on distal axons and terminals (*Fritschy and Panzanelli 2014*). presumably regulating neuronal synchronization and mediating presynaptic afferent depolarization, as well as regulating neurotransmitter release in some cell types (*Bowery and Smart 2006*).

Outside the CNS, $GABA_A$ receptors have been found in the liver where they inhibit cell proliferation (*Erlitzki et al. 2000*). For instance, β3 subunit levels are decreased in hepatocellular carcinoma, which correlates with increased tumor growth (*Minuk et al. 2007*). In smooth airway muscles of the lung, $GABA_ARs$ facilitate relaxation (*Mizuta et al. 2008*) and in several types of immune cells, $GABA_AR$ activation decreases cell proliferation (*Alam et al. 2006*; *Bjurstöm et al. 2008*).

1.3.6. Assembly and trafficking of $GABA_A$ receptors

$GABA_ARs$ serve as a chloride ion-selective channel that opens when GABA binds to its agonist binding site, thus increasing the chloride entrance into the cell. The membrane then hyperpolarizes, inhibitng the firing of new action potentials. Given the relevant role of the GABAergic neurotransmission for the proper CNS function, regulating the number of $GABA_ARs$

in the cell surface is fundamental (Figure 5). $GABA_AR$s are assembled in the endoplasmic reticulum (ER) in a specific process regulated by residues at the N-terminal domain in each subunit, which limits the possible subunit combinations (*Luscher et al. 2011*). Mutations in the N-terminal domains of different subunits abolish the subunit assembly and receptor generation (*Korpi et al. 1994*; *Tan et al. 2007*). The assembly begins with the formation of αβ heterodimers with the assistance of ER-associated chaperones, including calnexin and binding immunoglobulin protein (BiP) which monitor the fidelity of protein folding and assembly (*Connolly et al. 1996*; *Bradley et al. 2008*). This step is of a high relevance since the depletion of either α or β subunits results in the loss of the corresponding receptors whereas the loss of the γ2 leads to just a modest decrease of GABA binding sites (*Gunther et al. 1995*). Unassembled $GABA_AR$ subunits are bound to ER-chaperones that retain them until degradation (*Bollan et al. 2003*). Although the regulation of the differential subunit assembly in cells that co-express different $GABA_AR$s is still unknown, it is thought that is driven by the co-translation of compatible subunits. In this sense, the ectopic expression of α6 subunit in mouse hippocampal cells leads to an increased number of α6βγ2 receptors located extrasynaptically whereas postsynaptic receptors decrease (*Wisden et al. 2002*).

Once assembled, $GABA_AR$s must leave the ER by exocytosis. This process is however limited by the constitutive degradation of both α and β subunits in the ER (*Saliba et al. 2007*; *Bradley et al. 2008*). The chronic blockade of neural activity increases the $GABA_AR$ degradation at the ER (*Saliba et al. 2009*). The release of $GABA_AR$s is helped by the interaction between α and β subunits with PLIC-1 (Protein that Links Integrin-associated protein with the Cytoskeleton-1), since PLIC-1 interacts with polyubiquitinated $GABA_AR$ subunits at the ER thus preventing ER-associated subunit degradation and enhancing their expression at the cell surface (*Bedford et al. 2001*; *Saliba et al. 2008*).

Another posttranslational modification that is involved in the control of $GABA_AR$ trafficking is palmitoylation. In particular, the Golgi-specific DHHC zinc finger protein (GODZ, zDHHC3) palmitoylates γ2 subunit at cytoplasmic cysteine residues facilitating the translocation of the γ2-containing receptor from ER to Golgi and enhancing the accumulation of $GABA_AR$s at inhibitory synapses (*Keller et al. 2004*). Actually, the downregulation of GODZ produces the selective loss of $GABA_AR$s at synapses and the corresponding decrease in the amplitude and frequency of mIPSCs along with whole cell currents (*Fang et al. 2006*).

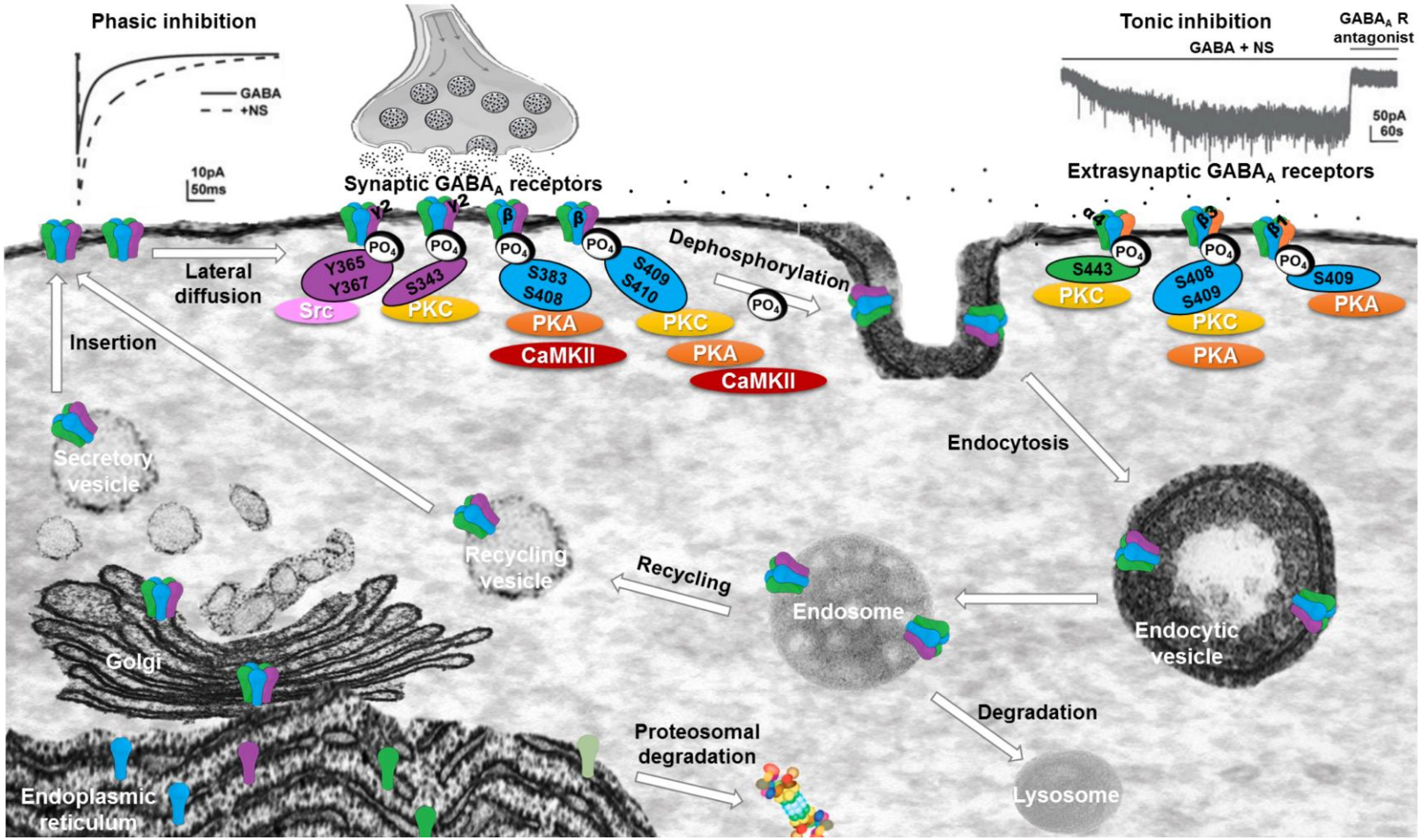

Figure 5: Modulation of GABA$_A$Rs trafficking by phosphorylation. GABA$_A$Rs are assembled in the ER, matured in the Golgi, secreted and inserted into the plasma membrane. Synaptic receptors reach their destination through lateral diffusion. GABA$_A$Rs subunits phosphorylation by several kinases regulates their function and their surface expression. Dephosphorylation of these subunits activates the internalization of the GABA$_A$R through its interaction with AP2 adapting complex. Endocyted receptors are transported to the endosomal system and further recycled to the cell surface or degraded in the lysosomes. Adapted from: Chuang and Reddy 2018**.**

Further, $GABA_ARs$ need to be translocated from Golgi to the plasma membrane. In this process, the brefeldin A-inhibited GDP/GTP exchange factor 2 (BIG2) interacts with the β subunits through its intracellular loop and facilitates the $GABA_ARs$ release from the Golgi to the plasma membrane (*Charych et al. 2004*). Besides, BIG2 is also a component of $GABA_ARs$ recycling endosomes (*Boal and Stephens 2010*). Apart from BIG2, the $GABA_ARs$ associated protein (GABARAP) interacts with all γ subunits easing the translocation of $GABA_ARs$ to the cell surface (*Leil 2004*). Moreover, GABARAP plays a role in rapid NMDA-induced functional plasticity of inhibitory synapses (*Marsden et al. 2007*). That is, upon NMDA receptor activation, there is an influx of Ca^{2+} that leads to a rapid accumulation of postsynaptic $GABA_ARs$ with the consequent increase in mIPSCs. This procedure also involves Ca^{2+} calmodulin-dependent kinase II (CaMKII), which is believed to phosphorylate the residue S383 of the β3 subunit (*Houston et al. 2007*).

Another important process for the correct regulation of the number of $GABA_ARs$ in the cell surface is the endocytosis. For this, adaptor proteins like clathrin adaptor protein AP2 are important for their interaction with β and γ subunits (*Kittler et al. 2000*). The AP2 binding motif in β subunits consists in a 10 basic amino acids sequence that includes a conserved phosphorylation site in the intracellular loop of β1-3 subunits (*Kittler et al. 2005, 2008*). Significantly, AP2 cannot interact with the β subunit when they are phosphorylated, i.e. AP2 interacts with $GABA_ARs$ promoting their internalization only when they are dephosphorylated. Consequently, neuronal perfusion with an unphosphorylated β3-derived peptide leads to an increase in mIPSCs and whole cell currents due to a decrease in the internalization of $GABA_ARs$ (*Kittler et al. 2005*). In fact, several kinases like PKA (Protein Kinase A), PKC, Akt and CaMKII can control phosphorylation of β subunits and consequently, endocytosis. Thus, PKA can phosphorylate β1 and β3 subunits at the AP2 interaction site (*McDonald et al. 1998*). PKC phosphorylates β1, β2 and β3 (*McDonald et al. 1998*; *Brandon et al. 2003*) and reductions in the phosphorylation state of β subunits by PKC inhibition have been involved in the loss of GABAergic inhibition present in animal models of status epilepticus (*Terunuma et al. 2008*). Apart from kinases endocytosis is also modulated by phosphatases. For instance, PP1α dephosphorylates β3 subunit at the AP2 interaction site promoting its endocytosis (*Terunuma et al. 2004*).

After their endocytosis, $GABA_ARs$ can be either recycled or degraded. Approximately 70% of the $GABA_ARs$ are reinserted into the membrane in an hour after endocytosis. The other 30% are targeted to endosomes for degradation in a process that takes about 6 hours (*Kittler et al. 2004*). The decision of whether endocyted $GABA_ARs$ undergo recycling or degradation is modulated by the interaction between β subunits and huntingtin-associated protein 1 (HAP1) through the cytoplasmic loop of the β subunit in a manner that when both proteins interact, there is a decrease

in the degradation of $GABA_A$Rs and an enhancement of their recycling (*Kittler et al. 2004*). In fact, it is believed that the neurodegenerative effects observed in Huntington's disease are, in part, due to a reduced expression and function of the $GABA_A$Rs (*Twelvetrees et al. 2010*). Those $GABA_A$Rs that fail to be recycled are ubiquitinated at lysine residues within the intracellular domain and further degraded at the lysosomes. Consistently, the blockade of lysosomal degradation results in an increase in the number of $GABA_A$Rs at the synapse and the consequent increase in the efficacy of the GABAergic inhibition (*Arancibia-Cárcamo et al. 2009*). In relation to β3 subunit, Saliba and co-workers showed that the ubiquitination of the β3 subunit is activity-dependent and proposed this targeting for proteasomal degradation as a mechanism to regulate the synaptic inhibition (*Saliba et al. 2007*).

Different studies (*Thomas et al. 2005*; *Bogdanov et al. 2006*) suggest that $GABA_A$Rs are exclusively inserted into or removed from extrasynaptic sites of the plasma membrane. In this manner, the lateral mobility of the receptors is necessary so that $GABA_A$R can be found at postsynaptic densities. Embedded proteins can move laterally in the membrane thanks to its physical properties of lipid bilayer as far as they are not stuck by intracellular interactors or they face obstacles. The final localization of the receptor depends on both the subunit composition of the receptor and the interaction of the receptor's subunits with scaffold proteins of the postsynaptic neuron such as gephyrin (*Tretter et al. 2012*) and radixin (*Hausrat et al. 2015*). Gephyrin is a subsynaptic scaffold protein that stabilizes $GABA_A$Rs at synapses. When the expression of gephyrin is downregulated in mouse cultured neurons, there is a selective reduction in the number of $GABA_A$Rs at the synapses. By contrast, radixin serves for the anchoring of α5-containing receptors extrasynaptically, which prevents thir accumulation at the synapses (*Loebrich et al. 2006*). However, after disruption of radixin-α5 interaction, α5-containing $GABA_A$Rs remain completely functional in mediating tonic current inhibition (*Loebrich et al. 2006*).

Besides, the neuronal activity is also important in adjusting the number of $GABA_A$Rs at synapses during synaptic plasticity (*Choquet and Triller 2013*) and in fact, after repetitive stimulation, desensitized $GABA_A$Rs laterally diffuse at neighboring GABAergic synapses where they decrease the amplitude of GABA-related synaptic currents (*de Luca et al. 2017*).

1.3.7. $GABA_A$ receptor function

In studies with heterologously expressed receptors, subsequent to GABA binding the α and β subunits rotate asymmetrically promoting the opening of the ion channel (*Horenstein et al. 2001*). Once opened, the $GABA_A$R-associated channel is selectively permeable to several anions that can flux in both directions (*Sakmann and Fassberg 1987*). Chloride is the principal anion passing

through the channel although other anions such as bicarbonate can also move through the $GABA_AR$-associated channel (*Kaila 1994*). In most cases, the opening of the $GABA_AR$-channel leads to the entrance of Cl^- into the cell, generating membrane hyperpolarization and neuronal inhibition. Still, if the intracellular Cl^- concentrations are higher, there is an efflux of Cl^- anion thus depolarizing the membrane. This phenomenon has been identified in the developing brain (*Obata et al. 1978*) and in primary afferent neurons (*Barker et al. 1975*).

The neural response upon $GABA_AR$ activation by GABA binding depends on the electrochemical driving force for Cl^-, which is fixed by the Cl^- equilibrium (E_{Cl}). E_{Cl} is determined by the relative expression of KCC2 (potassium chloride cotransporter 2) and NKCC1 (Na-K-Cl cotransporter) which varies during animal development and neural differentiation (*Andäng and Lendahl 2008*). KCC2 is a neuron-specific chloride potassium symporter thus mediating the synaptic inhibition and synaptic plasticity. During mammalian development, when neural networks are still being established, KCC2 levels remain low and they are upregulated during postnatal development (*Kaila et al. 2014*). On the other hand, NKCC1 is a cotransporter of sodium potassium and chloride. It is expressed widely throughout the body and importantly in many regions of the brain during development but not in adulthood (*Dzhala et al. 2005*). When NKCC1 is expressed, the internal chloride concentrations rise. In that manner, when the $GABA_AR$-associated channel opens there is an outflux of chloride anion thereby depolarizing the cell membrane. Altogether, the switch in KCC2 and NKCC1 expression levels are thought to be responsible for the alteration of the GABAergic responses from excitatory (early neural development) to inhibitory (maturity). This shift in the function of $GABA_ARs$ is essential for structural and functional maturation of neurons (*Tozuka et al. 2005*; *Ge et al. 2006*; *Cancedda et al. 2007*) as well as for termination of interneuron migration in the developing neocortex (*Bortone and Polleux 2009*).

1.3.7.1. Phasic and tonic inhibition

As mentioned above, $GABA_ARs$ mediate two distinct forms of inhibition. It is the subunit composition of $GABA_ARs$ that dictates their localization not only between brain regions but also within a neuron, which in turn determines the functional properties of the receptor. In that sense, receptors found in the postsynaptic density ($\alpha1\text{-}3\beta\gamma$) have EC_{50} (half maximal Effective Concentration) of ~6-14 μM whereas for peri- and extrasynaptic receptors ($\alpha4\beta\delta$, $\alpha5\beta\gamma$, $\alpha6\beta\delta$) the EC_{50} is approximately 0.5 μM. Hence, synaptic receptors mediate phasic inhibition (fast IPSPs) and extrasynaptic receptors that are continuously exposed to low concentrations of residual GABA, generate persistent tonic inhibition (*Farrant and Nusser 2005*).

Phasic activation of $GABA_ARs$ at the postsynaptic density is generated in response to action potential (AP)-induced and spontaneous quantal GABA release. That is, upon the arrival of an AP

at the nerve terminal, there is an influx of Ca^{2+} that triggers the fusion of synaptic vesicles with the presynaptic membrane and the consequent release of tens of thousands of GABA molecules into the synaptic cleft, thus generating a peak of GABA concentration in the millimolar range (*Mody et al. 1994*). On the other site of the synapse, at the postsynaptic density, a small number of receptors (from ten to few hundred) are clustered together (*Edwards et al. 1990*; *Mody et al. 1994*; *Nusser et al. 1997*; *Brickley et al. 1999*). These receptors undergo saturation even if only one neurotransmitter vesicle is released from the presynaptic neuron. For this reason, the amplitudes of IPSCs (Inhibitory Postsynaptic Currents) depend more on the number of $GABA_AR$ available for activation rather than on the amount of GABA release. Often multiple GABA vesicles are released from the presynaptic neuron in response to an AP generating spontaneous IPSC (sIPSC). However, sometimes single vesicles can be liberated without the need of an AP to generate miniature IPSC (mIPSC). The IPSC is finished within milliseconds due to the removal of GABA from the synapse by either diffusion or active transport. GABA that escapes from the synapse is further retaken by active transporters into neurons and astrocytes (*Glykys and Mody 2007a*). These transporters consist of high-affinity Na^+/Cl^- dependent membrane translocators of GABA and belong to the SLC6 family (*Chen et al. 2004*). Among them, the GABA transporter GAT-1 (SLC6A1) is the most common in neurons (*Glykys and Mody 2007a*). Due to their intrinsic capacity of regulating ambient GABA concentrations, GAT transporters become relevant modulators of GABA tonic currents. A second factor that contributes to the short lasting of the IPSC is the desensitization of the $GABA_ARs$ due to high agonist concentrations (*MacDonald and Twyman 1992*). In the state of desensitization, a $GABA_AR$ remains closed even when the agonist GABA is still bound. This phenomenon is important because of the high concentrations of GABA present at the synapses (*Jones and Westbrook 1996*).

Notably, if multiple synapses are triggered at the same time or if there is a repeated AP firing, it is possible that there is a large increase in the amount of released GABA, promoting its diffusion to peri- and extrasynaptic spaces or even to neighboring synapses (*Kullmann 2000*; *Farrant and Nusser 2005*). This phenomenon is known as neurotransmitter "spillover" and it is important to remark that the currents resulting from GABA spillover must still be considered phasic since they are temporally related to the release event (*Farrant and Nusser 2005*).

Residual GABA (100 nM – 2 μM) at the extracellular space is able to activate peri- and extrasynaptic $GABA_AR$ generating tonic currents. Tonic inhibition is responsible for 75% of the total inhibition currents received by hippocampal neurons (*Mody and Pearce 2004*). Different studies have shown that GABA-mediated tonic currents exist in granule cells of the dentate gyrus (*Nusser and Mody 2002*), thalamocortical relay neurons of the ventral basal complex (*Porcello et al. 2006*), layer V pyramidal neurons in the somatosensory cortex (*Yamada et al. 2007*), CA1 pyramidal cells and certain inhibitory interneurons in CA1 region of the hippocampus (*Bai et al.*

2001). However, the origin of the extracellular GABA is not well understood. Apart from GABA from spillover, Glykys and Mody showed that it could come from reversal of GATs (*Glykys and Mody 2007b*). Moreover, Liu et al. observed that GABA coming from astrocytes was also able to activate extrasynaptic currents since embryonic neurons co-cultured with astrocytes showed GABA tonic currents that were absent when no astrocytes were present (*Liu et al. 2000*).

1.3.8. Regulation of the $GABA_A$ receptors and their relation to diseases

1.3.8.1. Alterations in extrasynaptic $GABA_A$ receptors

Major changes in the $GABA_AR$ subunit expression patterns occur during development (*Laurie et al. 1992*). Nevertheless, the adult brain can suffer several changes in the expression of receptor subunits. The subunit composition of $GABA_ARs$ in each cell type, and as a consequence the function of the receptors, is determined by the expression levels of each subunit gene. Several physio- or pathological conditions can alter subunit levels.

Neurosteroids are steroid derivates that can be synthesized either in neurons and glia or in gonads and adrenals. This family comprises THP (3α-OH-5α-pregnan-20-one, allopregnanolone), which can selectively modulate the activity of $GABA_ARs$, specifically extrasynaptic $GABA_ARs$. During puberty in female mice, there is an increase in α4βδ $GABA_AR$ subtype in CA1 pyramidal neurons promoted by the rising levels of 17β-estradiol (E_2) and the decline in hippocampal levels of THP (*Keating et al. 2019*). However, in stress situations there is a release of THP that in pubertal female mice generates anxiety whereas it has an anxiety-reducing effect in adults by a mechanism that involves the downregulation of α4β2δ $GABA_ARs$ (*Shen et al. 2007*). Besides, THP is able to reduce the learning diminution that takes place at the onset of puberty by inhibiting α4β2δ $GABA_ARs$ (*Shen et al. 2010*). At the end of pregnancy, there is an increase in the expression of the δ subunit of the $GABA_ARs$ while the levels of γ2 subunit decrease and α4 subunit levels remain constant in the rat hippocampus (*Sanna et al. 2009*). Additionally, there is an increase in α4 subunit after delivery (*Sanna et al. 2009*). In a rat model of premenstrual syndrome, α4β2δ receptors are overexpressed at the hippocampus due to progesterone withdrawal. In this model, low doses of alcohol enhances $GABA_ARs$ function and decreases neuronal excitability (*Sundstrom-Poromaa et al. 2002*).

Ethanol is a depressant of the CNS that exerts behavioral effects similar to those promoted by other agonists of the $GABA_ARs$ such as benzodiazepines and barbiturates. The effects of ethanol on $GABA_ARs$ was reviewed by Davies and co-workers (*Davies 2003*). Extrasynaptic $GABA_AR$ are enhanced by ethanol concentrations lower than 30 mM (approximately the concentration achieved by social drinking) (*Sundstrom-Poromaa et al. 2002*; *Wallner et al. 2003*; *Wei et al.*

2004; *Hanchar et al. 2005*). Moreover, heterologous α4/α6 plus δ subunits containing $GABA_A$Rs are potentiated by concentrations of ethanol of 1-3 mM, which corresponds to less than a half glass of wine (*Sundstrom-Poromaa et al. 2002*; *Wallner et al. 2003*). In contrast, mice deficient in δ subunit of the $GABA_A$R showed diminished potentiation of tonic inhibition promoted by ethanol (*Wei et al. 2004*).

Besides, $GABA_A$Rs expression is altered in several pathologies, including depression and epilepsy. In humans, different studies with postmortem brains have described significant changes in subunit gene expression in depressed patients and suicide victims (*Klempan et al. 2009*; *Sequeira et al. 2009*). Such changes result in an alteration in the composition of $GABA_A$Rs which leads to the GABAergic deficit observed in major depression (*Luscher et al. 2011*). Epilepsy is a chronic disease characterized by seizures evoked by excessive electrical discharge of neurons in the brain (*Hesdorffer et al. 2013*). The term used to describe the complex process of acquired epilepsy development is termed "epileptogenesis" and pictures the plastic progression from a well neuronal excitation/inhibition balanced brain into a hyperexcitable brain. $GABA_A$Rs have been largely studied in both epileptic patients and epileptic animal models. In that sense, prolonged seizures (status epilepticus or SE) result in alterations in the expression and membrane localization of several $GABA_A$R subunits in hippocampus (*Brooks-Kayal et al. 1998*; *Peng et al. 2004*; *Zhang et al. 2007*). Structural and functional changes on $GABA_A$Rs have been described in neurons from surgically resected hippocampi from patients with intractable temporal lobe epilepsy (TLE) (*Brooks-Kayal et al. 1998*; *Shumate et al. 1998*; *Loup et al. 2000*). In addition, $GABA_A$Rs from TLE neocortex present a marked GABA-induced current run-down upon repetitive stimulation with GABA (*Goodkin et al. 2007*), which reflects $GABA_A$Rs instability and the desensitization of the receptor due to the shift of the $GABA_A$R-associated channel from an open to a desensitized state (*Sullivan 1992*). This mechanism is inhibited by BDNF (*Palma et al. 2005*) and phosphatase inhibitors (*Palma et al. 2004*). Further, Palma and co-workers demonstrated that this $GABA_A$-current run-down can actually be blocked by the antiepileptic drug levetiracetam (*Palma et al. 2007*). Thus, these results suggest that targeting $GABA_A$R activity could be a good strategy in the development of antiepileptic drugs.

In a mouse model of TLE, δ subunit expression decreases progressively after the pilocarpine-induced SE, while the expression levels for α4 and γ2 subunits increase over the same time course (*Peng et al. 2004*). This change in the expression pattern is thought to be due to the competition between δ and γ2 for their binding to α4 in the forebrain and with the α6 subunit in the cerebellum (*Tretter et al. 2001*). Notably, other studies done in experimental TLE found an increase in the expression of α3 α4, and δ subunits following the pilocarpine injection (*Schwarzer et al. 1997*; *Brooks-Kayal et al. 1998*; *Fritschy et al. 1999*). In a model of TLE in adult rats at the

time of the first pilocarpine-induced seizure, there is a significant reduction of the α1 subunit and increase in α4 subunit density that correlates with an enhancement of $GABA_A$-current run-down (*Mazzuferi et al. 2010*). In the pilocarpine model of SE, $GABA_AR$ α1 subunit mRNA decreases while α4 subunit mRNA expression increases in dentate granule cells of the hippocampus and animals go on to develop epilepsy. These changes in subunit mRNA levels correlate with decreased presence of α1βγ2 containing receptors (*Lund et al. 2008*) and increased presence of α4βγ2 containing receptors localized perisynaptically (*Zhang et al. 2007*; *Lund et al. 2008*; *Rajasekaran et al. 2010*). The change in receptor subtype from α1βγ2 to α4βγ2 may contribute to epileptogenesis, as α4 containing $GABA_ARs$ have been shown to desensitize rapidly, especially when assembled with β3 subunit (*Lagrange et al. 2007*). In primary cultured hippocampal neurons, transcriptional up-regulation of the α4 subunit gene after seizure is regulated by the PKC pathway, more specifically through the binding of the inducible early growth response factor (Egr3), whose mRNA levels also increase (*Roberts et al. 2005*; *Grabenstatter et al. 2014*). Additionally, inferior colliculi of both Wistar audiogenic rats (WAR) and the genetic audiogenic seizure hamster (GASH:Sal) present higher Egr3 gene expression than control animals (intact Wistar rats and Syrian hamsters respectively).

Different transgenic mice have been designed to bring about new insights on tonic inhibition. For instance, mice lacking the δ subunit of the $GABA_AR$ was first introduced in 1999 (*Mihalek et al. 1999*). $GABA_ARs$ deficient in δ subunit present lower affinity for the GABA agonist muscimol than WT mouse receptors. Moreover, δ KO mice show decreased sensitivity for anesthetic and anxiolytic drugs and are more exposed to the chemoconvulsants seizures caused by $GABA_AR$ antagonist. Also, $GABA_ARs$ without δ subunits are less sensitive to the action of neurosteroids and this fact can count for their increased susceptibility to seizure (*Mihalek et al. 1999*; *Spigelman et al. 2002*; *Porcello et al. 2003*; *Chandra et al. 2010*). Furthermore, mice lacking α4 have also been designed. In global α4 KO mice, there is a reduction of the inhibitory tonic currents in thalamus and dentate gyrus, as well as decreased gaboxadol sensitivity (*Chandra et al. 2006*). Importantly, α4 KO mice have defective migration and altered dendritic maturation in adult hippocampal neurogenesis (*Duveau et al. 2011*). β3 KO mice, on the other side, exhibit abnormalities in social and exploratory behavior and deficits in non-selective attention along with cerebellar vermis hypoplasia, all of them features associated with autism spectrum disorder (ASD) Moreover, large maternal deletion from UBE3A to GABRB3 genes (located on chromosome 15q11 and 15q13) causes impairments in motor function, learning and memory tasks related to the Angelman syndrome (*Jiang et al. 2010*).

1.3.8.2. Genetics of epilepsy

The development of epilepsy is, in part, due to alterations in the composition and function of $GABA_A$Rs that generate dysregulation of the neuronal activity. Genetic epilepsies are those caused by mutations in genes that modulate either activation or inhibition of the CNS. $GABA_A$R subunits can suffer mutations and lead to epileptogenesis. Notably, mutations in the α1 subunit encoding gene (GABRA1) and the gene coding for the β3 subunit (GABRB3) are related to childhood absence epilepsy (CAE) and juvenile myoclonic epilepsy (JME). Otherwise, mutations in the genes encoding the γ2 and δ subunits (GABRG2 and GABRD respectively) are associated with febrile seizures (FSs), generalized epilepsy with FS plus and Dravet syndrome (DS) (*Chuang and Reddy 2018*). Mutations in the genes coding for both synaptic and extrasynaptic $GABA_A$Rs subunits are reviewed by Galanopoulou, Chuang and Reddy (*Galanopoulou 2010*; *Chuang and Reddy 2018*). Here, we will focus on those mutations altering both GABRA4 or GABRB3 expression and/or function.

Concerning GABRB3 gene, 13 single nucleotide polymorphisms (SNP) are found in the promoter region causing diminished expression of the GABRB3 expression, a fact that has been related to CAE (*Feucht et al. 1999*; *Urak et al. 2006*; *Lachance-Touchette et al. 2010*). In exon 1, which codes for the signal peptide, two missense mutations (P11S and S15F) have been described (*Tanaka et al. 2008*) in families with remitting CAE. Another missense mutation in exon 2 (G32R) has been detected in CAE patients. This mutation causes a shift from αβ3γ2 receptors to αβ3 and β3 receptors and a consequent decrease in $GABA_A$R current density (*Gurba et al. 2012*). Experiments done with recombinant receptors containing these mutations suggest a possible mechanism because β3, when mutated is hyperglycosylated and that impedes the maturation and trafficking of the subunit thereby affecting $GABA_A$R function (*Tanaka et al. 2008*). In regard to GABRA4 gene, a polymorphism (T320A) has been described in idiopathic generalized childhood absence epilepsy although this polymorphism has also been observed in control patients (*Dibbens et al. 2009*). Nevertheless, different SNPs of the GABRA4 gene have been described in autism patients (*Ma et al. 2005*; *Collins et al. 2006*)

1.3.9. Regulation of $GABA_A$R activity through phosphorylation

The activity of $GABA_A$Rs can be regulated by several post-translational modifications such as phosphorylation that alter not only the number and localization but also the functionality of the receptor (reviewed in Connelly et al. 2013; Nakamura et al. 2015). These phosphorylations mainly occur in the major intracellular loop between TM3 and TM4 of the $GABA_A$R, which contains numerous consensus sites for tyrosine and serine/threonine (S/T) kinases. Although most phosphorylations target β and γ subunits, in the last decade several phosphorylation sites have

been identified on α subunits. Different kinases are known to phosphorylate $GABA_AR$ subunits, including PKA, PKC and CaMKII.

The S/T kinase PKA can either enhance or depress $GABA_AR$ function through the phosphorylation of its subunits. PKA is recruited by the A-kinase anchoring protein (AKAP) to $GABA_ARs$ containing either β1 or β3 subunits. PKA can phosphorylate β1 subunit on S409 inhibiting $GABA_AR$ function while the PKA phosphorylation of β3 subunits on S408 and S409 potentiates the activity of the receptor. Accordingly, mutation of S408 to alanine (S408A) in β3 subunit decreases $GABA_AR$ function at the same level as the β1 monophosphorylation on S409. By contrast, β2 subunit is not affected by PKA phosphorylation probably because it cannot bind AKAP. The effect of the β3 phosphorylation on the spontaneous activity of the extrasynaptic receptors is different depending on the subunit combination. Thus, the effect of PKA activation on α4β3δ is larger than for α4β3γ2 receptors. Nevertheless, it seems that PKA can function both as an activator and as an inhibitor of $GABA_AR$ activity depending on the cell context. For instance, in hippocampal pyramidal cells, cultured cerebellar granule cells, neostriatal neurons, superior cervical neurons and spinal cord neurons, PKA activation is to decreases $GABA_ARs$ function whereas in hippocampal dentate granule cells, cerebellar interneurons and olfactory bulb granule cells increases $GABA_ARs$ activity. Specifically, the activation of the PKA increases spontaneous α4β3δ and γ2 $GABA_AR$ currents (*Tang et al. 2010*).

PKC also has different effects on the $GABA_ARs$ depending on their subunit composition. PKC can phosphorylate S409/410 in β1-2 subunits, S408/409 in β3 subunit, S327 in γ2S/γ2L subunits and S343 in γ2L subunit. As noticed before the effect of the phosphorylation on the $GABA_AR$ can vary. Thus, in *Xenopus* oocytes the phosphorylation of γ2 on S343 increased the activity of the receptor while in fibroblasts expressing α1β1γ2L the constitutively activation of PKC results in a reduction of the $GABA_AR$-mediated currents. Actually, mutating γ2L S327 and S343 into alanine (S327A and S343A) prevents the enhancement of the $GABA_AR$ activity. In acute hippocampal slices, PKC inhibition leads to lower levels of β3-containing $GABA_ARs$ at the cell surface and to diminished tonic currents attributed to the lower levels of β3 phosphorylation on S383 (*Modgil et al. 2017*). In hippocampal pyramidal cells, PKC has no influence on mIPSCs while in dentate gyrus granule cells PKC enhances mIPSC amplitude. Besides, PKC can also phosphorylate α4 subunit on S443. Studies in COS7 cells show an enhancement of the α4 phosphorylation after phorphol 12-myristate 13-acetate (PMA)-induced PKC activation that results in an increase in the surface levels of α4β3 receptors. Consistently, the expression of the phosphomimetic mutant (S443E) showed that the accumulation of α4β3 was due to both increased stability and enhanced insertion levels at the cell surface. Opposing effects are observed in HEK293 cells expressing

heterologous α4β2δ receptors in which the activation of PKC decreased the surface levels of $GABA_A$Rs. This effect was accompanied by a reduction in GABA-mediated tonic inhibition. Tonic inhibition mediated by α4β2δ $GABA_A$Rs is modulated in a similar manner by PKC-dependent phosphorylation in the hippocampus and in the thalamus while phasic inhibition seems to be insensitive (*Bright and Smart 2013a*). In hippocampal neurons, PKC inhibition prevents α4 phosphorylation and surface expression of α4-containing receptors, apparently at odds with what happens at synaptic $GABA_A$Rs (*Connolly et al. 1999*; *Abramian et al. 2014*). Reassuringly, PKC activators were not able to potentiate surface expression or currents in cell lines expressing an α4 non-phosphorylatable mutant (S443A).

CaMKII can phosphorylate β3 subunit on S383 and in neuroblastoma-glioma hybrid (NG108-15) cells expressing α1β3 and α1β3γ2 receptors this phosphorylation potentiated GABA-evoked current amplitudes. Besides, the same group showed that the enhancement of GABA-evoked currents was also due to the phosphorylation of γ2 subunit on residues Y365/Y367 by endogenous tyrosine kinases indicating that the activation of CaMKII enhances GABA-evoked currents not only by direct phosphorylation of β3 subunit but also through the activation of tyrosine kinases that phosphorylate γ2 subunit. In hippocampal neurons, CaMKII phosphorylation of β3 on S383 induces de rapid surface expression of $GABA_A$Rs leading to an increase in the tonic currents (*Saliba et al. 2012*).

1.3.9.1. $GABA_A$ receptor run-down regulation by phosphorylation

The run-down of the GABA response is a phenomenon in which the repeated exposure of the receptor to GABA results in a gradual decrease of the resulting currents. In electrophysiology, GABA receptor run-down can be measured and it is used to evaluate the activity of the receptor.

It is well known that the phosphorylation of receptor subunits influences in its activity, including receptor run-down (*Kittler and Moss 2003*). In HEK293, neurosteroids enhance the GABA-mediated currents by promoting PKC phosphorylation of S443 in α4 subunit. This effect is also observed in hippocampal neurons, where the application of THDOC selectively enhances GABA-mediated tonic currents (*Abramian et al. 2014*).

Also, GABA run-down has been prevented or decreased by the inclusion of Mg-ATP or Mg-ATPγS in the intracellular solution of the whole-cell patch clamp recordings in pyramidal cells dissociated from the hippocampus of mature guinea-pigs, suggesting that receptor run-down may be a consequence of dephosphorylation of some targets closely associated with the $GABA_A$R (*Chen et al. 1990*).

1.3.9.2. Dysregulation of $GABA_A$ receptor phosphorylation in epilepsy

Epilepsy appears due to the imbalance between excitatory and inhibitory neuronal signaling. In that manner, alterations in $GABA_AR$ expression, trafficking and activity can lead to epileptogenesis. Since many $GABA_AR$ subtypes are regulated by phosphorylation, modifications in the phosphorylation pattern of the subunits are often related to epilepsy. Thus, in a model of pilocarpine-induced SE there is a decrease in the PKC-mediated β3 phosphorylation on S383, which is responsible for the loss of $GABA_ARs$ via enhanced endocytosis. Also in pilocarpine-treated rats, at the time of the first spontaneous seizure, there is an increased run-down in the hippocampus probably due to an increase in α4-containing receptors relative to α1-containing $GABA_ARs$.

The efficiency of $GABA_ARs$ in epileptic patients is often studied by injecting membranes from human nervous tissue into oocytes and then performing electrophysiological recordings are done. Results obtained with this model also show the relevance of $GABA_AR$ subunit phosphorylation in epilepsy since $GABA_ARs$ from the TLE temporal neocortex exhibit a marked current run-down. Besides, Palma et al showed that the inhibition of phosphatases stabilizes the epileptic $GABA_AR$ and enhances GABA inhibition in oocytes injected with TLE membranes (*Palma et al. 2004*). In this study, these authors also demonstrate that okadaic acid inhibition of protein phosphatases results in hyperphosphorylation of the β3 subunit, yielding an enhanced activity of the $GABA_AR$. In the same model, it was later demonstrated that $GABA_ARs$ run-down is also prevented by BDNF (*Palma et al. 2005*).

HYPOTHESIS AND OBJECTIVES

2. HYPOTHESIS AND OBJECTIVES

2.1 Hypothesis

Ccnd1 is required for NGF-induced neurite outgrowth in PC12 pheochromocytoma cells, is detected in the cytoplasm of cortical neurons at 4 days of *in vitro* differentiation, and mice without Ccnd1 show neurological abnormalities. Moreover, CCND1 mRNA has been abundantly detected by *in situ* hybridization in the adult mouse brain, specifically enriched in the hipoccampus, as well as in the adult human brain in different regions by DNA microarray expression profiling. And in a two hybrid screen previously carried out in our lab, Ccnd1 was found to interact with the α4 subunit of the GABA type A receptor.

Hence our hypothesis is that Ccnd1 may have a role, likely a cytoplasmic function, both during the development of the central nervous system and in the normal physiology of the adult brain. More specifically we want to test in this study whether the process of neuritogenesis may be modulated by Ccnd1 and whether Ccnd1 may be involved in the regulation of the GABA receptors.

2.2 Objectives

In order to elucidate the hypothesis, the study was divided in two main objectives These general objectives may be broken down into more specific ones.

I. Study of the role of cytoplasmic Ccnd1 in neuritogenesis in embryonic cortical neurons.

1. Evaluation of the overexpression of cytoplasmic Ccnd1 in neurite outgrowth in cultured cortical neurons.
2. Analysis of the effect of endogenous Ccnd1 downregulation in neuritogenesis.
3. If a role of Ccnd1 in neuritogenesis is uncovered, we will test paxillin as a possible downstream effector.

II. Dissection of the role of cytoplasmic Ccnd1 in the regulation of $GABA_A$ receptors

1. Defining the interaction between Ccnd1 and the α4 and β3 subunits of the $GABA_A$ receptor by *in vitro* and *in vivo* assays.
2. Characterization of the α4 and β3 subunits of the $GABA_A$ receptor as phosphorylation substrates of Ccnd1-Cdk4.
3. Examining functional effects mediated by cytoplasmic Ccnd1 on heterologously expressed $GABA_A$ receptors by electrophysiology in tsA201 cells.
4. Analysis of functional effects mediated by the Ccnd-Cdk4/6 complex on GABA receptors by electrophysiology in rat hippocampal slices.
5. Study of the regulation of α4 and β3 subunits trafficking and cell surface abundance by cytoplasmic Ccnd1.

MATERIALS AND METHODS

3. MATERIALS AND METHODS

3.1 Molecular biology techniques

3.1.1. Plasmid constructions

Coding sequences and fusion proteins of interest are cloned into pcDNA3, pCMV-SPORT6 or pNBM470 (as pcDNA3 but with N-terminal 6His-3HA epitopes). These vectors contain the CMV promoter, although sometimes this promoter is changed to the polyubiquitin C gene promoter (Ubi) (Table 1).

Site-directed mutagenesis (PCR-SDM) follows a previous protocol (Weiner et al. 1994) with some modifications. We have developed a facile procedure for rapid PCR-based site-directed mutagenesis of double-stranded DNA. Increasing the initial template concentration and decreasing the PCR cycles to 5-10 allows us to reduce the rate of undesired second-site mutations and dramatically saves time. Following PCR, DpnI treatment is used to select against parental DNA molecules since DpnI only cuts methylated or hemimethylated DNA, which comes from bacteria. Pfu DNA polymerase is used, prior to intramolecular ligation of the linear product, to remove any bases extended onto the 3' ends by the Taq DNA polymerase. The recircularized DNA vector incorporating the desired mutations is transformed into *E. coli*. This method can be used independently of any host strain and vector. When possible, a restriction site is generated at the mutation point so that it is possible to track the mutation and select the mutant clones.

Both cyclin D1 wild type and the cyclin D1 K112E allele are fused to three copies of the FLAG or HA epitopes under the CMV promoter in pcDNA3. Cyclin D1 K112E is a point mutant of cyclin D1 that contains a lysine to glutamic acid substitution at amino acid position 112. This mutant binds Cdk4/6 with an affinity similar to that of wild type cyclin D1, but it is unable to activate the catalytic activity of the partner kinase and cannot transform primary rodent cells (*Hinds et al. 1994*; *Baker et al. 2005*). To construct the variants of cyclin D1 associated to the membrane, the 3'coding sequence of the K-Ras gene, which contains the CAAX motif (GGC TGT GTG AAA ATT AAA AAA TGC ATT ATA ATG TAA) is fused to the 3' end of the coding sequence of either cyclin D1 or cyclin D1 K112E (*Fusté et al. 2016*).

Mus musculus GABRA4 (IMAGE ID 6828002, BioScience) and *Homo sapiens* GABRB3 (IMAGE ID 3871111, BioScience) are used to obtain a GST fusion protein in pGEX-KG (Clontech). Moreover, in some cases those proteins are tagged with either the FLAG or GFP epitope. GST-GABRA4 contains the full-length protein, while GST-C-terminus contains the sequence corresponding to amino acids 354 to 552.

GABRA4 cDNA is also cloned into the pEGFP-N1 mammalian expression vector to generate a GFP fusion protein. PCR-SDM is carried out to produce the non-phosphorylatable and the phosphomimetic mutants.

For cyclin D1 downregulation with interference ARN, shRNA TRCN0000026883 cloned into pLKO.1-puro is purchased from Sigma- Aldrich.

Plasmids are isolated from cultures of *E.coli* DH5α using a miniprep plasmid purification kit (Qiagen) according to manufacturer's instructions and are outlined in Table 1. To test integrity, DNA is subjected to agarose gel electrophoresis and to ethidium bromide (EtBr) staining. DNA concentration is determined with a spectrophotometer NanoDrop ND-1000 (NanoDrop Technologies). Constructions are checked by restriction analysis and the expressed proteins are checked by Western blotting. Mutations created by PCR-SDM are also checked by DNA sequencing.

Table 1. List of the plasmids used in this thesis.

NAME	PLASMID VECTOR	DESCRIPTION
pcDNA3	CMVp-3FLAG	Expression vector with CMV promoter tagged with FLAG
pNBM470	pcDNA3-6His-3HA-MCS	Expression vector with CMV promoter tagged with 6His and 3HA.
pEGFP-N1	CMVp-EGFP	GFP containing expression vector with CMV promoter
pGEX-KG	pGEX-2T derivate	Bacterial expression plasmid containing GST. Tac promoter.
pCYC193	CMVp-pcDNA3-FLAG5'-Ccnd1	pcDNA3 vector containing Ccnd1 tagged with FLAG under CMV promoter.
pCYC2057	3HA-Ccnd1-CAAX	Mm Ccnd1-CAAX cloned into pNBM470 expression vector under CMV promoter. Tagged with 3HA
pCYC2058	3HA-Ccnd1^{K112E}-CAAX	Ccnd1^{K112E}-CAAX cloned into pNBM470 expression vector under CMV promoter. Tagged with 3HA
pCYC2076	Ubip-3HA-Cdk4-CAAX	MmCdk4-CAAX cloned into pPDSL. Contains Ubi promoter and 3-HA tag
pCYC2111	shRNA SCR (scramble)	Control vector shRNA SCR pLKO.1-puro (Sigma-Aldrich)
pCYC2136	Ccnd1 shRNA83	shRNA for *Mus musculus* cyclin D1 in pLKO.1-puro vector. TRCN0000026883 (Sigma- Aldrich)
pCYC2084	3HA-CBP-Pxn	Mm Pxn cloned into pPDSL. Contains Ubi promoter and 3HA and CBP tags
pCYC2104	3HA-CBP-Pxn (S83A; S178A; S244A)	Non-phosphorylatable mutant of Pxn cloned into pPDSL. Contains Ubi promoter and 3HA and CBP tags

NAME	PLASMID VECTOR	DESCRIPTION
GABRA4	Mm GABRA4	IMAGE ID 6828002, BioScience
pCYC2123	GABRA4 in pGEX-KG	Mm GABRA4 cloned into the pGEX-KG bacterial expression plasmid containing GST. Tac promoter
pCYC2153	GABRA4 T423A, S431A in pGEX-KG	Mutant Mm GABRA4 cloned into the pGEX-KG bacterial expression plasmid containing GST. Tac promoter
pCYC2155	GABRA4 S456A S458A in pGEX-KG	Mutant Mm GABRA4 cloned into the pGEX-KG bacterial expression plasmid containing GST. Tac promoter
pCYC2157	GABRA4 T500A in pGEX-KG	Mutant Mm GABRA4 cloned into the pGEX-KG bacterial expression plasmid containing GST. Tac promoter
pCYC2127	Cterminal-GABRA4 in pGEX-KG	C-terminal fragment of GABRA4 cloned into the pGEX-KG bacterial expression plasmid containing GST. Tac promoter
pCYC2237	GABRA4 C-terminal T423A S431A in pGEX-KG	Mutant Mm GABRA4 C-terminal fragment GABRA4 cloned into the pGEX-KA bacterial expression plasmid containing GST. Tac promoter
pCYC2206	GABRA4 in FCIV1	Mm GABRA4 into FCIV vector under Ubi-c promoter. Contains an IRES element driven venus protein
pCYC2207	GABRA4 T423A S431A in FCIV1	Mutant Mm GABRA4 into FCIV vector under Ubi-c promoter. Contains an IRES element driven venus protein
pCYC2224	GABRA4 T423E S431E in FCIV1	Mutant Mm GABRA4 into FCIV vector under Ubi-c promoter. Contains an IRES element driven venus protein
pCYC2121	GABRA4 in EGFP-N1	Mm GABRA4 cloned into pEGFP-N1. Contains GFP and CMV promoter
pCYC2183	Mm GABRA4 T423A, S431A in EGFP-N1	Mutant Mm GABRA4 cloned into pEGFP-N1. Contains GFP and CMV promoter
pCYC2261	Mm GABRA4 T423E, S431E in EGFP-N1	Mutant Mm GABRA4 cloned into pEGFP-N1. Contains GFP and CMV promoter
pCYC2213	GABRB3-FLAG in pBI-EGFP	Hs GABRB3 cloned into pBI-EGFP. Contains FLAG tag
GABRB3	Hs GABRB3	IMAGE ID 3871111, BioScience
pCYC2181	GABRB3 in pGEX-KG	Hs GABRB3 cloned into the pGEX-KG bacterial expression plasmid containing GST. Tac promoter
pCYC2275	Hs GABRB3 in EGFP-N1	Hs GABRB3 cloned into pEGFP-N1. Contains GFP and CMV promoter

3.1.2. RNA extraction and RT-qPCR

Ccnd1 mRNA levels are analyzed by performing an mRNA extraction protocol from mice embryonic cortical neurons followed by RT-qPCR. To this end, cortical neurons are obtained as described in 3.2.2 and collected at different time points (0 hours, 4 hours, 1 day or 3 days) of *in vitro* differentiation in RLT buffer of the RNeasy Mini Kit (QIAGEN) containing β-mercaptoethanol. Samples are stored at -80ºC until RNA extraction is carried out using this kit and following the manufacturer's instructions. Afterwards, samples are treated with the On-Column DNase I Digestion Set from Sigma. RNA integrity and purity are measured by agarose gel electrophoresis and NanoDrop ND-1000 spectrophotometry (NanoDrop Technologies). For retrotranscription, up to 5 μg of RNA are converted into cDNA with the SuperScript Reverse Transcriptase (Thermofisher) using random hexamers as oligonucleotides. The reaction is performed according to manufacturer's instructions. This cDNA obtained is used for qPCR. In this case, samples are added to a SYBR Green master mix (Applied Biosystems™ SYBR™, Thermofisher) together with both the forward and reverse primers (see Table 2). As an internal control, the house keeping gene GAPDH is amplified and quantified. qPCR is performed in the C1000 Thermal Cycler CFX96 Real-Time System from Bio-Rad Laboratories. A scheme of the conditions used for the qPCR is shown in Figure 6.

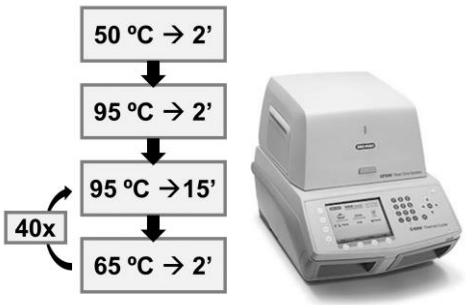

Figure 6: Scheme of the conditions used for qPCR.

Table 2: Primers used in qPCR.

TARGET	DIRECTION	DESCRIPTION	SEQUENCE (5' – 3')
CCND1	Forward	To amplify Mm CCND1 (183bp). Tm: 62.5 (exon1-2)	GCGTACCCTGAC ACCAATCTC
	Reverse	To amplify Mm CCND1. Tm: 62.4 (exon1-2)	CTCCTCTTCGCAC TTCTGCTC
GAPDH	Forward	To amplify Mm GAPDH (123bp). Tm: 62.6 (exon1-2)	AGGTCGGTGTGA ACGGATTTG
	Reverse	To amplify Mm GAPDH. Tm: 60.2 (exon1-2)	TGTAGACCATGT AGTTGAGGTCA

3.2 Cellular biology techniques

The different cell types, both primary and cultured lines, used in this thesis are listed in Table 3.

Table 3: Mammalian cell types used in this study.

Cell type	Description	Obtained from	Use
HEK293T	Human Embryonic Kidney cells	American Type Culture Collection (ATCC)	Used for virus production, immunoprecipitation assays and immunofluorescence
HEK tsA201	Human Embryonic Kidney SV40 transformed cells	Dr. David Soto's lab	Whole-cell patch clamp studies
MEFs (immortalized)	Immortalized Mouse Embryonic Fibroblasts	Dr. Sicinsky's lab	Used for shRNA testing
Cortical neurons	Primary cortical neurons from mice E15.5 embryos	Mice embryos (E15.5)	Neuritogenesis studies and immunofluorescence
Hippocampal slices	Organotypic hippocampal slices	Newborn rats (P5-7)	Whole-cell patch-clamp recordings and western blot
Hippocampal cells	Whole hippocampus	Adult female mice	Immunoprecipitation

All centrifugations at 4 ºC are done using the F45-24-11 rotor (Eppendorf), centrifugations of cell cultures are done using the S-4-72 rotor (Eppendorf). For bacterial cultures centrifugation, the A-4-81 rotor (Eppendorf) is used.

3.2.1. Growing and harvesting cells

HEK and MEFs cells are sub-cultured when a cell density greater than 80% confluence is reached, every 3-4 days, cells are sub-cultured. In brief, the medium is aspirated and cells are washed in pre-warmed phosphate-buffered saline (PBS). To detach the cells from the plate, cells are then incubated with trypsin (Sigma) at 37ºC for 5 min. To inactivate trypsin, a 3-volume aliquot of pre-warmed medium is added. Cells are then collected and centrifuged at 1000 rpm for 5 min. Pelleted cells are resuspended in 1 ml medium and then a Neubauer chamber is used for cell counting when an accurate cell number for seeding is necessary. Alternatively, a 1:10 or 1:20 dilution (depending on cell type) is directly used. Cells are maintained in a wet atmosphere with 5% CO_2 at 37ºC. Mycoplasma detection tests are performed with PlasmoTest (Invivogen, code: rep-pt1)

For cell freezing, cells are harvested at 1000 rpm after trypsinization, and resuspended in 1 ml freezing medium (90% FBS+ 10% DMSO). Aliquots of approximately $1\text{-}2\cdot10^6$ cells are stored in 2 ml polypropylene vials, first at least 24 hours at -80ºC and then permanently in the gas phase of a liquid nitrogen vessel (at -180ºC). To unfreeze cells, they are rapidly thawed at 37ºC and then mixed with 9 ml DMEM (supplemented with 10% FBS + P/S). They are centrifuged at 1000 rpm for 5 min and resuspended in 1 ml medium. The whole aliquot is added to a 100 mm plate containing 9 ml DMEM (with 10% FBS, P/S), and incubated at 37ºC, 5% CO_2.

3.2.2. Primary culture of cortical neurons

Timed-pregnant females are killed by cervical dislocation, and embryos are removed at the appropriate age (embryonic day E15.5) and placed on ice-cold HBSS-MHPS (Hank's Balanced Salt Solution, 10 mM $MgSO_4$, 10 mM HEPES pH 7.2 adjusted with NaOH) and 10^4 U/L P/S. The E15.5 age is chosen because most cortical neurons are forming while the appearance of glial cells can be avoided (*Sciarretta and Minichiello 2010*). All the dissection protocol is done on ice in order to preserve the cells. The embryo heads are collected in fresh ice-cold HBSS-MHPS medium and then cortexes are obtained with the help of a magnifying glass (Leica Microsystems). Briefly, skulls are opened laterally, the two cortexes dissected and meninges removed. Dissected cortexes are placed in 10 ml Falcon tubes (maximum 8 hemicortexes per tube) containing 4 ml ice-cold HBSS-MHPS. After removing the medium, 1.5 ml freshly-prepared filtered papain solution (1 mg/ml papain in HBSS-MHPS) is added to each tube. We prepare a papain (Sigma-Aldrich) stock solution at 10 mg/ml in water and store it at 4ºC. For proper digestion and protein hydrolysis, tissue is incubated in a water bath at 37 ºC for 23 min. During the enzymatic digestion, two Pasteur pipettes are prepared to the flame for further triturating the tissue: one with the round rim (pipette A) and the other with the round rim but with smaller diameter (pipette B). After the incubation with papain, the enzyme is inhibited by washing the tissue three times with 1 ml of 10 mg/ml trypsin inhibitor (ThermoFisher) in HBSS-MHPS (filtered). Additionally, one more wash is done with 1 ml neurobasal medium supplemented with B27 (1:50), 2 mM Glutamax and 1 mM sodium piruvate (NB27, ThermoFisher) at room temperature. Another milliliter is added to each tube and tissue is triturated by passing it through the two pipettes (A and B) no more than 10 times each. After the mechanical disgregation, the supernatant of 1 min incubation containing mostly single cells is transferred to a Falcon tube with 9 ml NB27 medium and centrifuged at 650 rpm for 4 min. Next, the pellet is resuspended in 1 ml NB27 using the pipette B no more than 5 times.

If needed, cells are counted in a Neubauer chamber. Trypan Blue (1:1) is used to stain dead cells so that only living cells are counted. For biochemical studies as well as for transfections, high density cultures are needed. Given so, approximately $5.5\cdot10^4$ cells/cm^2 are seeded. On the other

hand, for conditioned medium production, low density cultures (3 cortexes in a 100 mm plate) are needed since they must be in the incubator for 7-10 days without refreshing the media. Following the incubation, the medium is filtered and stored at -20ºC.

For the seeding of the primary cortical neuron culture, Neurobasal medium with B27 supplements (1:50), 2 mM Glutamax and 1 mM sodium piruvate is used. However, when cells are transfected, NB27 medium is diluted 1:1 with conditioned media.

3.2.2.1. Genotyping and protein extraction from wild type and cyclin D1 knockout mice

CCND1 knockout mice were obtained from P. Sicinski (*Sicinski et al. 1995*) (Figure 7A). Transgenic mice are maintained in a mixed background of C57BL/6 and SV129. Ccnd1 KO embryos are obtained from the crossing of two heterozygotes of Ccnd1. In order to process all embryos of the same genotype together, it is necessary to differentiate between KO and WT embryos prior to the primary cortical neurons culture. To that end, embryo's tails are collected and warmed at 54 ºC in a solution containing genotyping buffer (100 mM Tris-HCl pH8.0, 50 mM EDTA pH8.0, 1% SDS, 500 mM NaCl) and proteinase K (20 mg/ml) for 20 minutes while shaking at 950 rpm with a Thermo-Shaker (Eppendorf). Dissolved tails are then centrifuged for 5 minutes at 10000 rpm. Supernatant is collected and heated at 65 ºC to inactivate the proteinase K. Next, DNA is precipitated with isopropyl alcohol, washed with 70% ethanol, and eventually resuspended in water.

Genotyping is performed by PCR using genomic DNA extracted from the tail (as described above) and three different primers: one hybridizes with a sequence of CCND1 gene present in both WT and KO mice (1) (5'-TAGCAGAGAGCTACAGACTTCG-3') (Integrated DNA Technologies); a second primer is targeted to the gene region removed in the knockout construct, hence it uniquely hybridizes with the WT gene sequence (2) (5'-CTCCGTCTTGAGCATGGCTC-3') and the third primer hybridizes with the neomycin-gen introduced during knockout construction (3) (5'-CTAGTGAGACGTGCTACTTC-3') (Sicinski et al. 1995). PCR is performed in a Thermal Cycler (T100 Bio-Rad) with the program showed in Figure 7C. PCR products are analyzed in a 1.5 % agarose gel. After running, gel is stained in an EtBr solution for 10 min and visualized with a UV light transilluminator. The expected band pattern for WT (224 bp), heterozygous (224 and 391 bp) and KO (391 bp) animals is shown in Figure 7B.

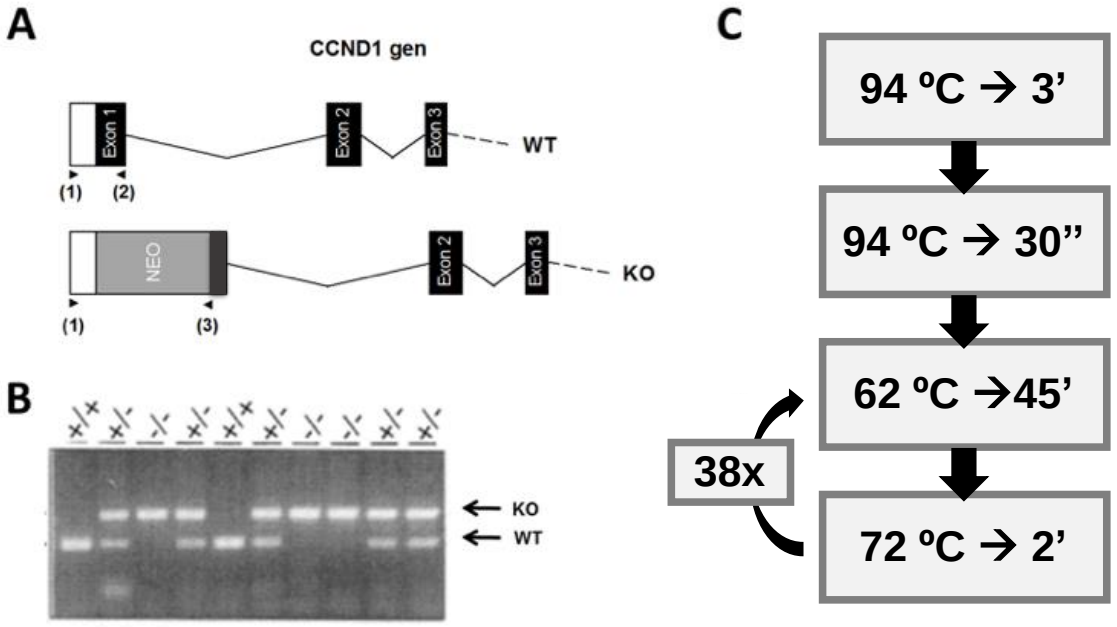

Figure 7: Disruption of CCND1 gene. A) Restriction map of Mm CCND1 and the structure of the mutated locus by homologous recombination. Black boxes show the coding exons numbered; open box represent the noncoding portion of the first exon. Arrows denote PCR primers (1, 2 and 3) used for genotyping the animals. **B)** PCR amplification products of DNA extracted from mouse tails. The sizes of amplification products of either WT or KO alleles are shown. The genotypes of the animals are represented above the lanes. Extracted from (*Sicinski et al. 1995*). **C)** Scheme of the conditions used for the PCR.

Moreover, Ccnd1 protein expression is confirmed by Western Blot. Protein extraction in this case, is performed from a paw of the animal which is introduced in 15 µl of urea with glass beads and 50 µl of 1x SR (2% SDS and 0.125 M Tris-HCl, pH adjusted to 6.8). The mix is vortexed and boiled at 95 ºC for 3 minutes. After that, sample is homogenized at high speed twice for one minute so that cells are broken (Minibead-beater-24, BioSpec). Finally, 25 µl of 1x SR are added and the supernatant is collected. The recovered volume (~40 µl) is mixed with 4xSS (20% sucrose and 0.02% bromophenol blue, 0.1% sodium azide) and 1% β-mercaptoethanol. Cyclin D1 levels in samples are analyzed by Western blot with a Ccnd1 antibody (see Table 5).

3.2.2.2. Plate coating for primary neuronal culture with poly-D-lysine and laminin

For the primary cortical neuron culture, it is necessary to coat the plates with filtered poly-D-lysine 0.5 mg/ml in borate buffer pH 8.4. After incubation at 37 ºC overnight (O/N), plates are washed three times with distilled water. For neuron transfections, plates are additionally coated with laminin (5 mg/ml in DPBS - Dulbecco's phosphate-buffered saline, Gibco). These plates are incubated at 37 ºC for at least 2 hours, and then they are washed three times with DPBS (Gibco) avoiding that the bottom of the plate dries up. Finally, 1:1 NB27 conditioned medium is added

and plates are left in an incubator until the moment of seeding the cells. In this way, a proper matrix is generated allowing the adherence of the cells.

3.2.3. Organotypic hippocampal slices preparation

Organotypic hippocampal slice cultures are prepared as previously described (Gähwiler et al, 1997) and shown in Figure 8. Briefly, newborn rats (postnatal days 5-7) are decapitated, and whole brains are dissected and placed in ice-cold Ca^{2+}-free dissection solution (10 mM D-glucose, 4 mM KCl, 26 mM $NaHCO_3$, 8% sucrose, 5 mM $MgCl_2$, 1:1000 Phenol Red) saturated with 5% CO_2 / 95% O_2, enabling the brain to chill for 1 min. Hippocampi are then isolated with the help of a magnifying glass, cut in slices (400 μm) in the same solution using a tissue chopper (Stoelting), and maintained at 35.5ºC in culture on semipermeable membranes in a medium containing 20% horse serum, 1 mM $CaCl_2$, 2 mM $MgSO_4$, 1 mg/l insulin, 0.0012% ascorbic acid, 30 mM Hepes, 13 mM D-glucose, and 5.2 mM $NaHCO_3$. Culture medium is replaced with fresh one every 2-3 days. The slices are used at 4-8 days i*n vitro*.

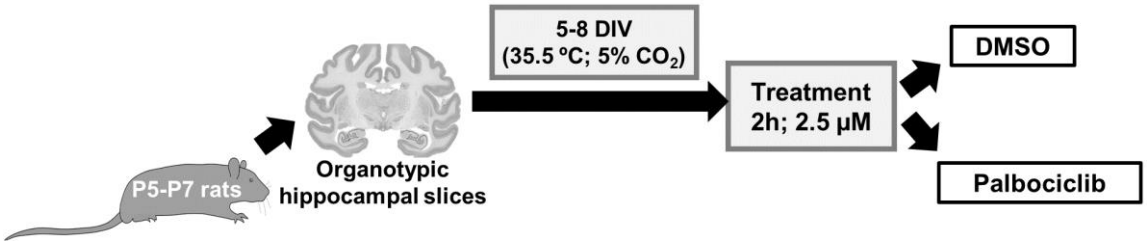

Figure 8: Scheme of the workflow followed for hippocampal slice preparation for whole-cell recordings.

3.2.4. Cell transfection

3.2.4.1. Lipofectamine 2000

For transient transfection of plasmid vectors, Lipofectamine 2000 (Invitrogen) transfection reagent is used. The day prior to transfection, cells are seeded in either 4-well plates (16 mm), 6-well dishes (35 mm), 60 mm or 100 mm plates. For HEK293T cells, plates are coated with 100 μg/ml collagen in 0.02 M acetic acid. Cells are transfected at ~70% confluency. For the amount of reagents, we follow manufacturer's recommendations (Table 4). The appropriate volume of Opti-MEM medium (GIBCO-Invitrogen) is mixed with DNA. Concurrently, Opti-MEM is mixed with Lipofectamine 2000 and incubated at room temperature for 5 min. Then, Lipofectamine mixture is added to the DNA mixture, gently mixed and left for 20 min at room temperature. During this time, cells are washed with Opti-MEM. The DNA – Lipofectamine mixture is then added to the

cells in a dropwise manner and gently swirled to mix. Cells are incubated at 37 ºC, 5% CO_2 for 15 min. Finally, transfection mixture is removed and DMEM (10% FBS, P/S) is added. Cells are grown at 37ºC, 5% CO_2 with humidity for a further 24 to 48 hours.

Lipofectamine 2000 reagent is also used for the "in tube" transfection of primary cortical neurons as long as this method guarantees a more efficient DNA entry to the cells (*Halterman et al. 2009*). In this case, 400 ng of DNA and 0.5 µl of Lipofectamine are mixed with 50 µl Opti-MEM for every $2 \cdot 10^5$ dissociated cortical neurons in 100 µl Neurobasal medium. Incubating times are the same as in HEK293 transfection, but cells must be incubated with the DNA – Lipofectamine mix for 40 min at room temperature prior to seeding. Plates are incubated 24 hours at 37 ºC and then used for different analyses.

3.2.4.2. Polyethylenimine

Polyethylenimine (PEI, Sigma-Aldrich) consists of a stable cationic polymer that is used to introduce DNA into a host cell, since it condenses the DNA into positively charged particles that bind to anionic cell surfaces (*Boussif et al. 1995*). As a consequence, the DNA:PEI complex is endocytosed by the cells and DNA is released into the cytoplasm.

Conditions prior to transfection are as described above for Lipofectamine 2000 in all respects. For the transfection procedure, 10 µM PEI and DNA are diluted separately in Opti-MEM (Table 4). After 5 min incubation, the diluted PEI is added to the diluted DNA and the mixture is incubated for 15 min at room temperature. During this time, cells are washed once with pre-warmed Opti-MEM and then, the PEI-DNA mixture is gently added to the cells. Plates are incubated for 1 hour at 37 ºC in the incubator. After this time, PEI-DNA mixture is removed from the cells and pre-warmed fresh medium (DMEM 10% FBS, P/S) is added. Finally, plates are placed at the 5% CO_2 incubator O/N. After 24-48 hours, cells are harvested and used for different analyses.

Table 4: Volumes of DNA, Opti-MEM, lipofectamine 2000 and PEI used for cell transfection in this thesis

PLATE (Ø)	DNA + Opti-MEM	Lipofectamine + Opti-MEM	PEI + Opti-MEM
16 mm	0.8 µg + 50 µl OPT	2 µl + 50 µl OPT	
23 mm	1,6 µg + 100 µl OPT	4 µl + 100 µl OPT	
35 mm	4 µg + 250 µl OPT	10 µl + 250 µl OPT	
60 mm	8 µg + 500 µl OPT	20 µl + 500 µl OPT	80 µl + 420 µl OPT
100 mm	24 µg + 1.5 ml OPT		240 µl + 1.26 ml OPT
150 mm	50 µg + 3.4 ml OPT		540 µl + 2.84 ml OPT

3.2.4.3. tsA201 cells transfection for electrophysiology

All electrophysiological experiments are done with mycoplasma-free tsA201 cells. This cell line (also known as HEK293T cells) is a transformed human kidney cell (HEK293) line stably expressing an SV40 temperature-sensitive T antigen, which produce high levels of recombinant proteins. tsA201 cells are kindly provided by Prof. F. Ciruela (Universitat de Barcelona) and purchased from the American Type Culture Collection (ATCC, CRL-3216, RRID: CVCL_0063). Mycoplasma detection tests are performed with PlasmoTest (Invivogen, code: rep-pt1).

Cells are transiently co-transfected with 1 μg total cDNA using polyethylenimine (PEI) transfection reagent (1 mg/ml) in a 3:1 ratio (PEI:DNA). In all transfections the DNA ratio used is 1:1:2 (plasmid A : plasmid B : plasmid C), where A is α4 or α4(T423E,S431E), B is β3: and C is CAAX or CAAX-Ccnd1 codifying plasmid. Cells are re-plated on poly-D-lysine coated glass coverslips to allow optimal density with isolated cells. All experiments are performed 48 h after transfection.

3.2.4.4. Electroporation

For faster expression, nucleofection is used. It applies an electrical pulse that allows DNA to enter directly into the nucleus. Specifically, for cortical neurons program 005-O of the Amaxa Nucleofector is used with its convenient electroporation solution (Ingenio, Mirus).

In the case of electroporation, $2 \cdot 10^6$ cells are centrifuged at 650 rpm for 4 min. Medium is removed, cells resuspended in 100 μl of electroporation solution, and 2 μg DNA added. This mix is then transferred to an electroporation cuvette and submitted to an electrical pulse. After that, 500 μl NB27 (37ºC) are added and cells collected and seeded in 4-well plates at a density of 10^5 cells/well (2 cm^2 area) and incubated at 37 ºC, 5 % CO_2 for 2 hours. Afterwards, transfection solution is removed and fresh medium at 37 ºC (1:1 conditioned medium: NB27) is added.

3.2.5. Competent cells transformation

Escherichia coli DH5α cells are thawed on ice and 1-50 ng DNA is added. Cells are incubated 30 for 30 min on ice. Subsequently, a heat-pulse at 42 ºC is done in a preheated water bath for 20 seconds. Reactions are then incubated on ice for 2 minutes and further 900 μl LB (Luria-Bertani medium) medium are added and incubated 1 hour at 37 ºC. Finally, using a sterile spreader, transformed cells are spread onto LB agar plates containing the appropriate antibiotic.

3.3 Microscopy techniques

3.3.1. Immunofluorescence

For protein detection by immunofluorescence, cells are fixed in the primary cortical neuron plate so that both the cellular and subcellular architecture are maintained. All solutions are filtered before use. First, cells are washed with cold PBS-MC (1 mM $MgCl_2$; 0.1 mM $CaCl_2$), and fixed by adding 4% PFA and 4% sucrose in PBS for 15 min (500 µl mix for a 2 cm^2 area well). Later, cells are washed with PBS and permeabilized with 0.1% Triton in PBS (300 µl mix for a 2 cm^2 area well) for 3 min. This step allows the entrance of the antibody into the cell. Subsequently, cells are washed with PBS and blocked with 3% Bovine Serum Albumin (BSA) for 30 min. This blocking step reduces the non-specific binding of the antibody. Primary antibody in 0.3% BSA in PBS is added to the sample and incubated at 4 ºC O/N at the concentrations indicated in the Table 5. The following day, wells are washed three times with PBS to remove unbound or weakly bound antibody. Primary antibodies are combined with the corresponding secondary antibodies labeled with Alexa488 or Alexa594 (Molecular Probes) diluted 1:1000 in 0.3% BSA in PBS, and incubated together with Hoechst (1:10000 Sigma-Aldrich) to stain the nuclei for 45 min at room temperature in the dark. Epifluorescence images are obtained with the objectives 10x and 20x of an inverted Olympus IX71 microscope and its Controller software. Confocal images are obtained with 40x and 60x objectives of the confocal microscope FV1000i (Olympus) and its Olympus Fluoview FV10-ASW4.1 Viewer. Table 5 lists primary antibodies. For neurite and axon length quantification, the NeuronJ plugin of the ImageJ software is used.

3.4 Biochemical analyses

3.4.1. Antibodies

Different antibodies have been used in several techniques such as immunofluorescence or Western blot. All primary and secondary antibodies used are listed in Table 5 and Table 6, respectively.

Table 5. List of primary antibodies employed and their experimental conditions in immunofluorescence, immunoprecipitation and western blot techniques.

ANTIGEN	BIOLOGICAL SOURCE	REFERENCE	CONCENTRATION OF USE	
			WESTERN BLOT	IMMUNO-FLUORESCENCE
α-Tubulin	Mouse monoclonal	Clone B-5-1-2, Sigma-Aldrich #T5168	1:10000	-
β-Actin	Mouse monoclonal	Clone AC-15, Sigma-Aldrich #A1978	1:4000	-

ANTIGEN	BIOLOGICAL SOURCE	REFERENCE	WESTERN BLOT	IMMUNO-FLUORESCENCE
Cyclin D1	Mouse monoclonal	Clone DCS-6, BD Pharmigen #556470	1:500	-
Cyclin D1	Rabbit monoclonal	Clone EP12, Dako #M3642	1:500	-
Cdk4	Rabbit polyclonal	Clone C-22, Santa Cruz Biotecnology #sc260	1:250	-
FLAG	Mouse monoclonal	Clone M2, Sigma-Aldrich #F3165	1:1000	-
FLAG	Rabbit polyclonal	Invitrogen #11508721	1:500	-
GABRA4	Rabbit polyclonal	AB5459, Sigma-Aldrich	1:1000	
GFP	Mouse monoclonal	Clone 13.1; Roche #11811460001	1:1000	
GFP	Mouse monoclonal	Clone 3E6, Invitrogen #A11120	-	1:200
GST	Goat polyclonal	GE Healthcare Life Sciences #27-4577	1:2000	-
HA	Rat monoclonal	Clone 3F10, Roche #11867431001	1:2000	1:200
Pxn	Mouse monoclonal	Clone 349; BD Transduction laboratories #610051	1:1000	-
Pxn phospho-Ser83	Rabbit polyclonal	ECM Biosciences #PP1341	1:500	-
Pxn phospho-Ser178	Rabbit polyclonal	Calbiochem #ST1069	1:500	-
TFRC	Mouse monoclonal	Clone H68.4; Invitrogen #13-6800	1:1000	-
Ubiquitin	Mouse monoclonal	Santa Cruz Biotecnology #sc8017	1:200	-

Table 6: List of secondary antibodies used in this thesis.

IMMUNOGEN	BIOLOGICAL SOURCE	REFERENCE	APPLICATION
Mouse IgG	HRP-linked whole Ab (from sheep)	GE Healthcare	Western blotting (1:10000)
Rabbit IgG	HRP-linked whole Ab (from donkey)	GE Healthcare	Western blotting (1:10000)
Rat IgG	HRP-linked whole Ab (from goat)	GE Healthcare	Western blotting (1:10000)
Mouse IgG	Alexa Fluor 488 conjugated antibody (from rabbit)	Thermo Fisher Scientific	Immunofluorescence (1:1000)
Rat IgG	Alexa Fluor 594 conjugated antibody (from rabbit)	Thermo Fisher Scientific	Immunofluorescence (1:1000)

3.4.2. Protein extraction and immunodetection by western blot

Immunodetection by western blot is used to study the expression pattern of expression of different proteins. For protein extraction from a cell culture, medium is removed and cells washed with cold 1x PBS. This step is important in order to avoid detection of proteins from the medium in the western blot. Then, cells are collected in 1x SR buffer (2% SDS, 0.125 M Tris-HCl pH 6.8) and sonicated (Soniprep 150 MSE) in short bursts of high-frequency sound waves (15'' at power 8). If needed, protein quantification is carried out with the Lowry method (Bio-Rad). Next, a mixture of 4x SS (20% sucrose, 0.02% bromophenol blue, 0.1% sodium azide) and 1% β-mercaptoethanol is added. Samples are boiled for 5 min at 95 ºC, spun and either stored at -20 ºC or used immediately.

In order to extract protein from hippocampal slices, 3-5 slices are collected in 80 µl 1x SR buffer and homogenized 2x 10 seconds with a Pellet Mixer (VWR ®Radnor). Protein is quantified by the Bradford method (Bio-Rad). Finally, 4x SS and 1% β-mercaptoethanol are added and samples boiled for 5 min at 95 ºC.

3.4.3. Electrophoresis (SDS-PAGE)

Denaturing electrophoresis (SDS-PAGE) is achieved using different concentrations of acrylamide/bisacrylamide (37.5:1, Bio-rad) are used depending on the molecular weight of the protein of interest, this ranging from 7.5% to 15%. Stacking gels to deposit the samples are 5% acrylamide/bisacrylamide. To determine protein size, 5 µL of a molecular weight marker (PageRuler prestained protein ladder, ThermoFisher) are loaded into each gel. The electrophoretic separation is performed in electrophoresis cells from BioRad (Mini-PROTEAN II, #165-2940) filled with a buffer solution (25 mM TRIS, 1.44%, 0.1% SDS) and applying constant amperage of 20 mA/gel for 1 hour approximately.

3.4.4. Electroblotting

After electrophoretic protein separation, proteins are transferred to a PVDF (polyvinilide difluoride) membrane (Immobilon-P, #IPVH00010, Millipore) previously activated by incubation with methanol for 5 seconds and equilibrated with transfer buffer (25 mM TRIS, 192 mM glycine, 20% methanol). The separating gel is in touch with the PVDF membrane inside a sandwich system for a semidry transfer in a Hoefer TE77XP semidry system. The amperage applied was constant at 60 mA per membrane for 75 min.

3.4.5. Membrane blocking

Once proteins are transferred, the chemically active groups in the PVDF membrane are blocked to avoid non-specific binding of antibodies. Two different blocking solutions are used depending on the primary antibody: 3% BSA in PBS-T (phosphate buffered-saline 10 mM, Tween-20 0.05%) for phosphorylation-antibodies or 5% skimmed milk in PBS-T for the rest. Membranes are blocked for 1 hour at room temperature or O/N at 4 ºC, then washed for 5 min with PBS-T in order to remove excess of blocking solution.

3.4.6. Immunodetection

Membranes are incubated with the primary antibody in 0.25% milk in PBS-T or in 0.3% BSA in PBS-T overnight at 4 ºC and mild shaking. Primary antibodies used in this work are summarized in Table 5. After incubation with the primary antibody, three washes of 10 min each are performed with PBS-T and then membranes are incubated with the appropriate secondary antibody linked to horseradish peroxidase (GE Healthcare) (Table 5 and Table 6) in 0.3% BSA or 0.5% milk and incubated for 1 hour with mild shaking at room temperature. Afterwards, membranes are washed three times for 10 min each with PBS-T.

3.4.7. Chemiluminescent detection and data analysis

For detection, PVDF membranes are incubated at room temperature for 5 min with a chemiluminescent substrate (Luminol™ Western Chemiluminescent HRP Substrate, Millipore). The luminescent emission is detected with a ChemiDoc™ MP imaging System from Bio-Rad and analyzed with the Image Lab v4.0 software (Bio-Rad). The amount of luminescence is directly proportional to the amount of protein in the membrane, when this is not overexposed. Usually, the level of a protein is relativized to a loading control: actin or Coomassie Blue staining.

3.5 Protein interaction assays

3.5.1. Immunoprecipitation using anti FLAG M2 agarose beads

Flag tagged proteins are recognized and bound by the anti-FLAG-M2 antibody (Table 5) and efficiently pulled-down using anti-FLAG-M2-conjugated agarose beads.

For heterologous expression of proteins, HEK293 cells are transfected with the plasmid of interest. After 24 h, cells are placed on ice and washed with ice-cold PBS. Cells are collected by scraping them in ice-cold lysis RIPA buffer (50 mM Tris-HCl pH 7.5, 150 mM NaCl, 1% NP-40, 0.1% Na·Deoxycolate, 0.1% SDS, 5 mM EDTA, 1x protease and phosphatase inhibitor mix). Collected cells are transferred to a pre-cooled microcentrifuge tube, rolled for 30 min at 4 ºC and then centrifuged at 4 ºC, 300 g for 5 min. After centrifugation, supernatant is transferred to a fresh tube kept on ice; the pellet containing cell debris and membranes is discarded.

An aliquot of the supernatant is stored as input. The remaining is then incubated for 3 hours at 4 ºC with the agarose beads conjugated with the FLAG-M2 antibody. Next, beads bound to the antigen are washed 3 times with ice-cold lysis buffer and bound proteins are eluted in 1x SR (2% SDS, 0.125 M Tris-HCl pH 6.8) at 37ºC for 5 min. Afterwards, eluate is taken and mixed with 4xSS (20% sucrose, 0.02% bromophenol blue, 0.1% sodium azide) and β-mecaptoethanol, and further boiled at 95ºC for 5 min. Samples are then stored at -20 ºC or analyzed by western blot. Anti-ubiquitin antibody is used to detect ubiquitylated proteins.

3.5.2. Immunoprecipitation of endogenous cyclin D1 in adult hippocampus

For the immunoprecipitation of endogenous Ccnd1 in adult hippocampus, three hippocampi from adult females are taken, lysed in 1 ml RIPA buffer, and homogenized with 20x strokes in a douncer. Then, 2 ml RIPA buffer are added and samples are rolled for one hour at 4 ºC. After that, samples are centrifuged 5 min at 5000 rpm, 4 ºC. Supernatant is then incubated for 30 min at 4 ºC with 20 µl of pre-washed protein A magnetic beads (Dynabeads, Invitrogen) for a preclearing step to remove proteins that bind non-specifically to beads. Afterwards, beads are removed and the sample is divided into two tubes and one is incubated overnight at 4 ºC with 3 µg rabbit α-FLAG antibody and the other with rabbit α-cyclin D1. The following day, and prior to the incubation with the sample, 40 µl protein A dynabeads per sample are washed twice with RIPA buffer (without SDS). These washed dynabeads are incubated 2 hours at 4 ºC with the antigen-antibody sample. Finally, three washes are carried out with RIPA buffer (without SDS) and bound proteins are eluted from the beads with 1x SR (2% SDS, 0.125 M Tris-HCl pH 6.8) for 5 min at 37ºC. Eluate is taken and mixed with 4xSS (20% sucrose, 0.02% bromophenol blue,

0.1% sodium azide) and β-mecaptoethanol and further boiled at 95ºC for 5 min. Samples are then analyzed by western blot.

3.5.3. Affinity purification of GST-α4

Mus musculus GABRA4 (Image ID 6828002, BioScience) and C-terminus of GABRA4 (amino acids 354-552) are amplified by PCR and cloned into the expression vector pGEX-KG, which allows the fusion with the glutathione-S-transferase (GST) encoding gene. The resulting fusion proteins are able to bind to glutathione beads, and therefore these constructions allow us to express and purify from bacteria the fusion proteins for *in vitro* interaction analyses or *in vitro* kinase assays. To this end, *Escherichia coli* BL21 is transformed with either the GST-GABRA4 or GST-C-terminus GABRA4 vectors (see 3.2.5).

Vector-bearing bacteria are grown in 10 ml LB medium with 50 μg/ml ampicillin overnight at 37 ºC. The next day, culture is diluted into a new LB + ampicillin + 10% glycerol solution to an OD_{600} ~0.05 – 0.1 and cells are grown at 37 ºC for 2-3 hours. When the culture reaches an OD_{600} of 0.5, the expression of the fusion proteins is induced with 1 mM IPTG (Isopropyl β- D -1-thiogalactopyranoside) for 4 hours at 30 ºC until OD_{600} reaches 2-3. At this point, the culture is placed on ice for 30 min and then centrifuged at 700 rpm for 10 min at 4 ºC. The resulting pellet is resuspended in 2 ml cold distilled H_2O, divided into two tubes with 50 OD_{600} equivalents each, centrifuged at 10000 rpm for 5 min at 4 ºC. The resulting pellets are frozen and maintained at -80 ºC.

For protein purification, the pellet is resuspended in 1 ml lysis buffer (50 mM HEPES pH7.5, 150 mM NaCl, 1 mM EDTA, 1 mM DTT, 10% glycerol and a mix of protease and phosphatase inhibitors) with 0.5 mg/ml lysozyme and rolled at 4 ºC for 30 min. Then, to help dissolve the membranes, 0.5% Triton-X100 is added and incubated on ice for 5 min. Cell extract is sonicated three times for 10 seconds at power 6 (Soniprep 150 MSE) and centrifuged at 15000 rpm for 10 min at 4 ºC. At this time, an aliquot of the supernatant is taken as the soluble extract fraction and the rest is incubated with previously washed Glutathione-Sepharose 4B beads (GE, Healthcare Bio-sciences) rolling for 2 hours at 4 ºC. Afterwards, protein-bound beads are washed three times with lysis buffer containing 0.1% Triton-X100 and once with kinase buffer or binding buffer. Then, glycerol is added and samples are kept at –80 ºC. An aliquot of this purified protein together with the soluble extract is collected for a further analysis by SDS-PAGE. The gel is stained with Coomassie brilliant blue (EZblue^{TN} Gel Staining Reagent, Sigma- Aldrich). The final concentration and purity of the isolates are estimated by comparison with protein standards.

3.5.4. *In vitro* protein interaction assay

FLAG-Ccnd1 (pCYC193) is amplified by PCR (forward primer: CGCGCTAATACGACTCACTATAGGGAGACCCAAGCCCATGGGATCAC; reverse primer: TTTTTTTTTTTTTTTTTTTTTTTTTTTTTTGGCTGATCAGCGAGCTCTAG, transcribed *in vitro* with the T7 RNA polymerase (New England Biolabs), and *in vitro* translated with a rabbit reticulocyte lysate system (Promega). For the *in vitro* protein interaction assay, 400 ng of GST-α4 or GST-α4-C-terminal purified from *E. coli* and immobilized on Glutathione-Sepharose 4B beads (GE, Healthcare Bio-sciences) are incubated together with FLAG-Ccnd1 in binding buffer (20 mM HEPES-KOH pH7.5, 150 mM KCl, 5 mM $MgCl_2$, 0.5 mM EDTA, 0.1% NP-40, 1mM DTT, 1 mM PMSF, 10% glycerol and a mix of protease and phosphatase inhibitors) for 30 min at room temperature. After four washes in binding buffer, 50 µl 2xSSR is added and the samples are analyzed by SDS-PAGE and Western blotting (GST and Rabbit anti-Ccnd1 antibodies, see Table 5).

3.6 Kinase reaction assays

3.6.1. *In vitro* kinase assay

For kinase reactions, 0.2-0.5 µg substrate (GST-fusion proteins obtained in 3.5.3) are mixed with 10 µM cold ATP, 10 µCi γ-^{32}P-ATP (PerkinElmer, 3000 Ci/mmol) and 1.5 µl of the Ccnd1–Cdk4 active complex purified from baculovirus (C0620, Sigma- Aldrich) in 20 µl kinase buffer (50 mM Tris-HCl pH7.5, 10 mM $MgCl_2$, 0.5 mM DTT, 1 mM EGTA, 2.5 mM β-glycerophosphate). Either the kinase complex inhibitor palbociclib (S1116, Selleckchem) at 2 µM or DMSO as a control is added to the reaction mix. This mix is incubated for 20 min at 30 ºC and the reaction is stopped by adding 2xSSR (4% SDS, 0.25 M Tris-HCl pH6.8, 10% sucrose, 2% β-mercaptoethanol and 0.01% bromophenol blue) and boiling the samples for 5 min at 95 ºC. Proteins are loaded into a gel and separated by SDS-PAGE electrophoresis. After that, the gel is dried and exposed to a film at -80 ºC. Phosphorylated proteins are visualized by autoradiography in the automatic film processor OPTIMAX from PROTEC®.

3.6.2. Mass spectrometry (HPLC-MSMS)

Mass spectrometry experiments are performed with the GST-α4 or GST-α4-C-terminal obtained in 3.5.3 after an *in vitro* kinase assay as in 3.6 but with non-radioactive ATP or without ATP (control). After the kinase reaction, samples are run in a SDS-PAGE gel and stained with Oriole Fluorescent Gel Staining (BioRad). Detected bands are purified and prepared to be analyzed by

mass spectrometry (HPLC-MSMS) in the Proteomic Unit of the Institut d'Investigació Biomèdica de Bellvitge (IDIBELL).

3.7 Electrophysiology

3.7.1. Whole-cell currents measurements in tsA201 cells

The measurements of GABA-evoked whole-cell currents in tsA201, a human embryonic kidney cell line, were done in the laboratory of Dr. David Soto (Universitat de Barcelona). Cells are visualized with an inverted microscope (AxioVert A.1, Carl Zeiss) and maintained in extracellular flowing solution at a rate of 60 ml/h. The extracellular solution contains (in mM): 140 NaCl, 5 KCl, 10 HEPES, 11 glucose, 2.5 $CaCl_2$, 1.2 $MgCl_2$ (pH = 7.4 with NaOH; osmolarity 305 mOsm/Kg adjusted with sorbitol). Electrodes are fabricated from borosilicate glass (1.50 mm O.D., 1.16 I.D., Harvard Apparatus) pulled with a P-97 horizontal puller (Sutter Instruments) and polished with a forge (MF-830, Narishige) to a final resistance of 2–5 MΩ. The intracellular solution contains (in mM): 140 KCl, 2 $MgCl_2$, 2 $CaCl_2$, 10 HEPES, 1.1 EGTA, 2 Mg ATP (pH = 7.2 with KOH; osmolarity 295 mOsm/Kg adjusted with sorbitol).

Macroscopic $GABA_A$-mediated currents are recorded at room temperature (22-25˚C) in the whole-cell configuration from cells positive for venus and mCherry fluorescence at a holding membrane potential of -60 mV. Currents are recorded with Axopatch 200B amplifier, filtered at 2kHz and digitized at 5kHz using Digidata 1440A interface with pClamp 10 software (Molecular Devices Corporation). Series resistance is typically 5–20 MΩ, and is monitored at the beginning and at the end of the experiment. Cells that showed a change in series resistance greater than 20% are rejected.

Rapid application of the agonist GABA (1-2 ms exchange) is applied by switching between a continuously flowing control solution (extracellular solution diluted by 5%) and a GABA-containing solution (1 μM GABA and 2.5mg/ml of sucrose diluted in extracellular solution). Solution switching is achieved by piezoelectric translation of a theta-barrel application tool made from borosilicate glass (1.5 mm O.D.; Sutter Instruments) mounted on a piezoelectric translator (P-601.30; Physik Instrumente). Agonist is applied at 2 minutes interval and the magnitude of the peak current is measured (I_{GABA}). Electrophysiological recordings are analyzed using IGOR Pro (Wavemetrics Inc.) with NeuroMatic (Jason Rothman, UCL).

3.7.2. Whole-cell recordings in organotypic hippocampal slices

3.7.2.1. GABA tonic currents

Whole-cell voltage clamp is used to measure GABA tonic currents in cultured hippocampal slices. Prior to the electrophysiological recordings, slices are treated for 2 hours with either DMSO (control solution) or 2.5 μM Palbociclib (Cdk4/6 inhibitor) (Selleckchem). After that, slices are placed in a chamber and perfused with artificial cerebrospinal fluid [aCSF: 119 mM NaCl, 2.5 mM KCl, 1 mM NaH_2PO_4, 26 mM $NaHCO_3$, 11 mM glucose, 1.2 mM $MgCl_2$, 2.5 mM $CaCl_2$; osmolarity adjusted to 290 mOsm; pH7.5] supplemented with 100 μM AP5 (NMDA receptor antagonist), 10 μM CNQX (AMPA receptor antagonist), 1 μM strychnine (glycine antagonist), 4 μM 2-chloroadenosine (to stabilize the evoked neural response) and DMSO or Palbociclib as external solution gassed with 5% CO_2 at 29 ºC in the electrophysiology set-up. Patch recording pipettes (4-6 MΩ) are pulled from thin-walled borosilicate capillary glass (World Precision Instruments [WPI], Sarasota, FL) on a P-2000 laser electrode puller (Sutter Instrument, San Rafael, CA) and filled with high chloride internal solution (178 mM CsCl, 10 mM Hepes, 2.5 mM $MgCl_2$, 4 mM Na_2ATP, 0.4 mM Na_3GTP, 10 mM sodium phosphocreatine, 0.6 mM EGTA; pH adjusted to 7.2, osmolarity adjusted to 290 mOsm). The pipette potential is held at -60 mV during recordings. GABA inhibitory post synaptic currents are evoked with single voltage pulses (200 μs, <30 V) delivered through a bipolar electrode Axopatch 200B amplifier (Molecular Devices, Union City, CA) placed on Schaffer collaterals, and tonic currents are recorded from CA1 pyramidal neurons. At least 10 min of stable baseline synaptic responses and holding currents (HC) are recorded. The tonic $GABA_A$ R-mediated current is measured as an outward shift in holding current following application of picrotoxin (100 μM). For quantifications, each cell contributed with a holding current value obtained as a mean of one minute HC recording once the synaptic response was almost inhibited by picrotoxin action (Figure 9).

3.7.2.2. Miniature inhibitory postsynaptic currents

Recordings of miniature responses (mIPSC) are performed from hippocampal slices from P5-7 rats at -60 mV in the presence of 10 μM CNQX, 100 μM AP5, 1 μM strychnine and 1 μM tetrodotoxin (action potentials blocker). As for the GABA tonic current recordings, slices are treated for 2 hours with 2.5 μM Palbociclib or DMSO. These recordings are obtained with the gap-free program of pClamp. All electrophysiological data are collected with pCLAMP software (Molecular Devices). Data analysis is performed with pClamp software (miniature currents) or custom-mode Excel (Microsoft) macros (GABA tonic currents).

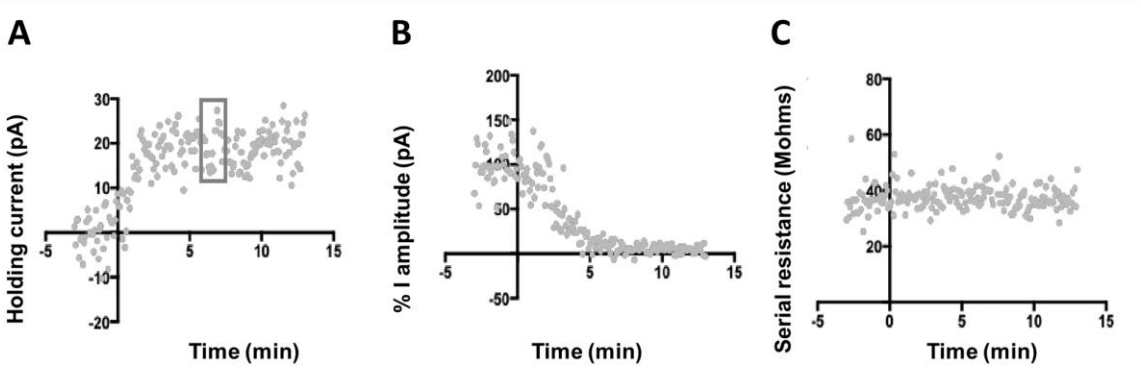

Figure 9: Representative examples of recordings of GABA tonic currents. A) Rat hippocampal slices are used for whole-cell patch clamp recordings performed at -60 mV. Recordings are aligned by the moment of 100 μM picrotoxin addition. The grey rectangle shows the selected minute in which the holding current (HC) for that cell is obtained. Baseline holding current is considered as the average of the HC during 3 minutes of stability. The shift in the HC is represented as the HC at the moment minus the baseline HC. **B)** Percentage of the intensity (I amplitude) of the evoked synaptic response. The amplitude of the response during the baseline is considered as 100%. The fall of the synaptic response is used as a control for picrotoxin activity. **C)** Serial resistance of each cell is followed as a control for cell viability and stability.

3.8 Surface biotinylation assay

A cell surface biotinylation assay provides a way to study trafficking of cell-surface proteins by their labelling with a biotin variant (EZ-link sulfo-nhs-SS-biotin, Fisher Scientific). In other words, the aim of this protocol is to analyze the processes of endocytosis and further destruction or "recycling" that contribute to the regulation of the amount of a specific protein in the membrane.

The biotin variant used in this assay is a small water-soluble molecule consisting of a charged sulfo group, a reactive N-hydroxysuccinimide ester group, a cleavable disulfide bond and biotin. Due to the strong charge imparted by the sulfo group, this biotin variant is membrane impermeable.

3.8.1. Biotin labeling of membrane proteins

Cells ($2 \cdot 10^6$ cells in a 100mm plate) are washed twice with ice-cold PBS. Then, 1 mg/ml of sulfo-NHS-SS-biotin in PBS is added and incubated on ice for 15 min. Low temperature restricts endocytosis, thus the NHS group of the reagent reacts covalently only with primary amines on surface proteins. After the treatment, cells are washed twice with TBS (Tris-buffered saline: 150 mM NaCl, 50 mM Tris-HCl, pH 7.6) in order to quench the non-conjugated biotin. Next, cells are lysed in RIPA buffer (50 mM Tris pH 7.4, 150 mM NaCl, 1% NP-40, 0.1% sodium deoxycholate,

0.1% SDS, 5 mM EDTA, 40 mM NaF, 1 mM Na_3VO_4 and 1x EDTA-free protease inhibitor cocktail) and centrifuged at 1800 rpm, 5 min at 4ºC. Supernatants are collected as cell lysates.

Biotinylated proteins are isolated by adding the cell lysates to streptavidin-coated synthetic beads (Neutravidin agarose beads, Fisher Scientific). To use the same amount of protein per condition, protein concentration of each cell lysate is measured with the Bio-Rad DC™ Protein assay kit. Then, cell lysates and Streptavidin-agarose beads are incubated together overnight at 4ºC on an orbital shaker and washed three times with RIPA buffer the next day. A final elution step in 2xSSR is performed to release bound proteins. The target proteins are then analyzed by Western blotting.

3.8.2. Receptor internalization assay using biotin labeling

Cells ($2 \cdot 10^6$ cells in a 100mm plate) are washed with PBS and labeled with 1 mg/ml of sulfo-NHS-SS-biotin in PBS on ice for 15 min. Next, two washes with TBS are carried out, and time 0 samples are collected. The other plates are placed at a 37 ºC incubator for 15 min with medium containing the lysosomal inhibitor leupeptin at 100 μg/ml to prevent lysosomal proteolysis of internalized proteins. Afterwards, cells are incubated twice for 15 min each with cleavage buffer (50 mM glutathione, 75 mM NaCl, 10 mM EDTA, 1% BSA, 0.075 N NaOH) on ice in orther to cleave biotin labels in cell-surface proteins (it breaks the disulfide bridge of the EZ-link sulfo-nhs-SS-biotin). Subsequently, cells are washed with PBS containing 5 mg/ml iodoacetamide, an alkylating reagent, and TBS. Finally, cells are lysed with RIPA buffer and a pull-down with Streptavidin-agarose beads is performed as in 3.8.1. Samples are analyzed by Western blot

3.8.3. Assessment of receptor insertion into the membrane by biotin labeling

Receptor insertion into the membrane is assessed by biotin labeling. First, cell-surface proteins are labeled with 1 mg/ml of sulfo-NHS-SS-biotin in PBS on ice for 15 min. After that, all labels are cleaved by incubation with cleavage buffer (50 mM glutathione, 75 mM NaCl, 10 mM EDTA, 1% BSA, 0.075 N NaOH) on ice twice for 15 min. Time 0 samples are collected at this moment. Then, cells are placed on an incubator at 37 ºC with fresh medium for 2 hours. Subsequently, cells are incubated again with biotin for newly inserted surface protein labeling, lysed with RIPA buffer and a pull-down with Streptavidin-agarose beads is carried out as in 3.8.1. Samples are analyzed by Western blot.

3.9 Statistical analysis

Different statistical analyses are used in this work. In every analysis, the minimum level of statistical significance is a p-value equal to 0.05. The significance level is represented in each graph as indicated.

In order to evaluate possible differences between two experimental groups a t-test is performed. When there is a multiple comparison, one-way ANOVA with a post-hoc test (Tukey) is performed. In whole-cell recordings in ts201A cells, comparisons between groups are done using the parametric student's t-test. For tonic currents comparison, Wilcoxon test is performed and in mIPSC amplitude and frequency, Mann-Whitney test is done. Microsoft Excel and GraphPad Prism v5.0 (GraphPad) are used for statistical analysis and graphical representation.

3.10 Ethical considerations

All procedures with animals follow the protocols approved by the Institutional Committee of Care and Use of Animals (Comitè Institucional de Cura i Ús d'Animals), and experiments are approved by the Ethics Committee of the University of Lleida (EAEC 18-01 / 12). Animals are housed and maintained in the animal facility of the University of Lleida with 12h:12h light/dark cycle and food/water available *ad libitum*. All efforts are made to minimize the number of animals and their suffering.

RESULTS

4. RESULTS

4.1 Role of cytoplasmic cyclin D1 in neuritogenesis

Several studies point to a role for Ccnd1 in normal development of the nervous system. Ccnd1 KO mice show neurological abnormalities (*Sicinski et al. 1995*), Ccnd1is required for NGF-induced neurite outgrowth in PC12 pheochromocytoma cells (*Marampon et al. 2008*), and is also detected in the cytoplasm of cortical neurons at 4 DIV (days *in vitro*) (*Sumrejkanchanakij et al. 2003*). All together these observations led us to consider a role -likely a cytoplasmic function- for Ccnd1 in neuritogenesis. We wanted to study this possibility by electroporating an HA-Ccnd1 construct in cortical neurons, but this caused nuclear Ccnd1 accumulation and apoptosis, detected by cleaved caspase 3 labeling and pyknotic nuclei (Figure 10). To prevent neuronal apoptosis due to nuclear Ccnd1 accumulation, HA-Ccnd1 was fused to CAAX, a farnesylatable motif that targets the protein to cell membranes, thus avoiding entrance to the nucleus (*Fusté 2016*). After electroporation of HA-Ccnd1-CAAX in cortical neurons, Ccnd1 localizes in the cytoplasm, cleaved caspase-3 labeling and pyknotic nuclei disappear, and apoptotic death is prevented. Therefore, the HA-Ccnd1-CAAX construct allows us to study the effects of cytoplasmic Ccnd1 in neurons.

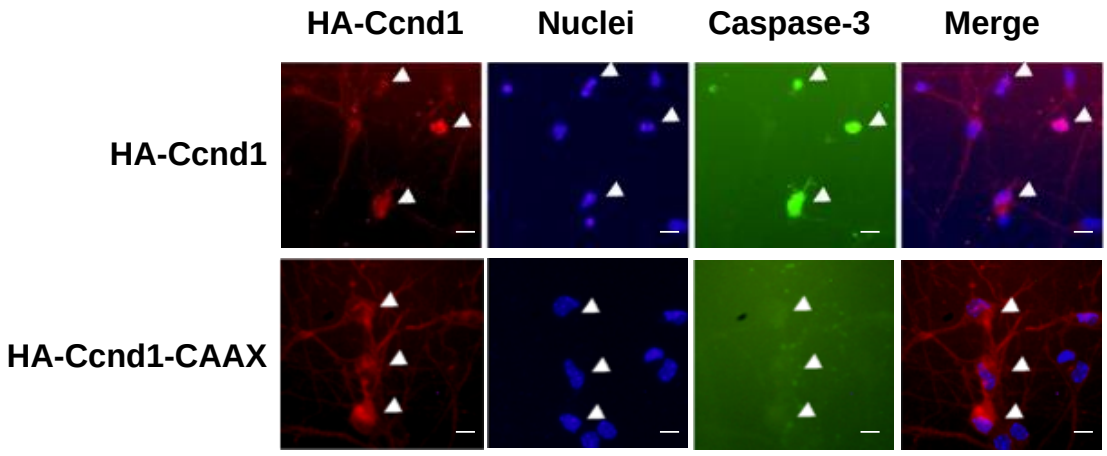

Figure 10. Cytoplasmic localization of cyclin D1 avoids apoptotic neuronal death. Mouse cortical neurons from E15.5 embryos are electroporated with HA-Ccnd1 or HA-Ccnd1-CAAX and cultured until 4 DIV. At 4 DIV, apoptosis is assessed by immunofluorescence. Representative images showing HA positive cells (red), pyknotic nuclei (Hoechst) and cleaved caspase-3 (green). Arrowheads show electroporated cells. Scale bar 10 μm

In consequence, to study the role of cytoplasmic HA-Ccnd1-CAAX in neuritogenesis in primary cortical neurons, we co-electroporated them with HA-Ccnd1-CAAX and GFP. GFP is used to

observe cell morphology under fluorescence. Neurite number and length are quantified with the NeuronJ plugin of ImageJ. The mean of each condition is obtained and normalized to a GFP control in each experiment. Then, the mean of the ratios is represented.

In these experiments, HA-Ccnd1-CAAX promoted an increase of both axon and neurite lengths (1.5-fold and 1.4-fold increase respect to a control vector, respectively) at 4 DIV. Also, neurite number per cell was increased when HA-Ccnd1-CAAX was overexpressed (from an average of 5.9 neurites per cell to 6.5 neurites per cell). Hence, overexpression of cytoplasmic Ccnd1 significantly induces neuritogenesis in cortical neurons at 4 DIV when compared to control cells (Figure 11).

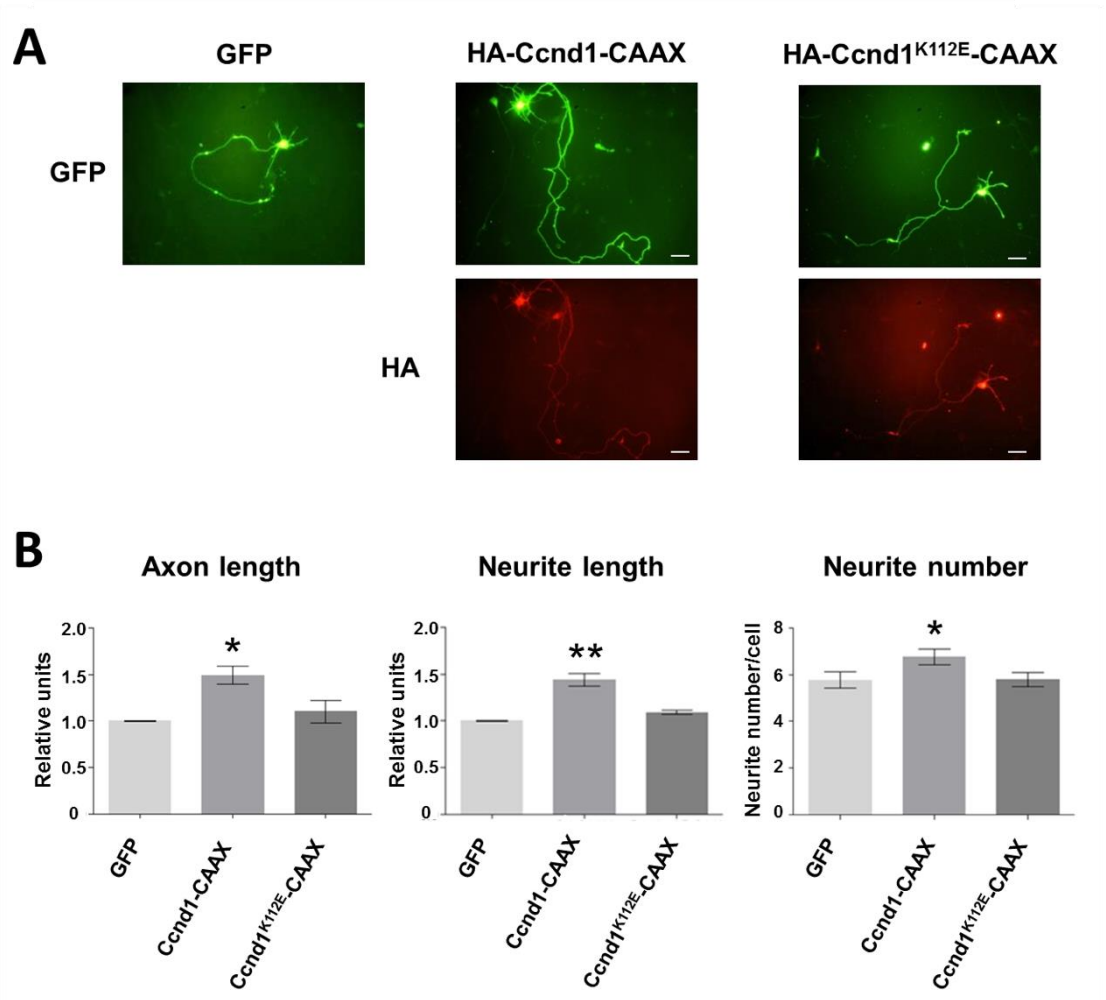

Figure 11: Cytoplasmic cyclin D1 induces neuritogenesis in cortical neurons at 4 DIV. A) Representative images of cortical neurons electroporated with GFP and HA-Ccnd1–CAAX, HA-Ccnd1^{K112E}-CAAX or a control vector. At 4 DIV, cells are observed by immunofluorescence against GFP (green) and HA (red). Scale bar 10 μm. **B)** Quantifications of axon length, neurite length and number of neurites per neuron of the experiments in A. Data obtained with the NeuronJ plugin of ImageJ. Values are expressed as mean±SEM (n=3 independent experiments, at least 25 cells per condition in each experiment). Statistical significance is determined by one way ANOVA and Tukey-HSD post-test (*p<0.05; **p<0.01, compared to control).

Furthermore, this effect is kinase-dependent since the overexpression of a Ccnd1 mutant (HA-Ccnd1^{K112E}-CAAX) that does not form an active complex with CDKs does not significantly increment either the number of neurites per cell or the lengths of neurites or axons (1.0-fold and 1.1-fold increase respect to control, respectively). Hence, we conclude that overexpression of cytoplasmic Ccnd1 induces axon and neurite outgrowth and increases neurite number per cell in a kinase-dependent manner.

Since the effect of cytoplasmic Ccnd1 observed in neurons at 4 DIV was dependent on the kinase activity, we reasoned that overexpressing Cdk4, the CDK partner of Ccnd1, might also elicit a similar effect. Therefore, HA-Cdk4 fused to CAAX was electroporated into primary cortical neurons. Indeed, overexpression of this membrane-targeted HA-Cdk4-CAAX construct in cortical neurons at 4 DIV also causes a significant increase (1.4-fold) of both axon and neurite lengths compared to a control group, neurons electroporated with a GFP and a control vector. Also, neurite number per cell was increased when HA-Cdk4-CAAX was overexpressed (from an average of 5.47 neurites per cell to 6.6 neurites per cell) (Figure 12).

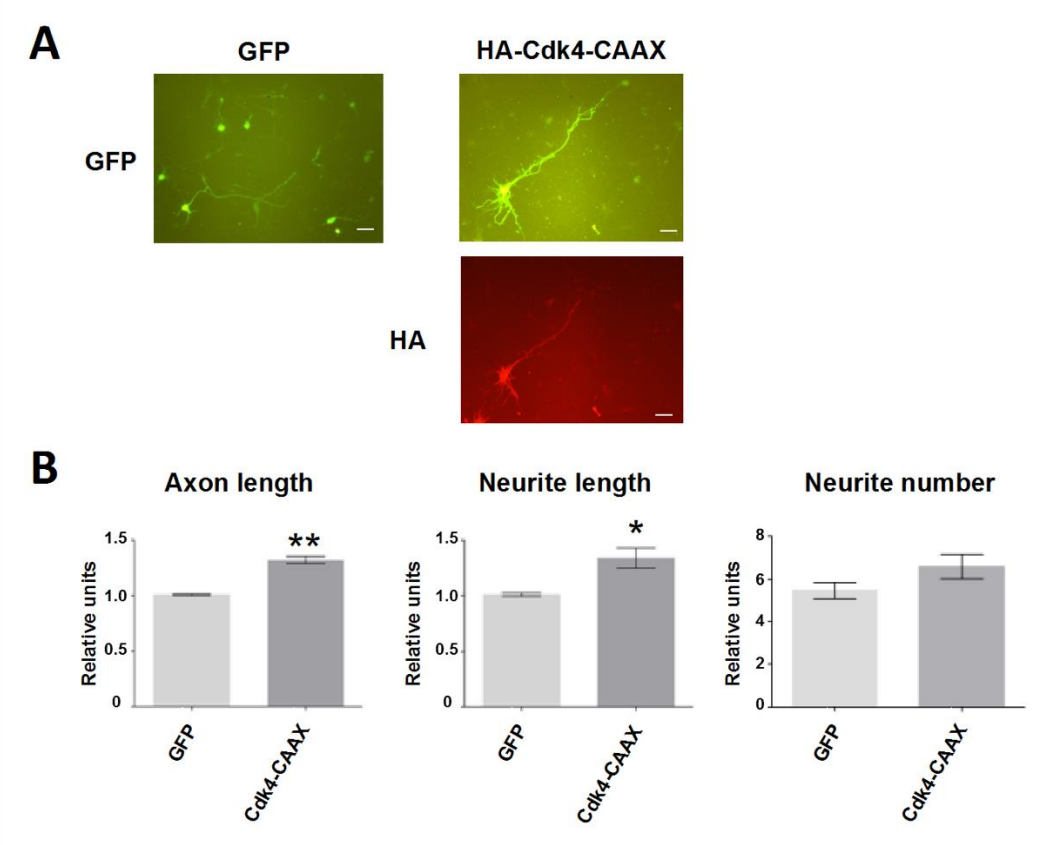

Figure 12: Cytoplasmic Cdk4 induced neuritogenesis in cortical neurons at 4 DIV. A) Representative images of cortical neurons electroporated with GFP and either HA-Cdk4-CAAX or a control vector. At 4 DIV, cells are observed by immunofluorescence against GFP (green) and HA (red). Scale bar 10 μm. **B)** Quantifications of axon length, neurite length and neurite number of experiments in A. Data obtained with the NeuronJ plugin of ImageJ. Values are expressed as mean±SEM (n=3 independent experiments, at least 25 cells per condition in each experiment). (*p<0.05; **p<0.01, t-test).

Because the overexpression of cytoplasmic Ccnd1 in mouse cortical neurons induces an increment in the length of both axons and neurites, we wanted to study the role of endogenous Ccnd1 in neurite outgrowth. To this aim, cortical neurons were isolated from E15.5 mouse embryos and cultured for 0 hours, 4 h, 1 DIV and 3 DIV, and then CCND1 mRNA was quantified by qRT-PCR. Endogenous CCND1 mRNA levels decrease significantly after 1 DIV and become very low at 3 DIV in comparison with 0 h and 4 h of *in vitro* differentiation (Figure 13).

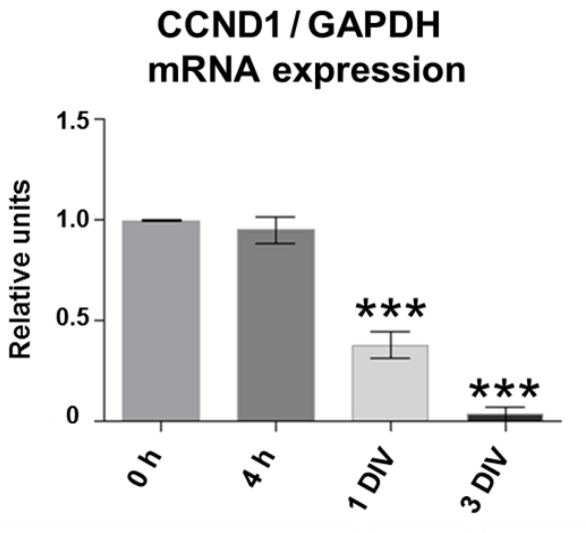

Figure 13: Cyclin D1 mRNA level drops at 1 DIV and continues to decrease at 3 DIV. CCND1 and GAPDH mRNAs expression are analyzed by qRT-PCR at different time points in cultured cortical neurons. CCND1 mRNA levels relative to GAPDH mRNA levels are represented. For all plots, values are expressed as mean ± S.E.M. Statistical significance is determined by one way ANOVA and Tukey-HSD post-test (***$p<0.001$, compared to time 0h).

Since downregulation of Ccnd1 in PC12 cells results in a diminution of neurite outgrowth (*Marampon et al. 2008*), we used interference RNA (shCcnd1) to downregulate the expression of Ccnd1 in cortical neurons. The efficiency of the shRNA was tested in MEFs (Figure 14A). Afterwards, cortical neurons were transfected before seeding with GFP along with a scramble control or with shCcnd1, seeded and cultured for 1 DIV. Next, cells were fixed and observed by immunofluorescence against GFP to allow quantifications (Figure 14B). Both axon and neurite lengths are significantly reduced (23% and 20% respectively) when Ccnd1 is downregulated, which also significantly decreases the neurite number per cell, from an average of 4.95 neurites per cell in the WT to 4.34 in shCcnd1-expressing neurons. Therefore, downregulation of endogenous Ccnd1 significantly affects neuritogenesis.

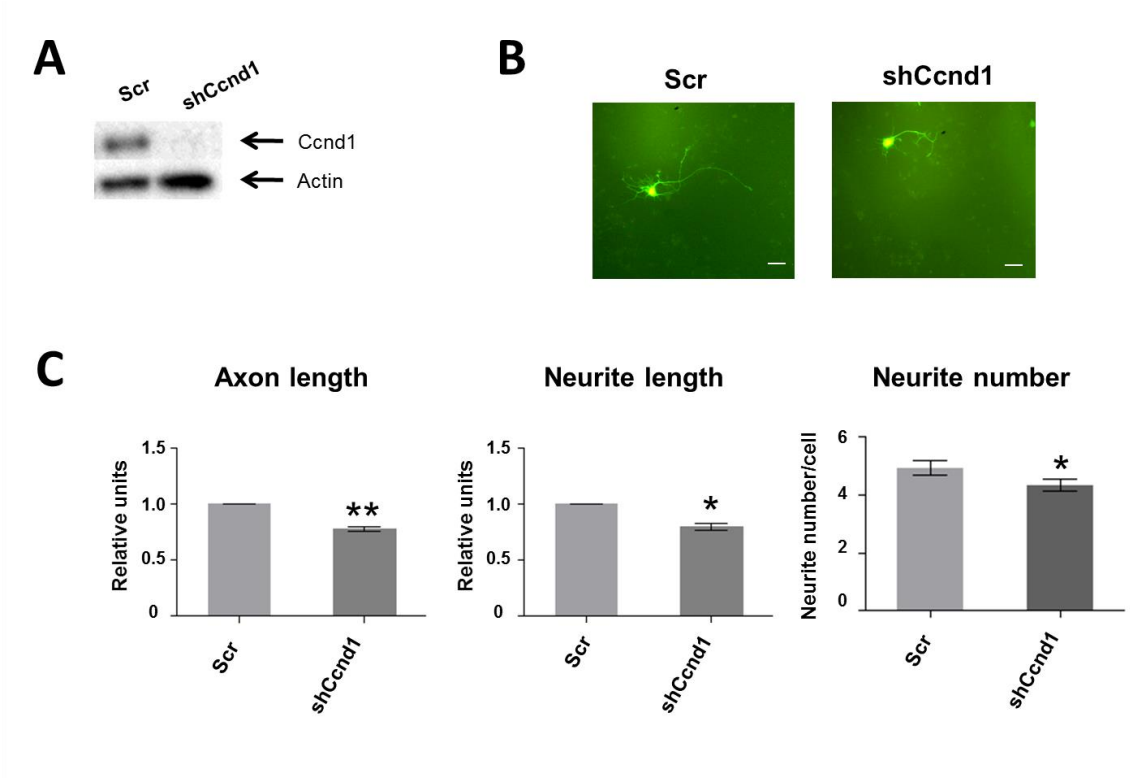

Figure 14: Downregulation of cyclin D1 affects neuritogenesis in cortical neurons at early stages of differentiation. A) Ccnd1 knockdown by interference RNA in MEFs. Immunoblot showing Ccnd1 protein levels (Dcs6 antibody) in control (Scr) and knockdown cells. Actin levels are used as a loading control. **B)** Cortical neurons are co-transfected with GFP and either a scramble shRNA or shCcnd1. Neurons are fixed at 1 DIV and observed by immunofluorescence against GFP. Scale bar 10 μm. **C)** Axon length, neurite length and neurite number per cell are quantified using the NeuronJ plugin of ImageJ. For all plots, values are expressed as mean ± S.E.M (n=3 independent experiments, at least 25 cells per condition in each experiment). Statistical significance is determined by t-test (*p<0.05; **p<0.01).

In addition, axon and neurite lengths and neurite number were determined for cortical neurons obtained from E15.5 WT and Ccnd1 KO mice (Figure 15). Prior to seeding, neurons were electroporated with GFP in order to follow neurites for quantification. Cells were cultured for 1 DIV, fixed and observed by immunofluorescence against GFP. Multiple images were taken and the axon length, the neurite lengths and the neurite number per cell quantified. Neurons lacking Ccnd1 had shorter axons (by 18%) and neurites (by 26%) in comparison with neurons obtained from WT mice. We do not find a statistically significant difference between the number of neurites in WT (3.09 average) vs Ccnd1 KO neurons (2.99 average).

All in all, apoptotic neuronal death induced by the overexpression of Ccnd1 is prevented by targeting the protein to the cytoplasm. We have shown a role of cytoplasmic Ccnd1 in neuritogenesis in a manner that depends on the kinase activity of Ccnd1-Cdk complex. This effect of Ccnd1 on neuritogenesis is seen under overexpression conditions and importantly also under endogenous conditions by downregulation of Ccnd1 with RNA interference and in Ccnd1 KO neurons.

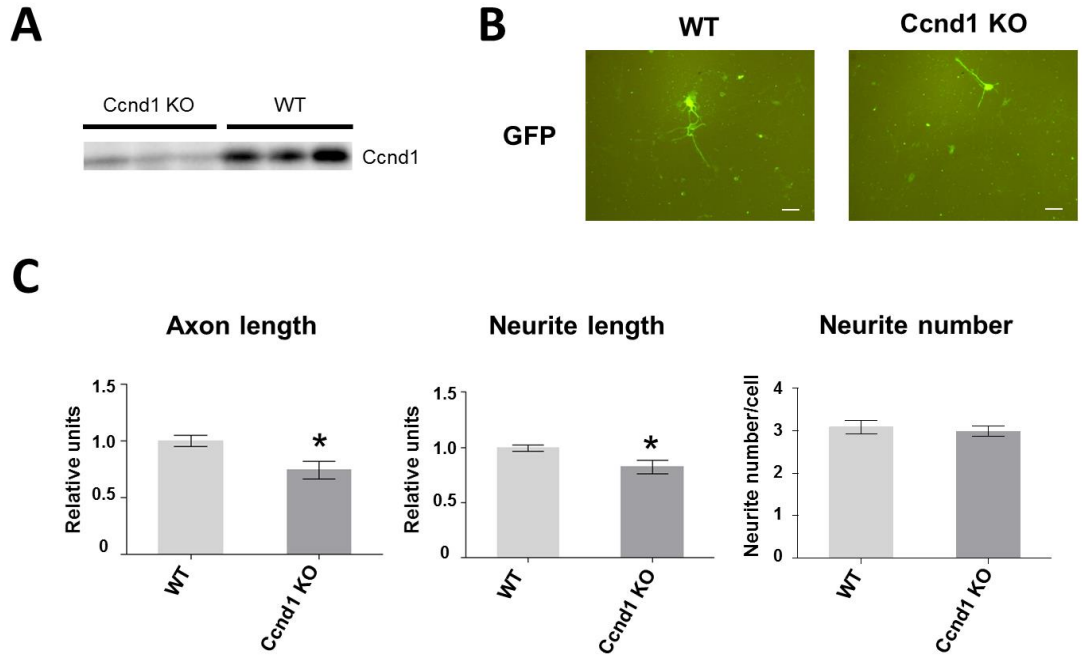

Figure 15: Cyclin D1 deficient cortical neurons have shorter axons and neurites at 1 DIV. Cortical neurons from Ccnd1 KO mouse embryos (n=6) and WT controls siblings (n=6) were electroporated with GFP and cultured for 1 DIV. **A)** Ccnd1 levels from paw of PCR-genotyped Ccnd1 KO embryos and sibling controls were analyzed by WB using Dcs6 antibody. **B)** Representative images of 1 DIV-cultured cortical neurons. Cells are fixed and observed by immunofluorescence against GFP. Scale bar 10 μm. **C)** Quantifications of axon length, neurite length and neurite number of the experiments in B using the NeuronJ plugin of ImageJ. For all plots, values are expressed as mean ± S.E.M (n=3 independent experiments, at least 25 cells per condition in each experiment). Statistical significance is determined by t-test (*$p<0.05$).

4.2 Effect of paxillin phosphorylation at S83 and S178 in neuritogenesis

Because Pxn phosphorylation at serine 83 (S83) and serine 178 (S178) is important for neuritogenesis in PC12 cells (*Huang et al. 2004*; *Yamauchi et al. 2006*) and Ccnd1 controls cell spreading and invasion through the phosphorylation of Pxn at serine 83 (S83) and serine 178 (S178) (*Fusté et al. 2016*), we wondered whether Pxn could be a downstream target of Ccnd1 in the control of neurite outgrowth. Hence, we tested the level of phosphorylated Pxn in cortical neurons from E15.5 mouse embryos. These neurons were cultured for 1 or 4 DIV and collected for the analysis of phosphorylated S83 (pS83), phosphorylated S178 (pS178) and total Pxn levels (Figure 16A). WB quantifications are shown in Figure 16B as a ratio between phosphorylated Pxn and total Pxn. pS83 Pxn/Pxn decreases up to 54% and pS178/Pxn drops 52% when 4 DIV is compared to 1 DIV. These results are in accordance with CCND1 mRNA levels in cultured cortical neurons, i.e, there is a correlation between CCND1 mRNA levels and Pxn phosphorylation at S83 and S178 during differentiation.

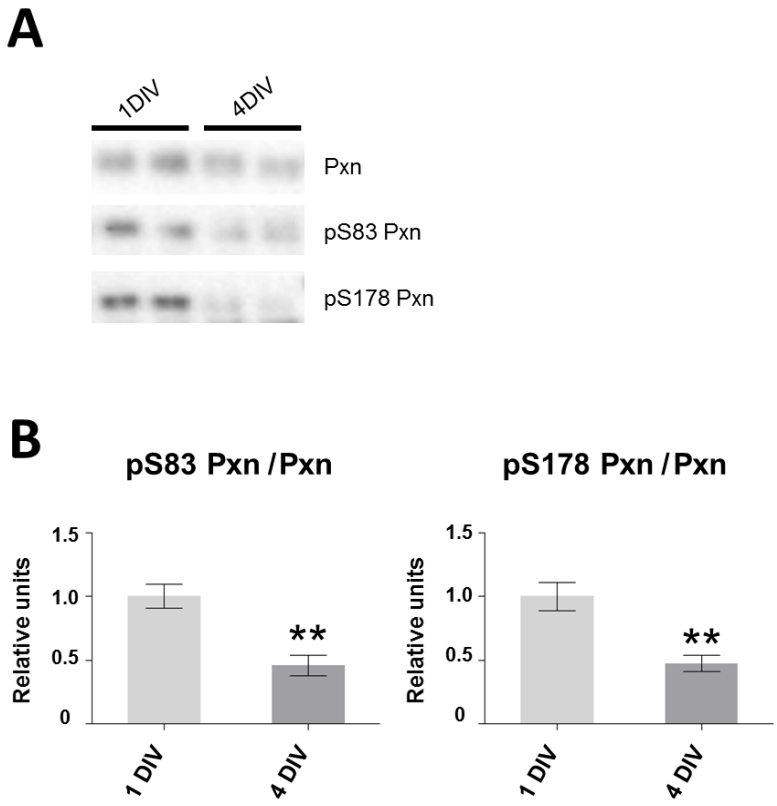

Figure 16: Paxillin phosphorylation at serines 83 and 178 is lower at 4 DIV in comparison to 1DIV. A) Endogenous levels of total Pxn and phosphorylated Pxn pS83 and pS178 in cortical neurons are analyzed at 1 DIV and 4 DIV by WB. **B)** Quantification of pS83 Pxn and pS178 Pxn versus total Pxn levels. Values are expressed as mean ± SEM (n=6). Statistical significance is determined by t-test (**p<0.01).

Paxillin can be phosphorylated *in vitro* by Ccnd1-Cdk4 at S83, S178 and S244 (*Fusté et al. 2016*). Next, we wanted to test whether these Pxn phosphorylations were important for neurite outgrowth. For this reason, cortical neurons were electroporated with GFP and either HA-Pxn or the triple non-phosphorylatable mutant $Pxn^{S83A,\ S178A,\ S244A}$ (HA–Pxn^{TM}) and cultured for 1 DIV. For this experiment, we chose to culture the cells for 1 DIV because at this time we can observe effects of endogenous Ccnd1 on neurite outgrowth (Figure 14B and Figure 15C) and there are good levels of Pxn phosphorylation at S83 and S178 (Figure 16A). After 1 DIV, neurons were fixed and observed by immunofluorescence against GFP and HA. Figure 17 shows the quantification of both axon and neurites lengths for HA-Pxn and for the mutant HA– Pxn^{TM}. This non-phosphorylatable mutant of Pxn causes a decrease of 18% in axon length and a decrease of 16% in total neurite length compared to control neurons electroporated with WT Pxn. Besides, neurite number per cell in the triple mutant (3.21 average) is lower than in the control (4.05 average). Hence, Pxn phosphorylation at S83, S178 and S244 significantly affects neuritogenesis

in cortical neurons at 1 DIV suggesting that Pxn could act as a downstream effector of Ccnd1 in the control of neurite outgrowth.

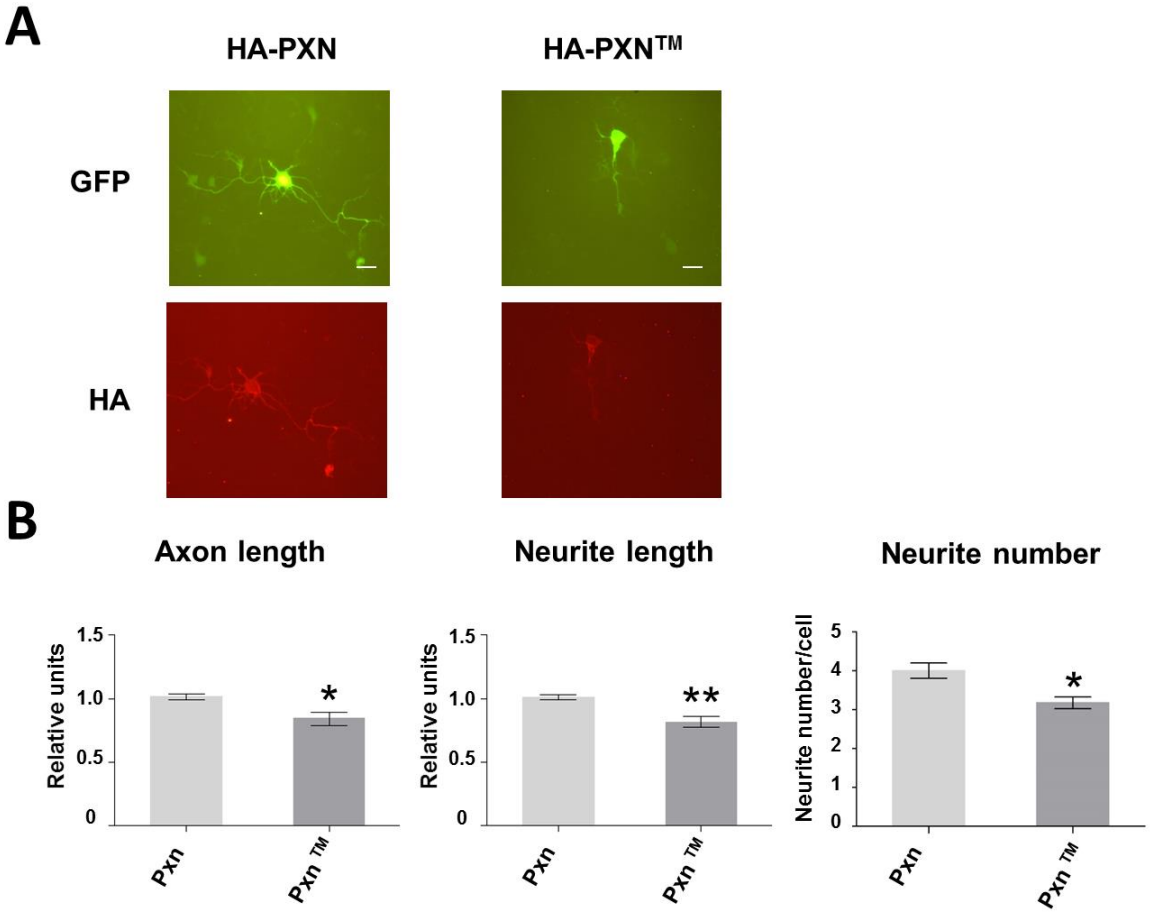

Figure 17: Phosphorylation of paxillin at serines 83, 178 and S244 is involved in early neuritogenesis control. A) Representative images of cortical neurons from E15.5 embryos electroporated with GFP and either HA–Pxn or a triple non-phosphorylatable mutant HA–Pxn^{TM} at 1 DIV. Neurons are fixed and observed by immunofluorescence against GFP (green) and HA (red). Scale bar 10 μm. **B)** Axon and neurite lengths are quantified using the NeuronJ plugin of ImageJ. Values are expressed as mean ± SEM (n=5 independent experiments, at least 25 cells per condition in each experiment). Statistical significance is determined by t-test (*p<0.05; **p<0.01).

4.3 Cyclin D1 effects on GABA$_A$ receptors

4.3.1. Interaction between cyclin D1 and α4 subunit of the GABA$_A$ receptor

Looking for Ccnd1 interactors in the brain, a yeast two hybrid screening had previously been carried out in our lab with Ccnd1 as a bait and an adult mouse brain cDNA library as prey. An interaction between Ccnd1 and the alpha 4 subunit of the type A GABA receptor (α4) was detected. Specifically, Ccnd1 interacted with three independent clones that contained the

intracellular loop found between the TM3 and TM4 domains of the α4 subunit (from amino acid 354 to 552) (Figure 24).

In order to confirm the interaction between Ccnd1 and α4, we performed both pull-down and immunoprecipitations (IP) experiments. In the GST pull-down assay, *in vitro* transcribed and translated FLAG-Ccnd1 directly and specifically interacts with both recombinant full-length GST-α4 and the C-terminus fragment isolated from the cDNA library (GST-α4-C-terminus) corresponding to the intracellular loop and TM4 (Figure 18). This interaction is further tested *in vivo* in HEK 293 cells transfected with HA-α4-C-terminus together with FLAG-Ccnd1. IP of FLAG-Ccnd1 specifically co-IP HA-α4-C-terminus (Figure 19).

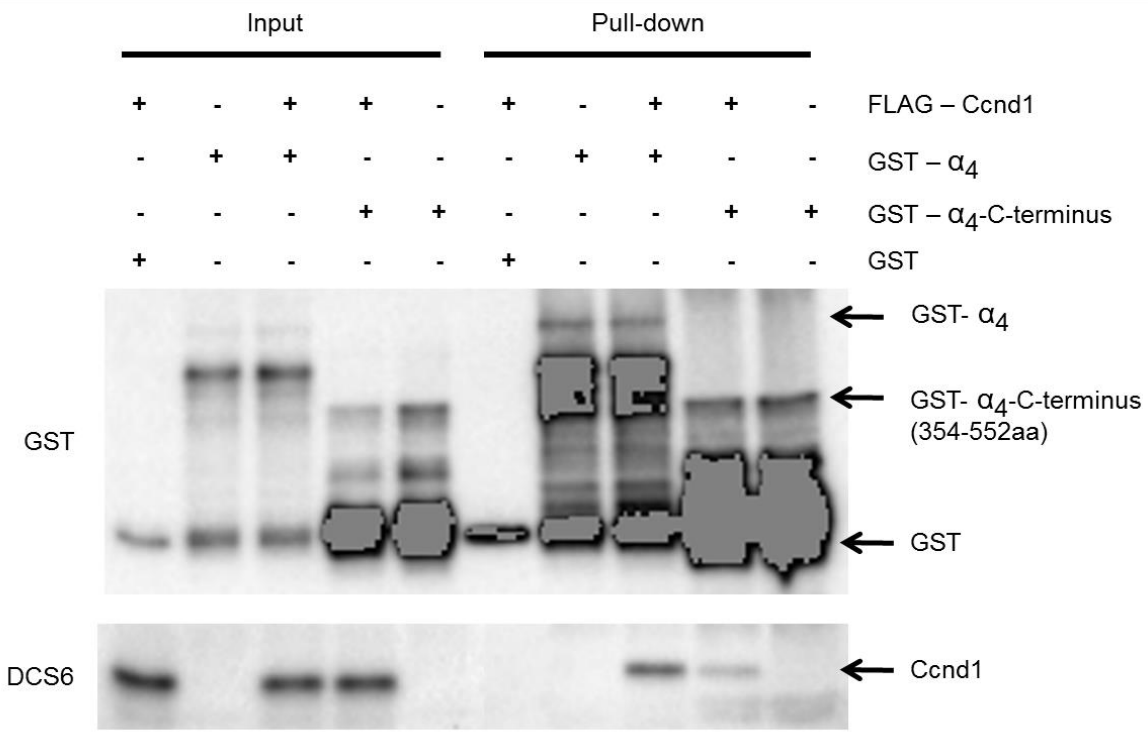

Figure 18: Ccnd1 interacts *in vitro* with the C-terminus of the α4 subunit of the $GABA_A$ receptor. GST, GST-α4 or GST-α4-C-terminus are purified from *E. coli* and immobilized on glutathione agarose beads, followed by incubation with *in vitro* transcribed and translated FLAG-tagged Ccnd1.Five separate reactions with the indicated components were set up. WBs using antibodies against GST and Ccnd1 before and after the pull-down are shown.

Therefore, these assays confirmed that Ccnd1 interacts with α4 through its C-terminal region that contains the intracellular loop between TM3 and TM4.

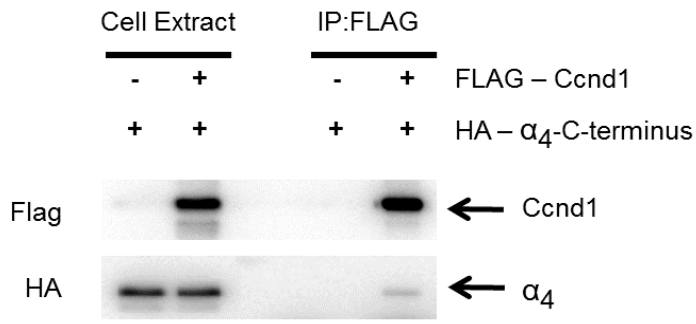

Figure 19: Heterologous Ccnd1 interacts with the C-terminus of α4 subunit of the type A GABA receptor. HEK 293 cells are co-transfected with HA-α4-C-terminus together with either FLAG-Ccnd1 or a control vector. After 24 h in culture, cells are collected for IPs with antiFLAG agarose beads. Cell extracts are collected before the addition of the antibody (inputs). WB of inputs and IP, antibodies used are listed on the left of the blot.

We wanted to study in a relevant model whether Ccnd1 and α4 co-localize. Detection of the endogenous proteins was precluded because the antibodies that were available did not work for immunofluorescence. Our goal was to use cortical neurons electroporated with Ccnd1 and α4. However, expression of Ccnd1 in these cells induces apoptosis (see Figure 10), consequently we had to use a Ccnd1-CAAX construct. Nonetheless, as a previous test, we checked the co-localization of overexpressed GFP-tagged α4 and HA-Ccnd1-CAAX in HEK293 cells by immunofluorescence and confocal microscopy (Figure 20). In this model, we observed mainly a cytoplasmic distribution of both proteins, which co-localized conspicuously at the cell boundary, presumably at the cell membrane.

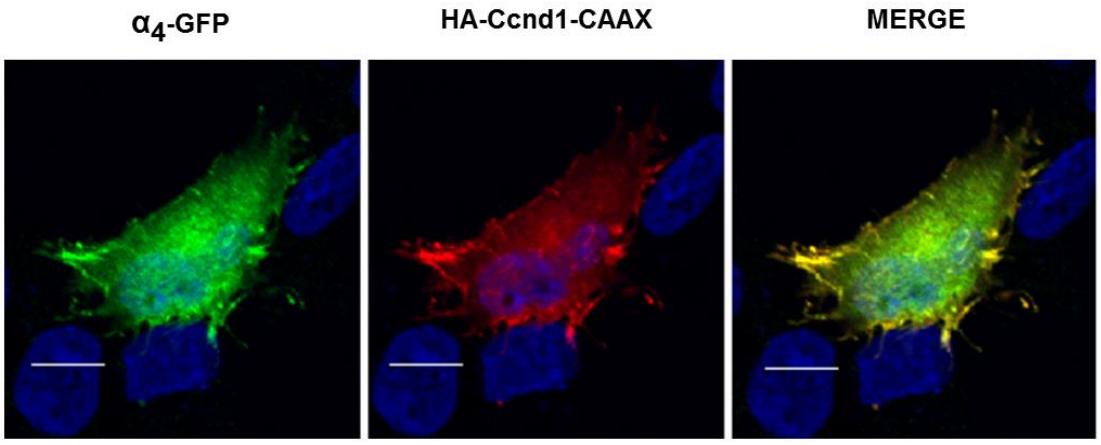

Figure 20: Cyclin D1-CAAX and α4 co-localize in HEK293T transfected cells. HEK 293 cells are co-transfected with α4-GFP and HA-Ccnd1-CAAX, fixed and labeled for immunofluorescence with anti-GFP (green) and anti-HA (red) antibodies. Co-localization can be seen as yellow color in the merge. Scale bar 10 μm. Images obtained by confocal microscopy.

Next, we used the same GFP-tagged α4 and HA-Ccnd1-CAAX to electroporate cortical neurons that were seeded, and fixed after 1 DIV. By immunofluorescence and confocal microscopy, both proteins co-localize in the soma as well as in the neurites (Figure 21). Thus, we can conclude that heterologously expressed α4-GFP and Ccnd1-CAAX co-localize in the cytoplasm, particularly in membranous regions, in both HEK293 cells and primary cortical neurons.

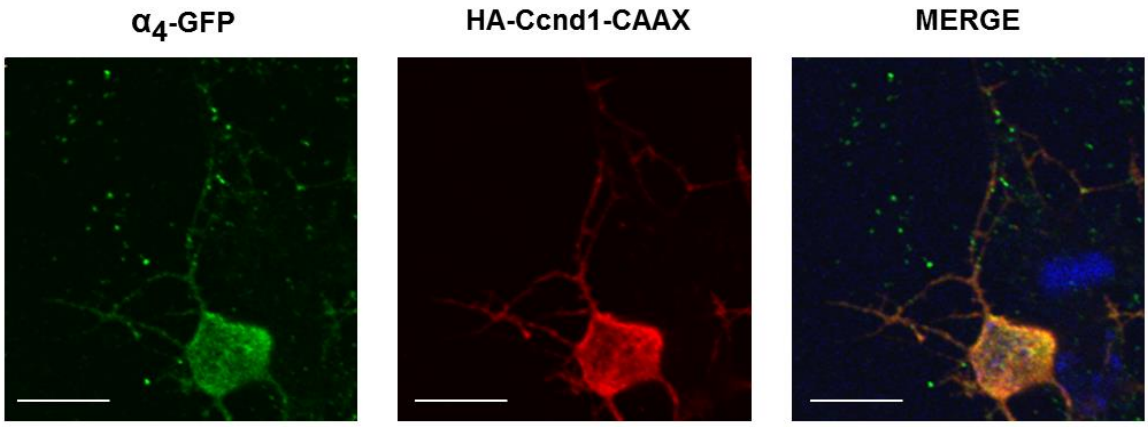

Figure 21: Heterologous α4 and Ccnd1-CAAX co-localize in primary cortical neurons. Mice cortical neurons are isolated from E15.5 mouse embryos and electroporated with HA-Ccnd1-CAAX and α4-GFP. At 1 DIV, cells are fixed and labeled with anti-GFP (green) and anti-HA (red) antibodies. Co-localization can be seen as yellow color in the merge. Scale bar 10 μm. Images obtained by confocal microscopy.

Finally, we wanted to detect the interaction between endogenous Ccnd1 and α4 to highlight its physiological significance. Hence, we looked at mRNA expression levels for α4 and Ccnd1 at the Allen brain atlas (Allen institute for brain science), and we realized that the two genes were highly expressed in the hippocampus of P56 adult mice (Figure 22).

Thus, we obtained hippocampi from adult female mice and performed an IP against Ccnd1 with a rabbit polyclonal antibody. As a control, we performed an IP in parallel with a rabbit polyclonal antibody against the FLAG epitope. In this experiment, we observed faint but specific co-IP of endogenous α4 with Ccnd1 (Figure 23).

Formerly, we have demonstrated not only the interaction between Ccnd1 and α4 subunit through the α4 intracellular loop, but also that both proteins co-localize at the cytoplasm and membranous regions when they are heterologously expressed in HEK293 cells and cortical neurons. Endogenously, we have detected the interaction between Ccnd1 and the α4 subunit of the $GABA_AR$ in the hippocampus of adult mice.

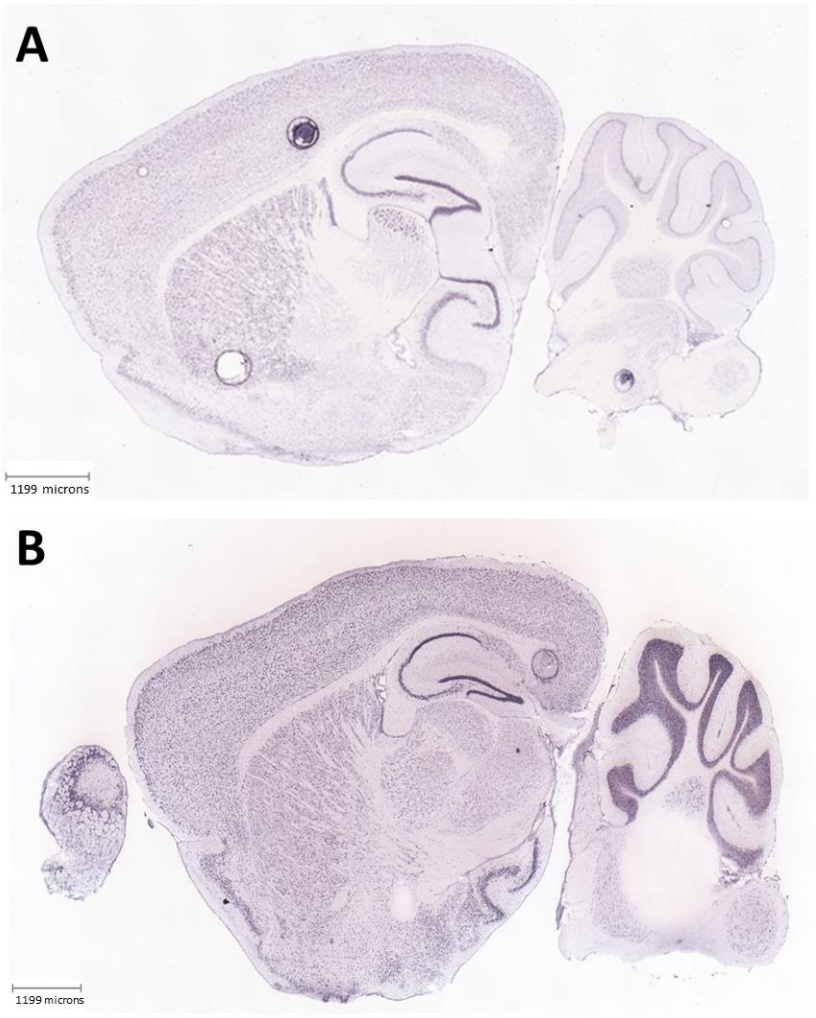

Figure 22: α4 subunit and CCND1 mRNA expression patterns in mouse adult brain. *In situ* hybridization results obtained for α4 **(A)** and CCND1 **(B)** in P56 mouse brain. Image credit: Allen brain atlas (Allen institute for brain science).

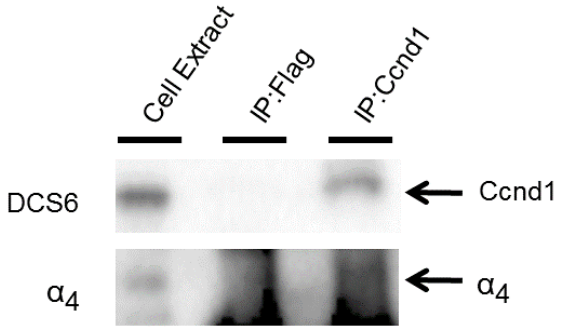

Figure 23: Endogenous Ccnd1 and α4 interact in adult hippocampus. Ccnd1 IP with a rabbit polyclonal antibody from an extract of adult mouse hippocampi. Whole cell extracts (WCE) are collected before the addition of the antibody for the IP. Lane IP Flag: control IP with rabbit polyclonal FLAG antibody. Lane IP Ccnd1: IP with rabbit polyclonal Ccnd1 antibody. WBs using antibodies against Ccnd1 and α4, before and after the immunoprecipitation are shown.

4.3.2. The alpha 4 subunit of the $GABA_A$ receptor as a phosphorylation target for cyclin D1-Cdk4 complex

The α4 subunit, as well as other $GABA_A$ receptor subunits, contains a large N-terminal extracellular loop, four transmembrane domains and an intracellular loop between TM3 and TM4 which is susceptible to phosphorylation (Figure 4A, Figure 24 and (*Abramian et al. 2010*)). α4 contains seven putative Cdk phosphorylation sites (serine-proline; threonine-proline), five of them located at the large intracellular loop between TM3-4 (Figure 24).

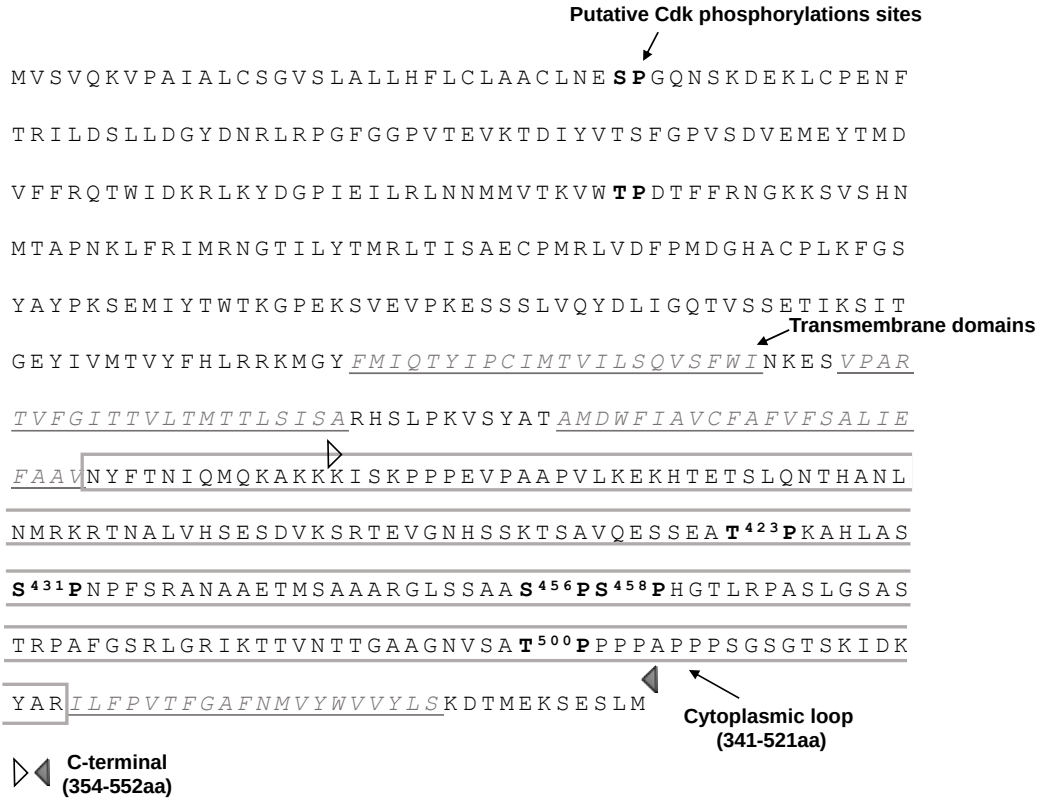

Figure 24: *Mus musculus* $GABA_A$ receptor α4 subunit amino acidic sequence. In bold, putative Cdk phosphorylation sites. In italics and underlined, four TM domains; framed, intracellular loop between TM3 and TM4. Between arrows, the C-terminal fragment from amino acid 354 to amino acid 552 found to interact with Ccnd1 in the yeast two hybrid assay.

Thus, we wondered whether Ccnd1-Cdk4 complex is able to phosphorylate this subunit of the $GABA_A$ receptor. For this, we carried out an *in vitro* kinase assay with a commercially available Ccnd1-Cdk4 complex purified from insect cells (Sigma) and a GST-α4 fusion protein purified from *E. coli* and γ-^{32}P-ATP. In this assay, we observed phosphorylation of GST-α4 that is dependent on the CDK complex and that is inhibited by Palbociclib, a specific inhibitor of Ccnd-Cdk4/6 complexes (Figure 25). Because Ccnd1-Cdk4 does not phosphorylate GST alone or fused

to a number of other proteins, we conclude that this CDK complex must phosphorylate α4 *in vitro*. To determine the precise α4 residues involved in the phosphorylation by the Ccnd1-Cdk4 complex different alleles of α4 were constructed by mutating the threonines and serines that are candidates to be targets of the complex in the intracellular loop. We changed threonines and serines for alanines resulting in non-phosphorylatable residues. Three different mutants were made: a double mutant T423 and S431 (T423A-S431A), another double mutant S456 and S458 (S456A-S458A) and a single mutant T500 (T500A).

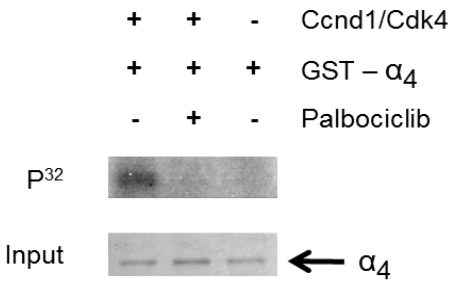

Figure 25: α4 is phosphorylated *in vitro* by the Ccnd1-Cdk4 complex. Ccnd1-Cdk4 complex (Sigma) is used in a kinase assay in the presence of γ-^{32}P-ATP to test the phosphorylation of GST-α4 purified from *E. coli*. The Cdk4/6 inhibitor Palbociclib (2 μM) is used to show that phosphorylation depends on Ccnd1-Cdk4 complex. Coomassie staining of α4 is shown in lower stripe (Input) as a loading control.

As shown in Figure 26, T423A-S431A results in a significant reduction of α4 phosphorylation in the kinase assay, while the other mutants display the same level of phosphorylation as WT.

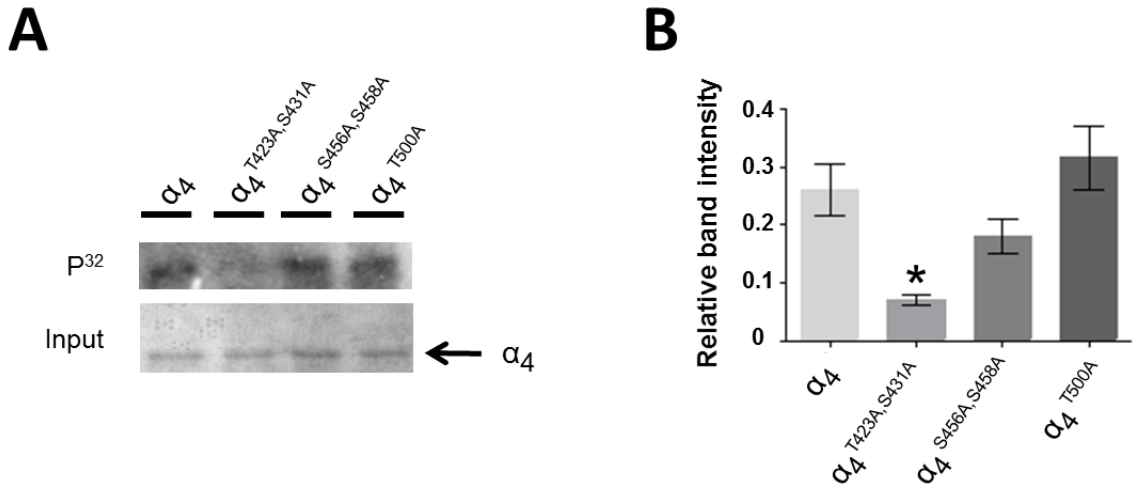

Figure 26: α4 T423A-S431A mutant has reduced phosphorylation by Ccnd1-Cdk4 complex. A) Ccnd1-Cdk4 complex (Sigma) is used in an *in vitro* kinase assay to detect the phosphorylation sites of α4. Three different non-phosphorylatable mutants of α4 are tested. Coomassie staining of the gel is shown in the lower stripe (Input) as a loading control. **B)** Quantifications of three independent experiments. Values are expressed as mean ± S.E.M. Statistical significance is determined by t-test (*p<0.05).

Moreover, the capacity of the Ccnd1-Cdk4 complex to phosphorylate the C-terminus region of α4 is tested *in vitro* (Figure 27). We found that the complex does phosphorylate α4 at the C-terminus (amino acids 354 to 552) and that there is a significant diminution in the phosphorylation levels when mutating T423 and S431 into non-phosphorylatable amino acids in two different clones.

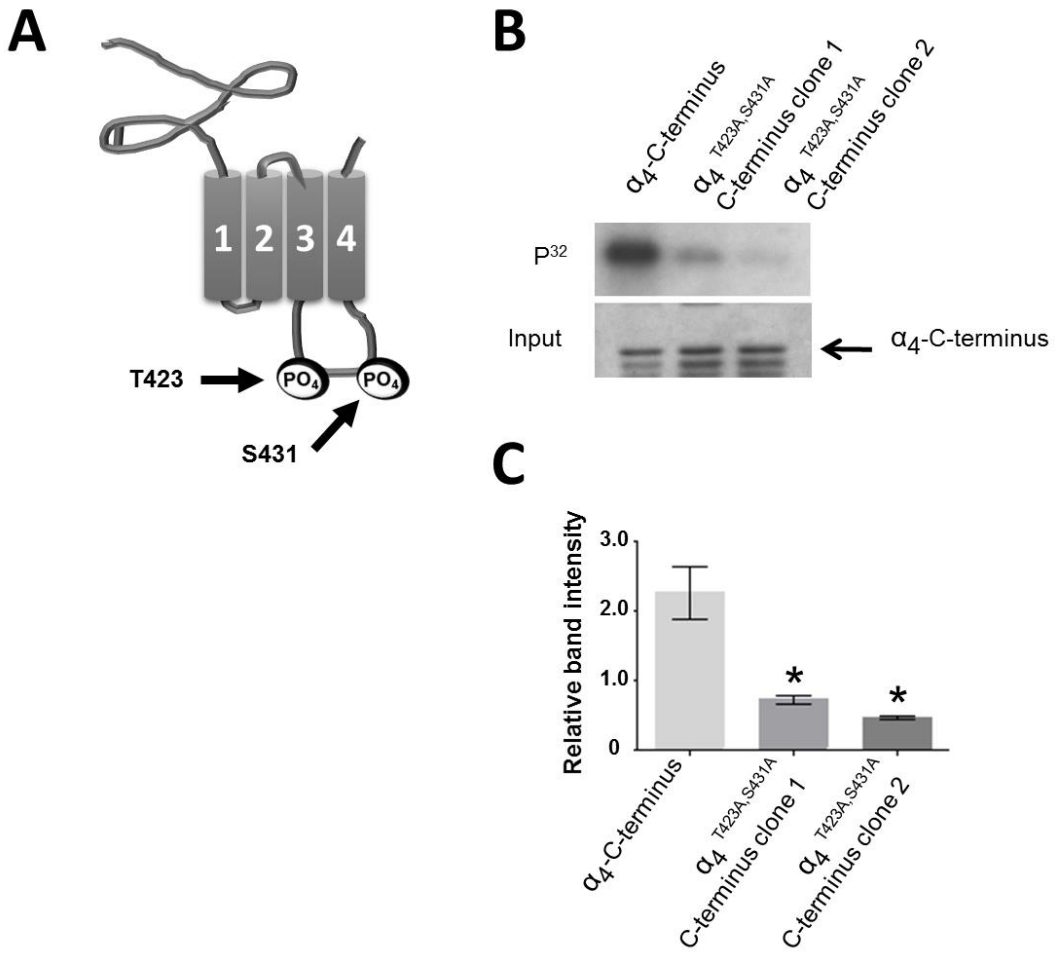

Figure 27: Residues T423 and S431 in the C-terminus of α4 are phosphorylated by Ccnd1-Cdk4 complex. A) Schematic representation of the Ccnd1-Cdk4 complex phosphorylation sites on α4 subunit of $GABA_A$Rs. Note their location at the intracellular loop. **B)** *In vitro* kinase assay performed with Ccnd1-Cdk4 complex (Sigma) using both GST-fused α4-C-terminus and two independent clones of GST-α4-$Cterminus^{T423A-S431A}$ non-phosphorylatable mutant. **C)** Quantifications of two independent experiments. Values are expressed as mean ± S.E.M. Statistical significance is determined by t-test (*$p<0.05$).

Furthermore, a non-radioactive kinase assay using GST-α4 C-terminus and Ccnd1-Cdk4 complex was analyzed by mass spectrometry (HPLC-MSMS). In this study (Table 7) only phosphorylation at T423 and S431 was detected. As a control, no phosphopeptides appeared when no ATP was added to the assay. Hence, all in all, we can conclude that residues T423 and S431 are the main, if not the only, phosphorylation targets of Ccnd1-Cdk4 in the α4 subunit of the $GABA_A$R.

Table 7: Mass spectrometry results of α4 phosphorylation by Cdk4-Ccnd1. Mass spectrometry of the peptides containing the different Cdk putative phosphosites in the presence (up) or absence (down) of ATP. Grey highlights show the phosphorylation of the threonine and the serine that correspond to those detected by the kinase assay. This phosphorylation is not observed when ATP is not present in the kinase reaction.

ID	Description	Score	Coverage	Proteins	Unique Peptides	Peptides	MW [kDa]
Q9D6F4	Gamma-aminobutyric acid receptor	309.37	33.70	1	16	17	60.8
Sample ATP	**Peptide sequence**	**Modifications**	**phoSite Probab**	**q-Value**	**M+H+ [Da]**	**ΔM [ppm]**	**RT [min]**
	TSAVQESSEATPK			0.002	1334.64	-1.09	15.99
	TSAVQESSEATPK	T11 (Phospho)	T(11): 100.0	0.012	1414.61	-1.91	15.92
	AHLASSPNPFSR			0.038	1283.64	-3.28	19.81
	AHLASSPNPFSR	S6 (Phospho)	S(6): 98.3	0.131	1363.61	-5.17	20.50
Sample no ATP	**Peptide sequence**	**Modifications**	**phoSite Probab**	**q-Value**	**MH+ [Da]**	**ΔM [ppm]**	**RT [min]**
	TSAVQESSEATPK			0.0000	1334.64	-0.91	16.33
	AHLASSPNPFS			0.0000	1283.64	-3.57	20.01

M+H+: proton adduct; ΔM: mass difference; RT: retention time; q-value: adjusted p-value.

4.3.3. Functional effects of the α4 phosphorylation by cytoplasmic Ccnd1-Cdk4 complex by whole-cell patch clamp in HEK tsA201 cells

Once we knew that Ccnd1-Cdk4 complex is able to phosphorylate the alpha4 subunit, we wanted to study if the $GABA_AR$ functionality is affected by this phosphorylation. One way to study the $GABA_AR$ functionality is by electrophysiology, measuring their run-down by whole-cell patch clamp. For this reason, we have collaborated with Dr. David Soto (Institut de Neurociències, Universitat de Barcelona), who has expertise in electrophysiology.

The run-down of the GABA response consists in a gradual loss of GABA-induced currents due to the repetitive GABA stimulation of $GABA_ARs$. To examine the run-down of GABA-mediated

currents by whole-cell patch clamp recordings, 1 μM GABA was applied to the cells once every 2 min (Figure 28).

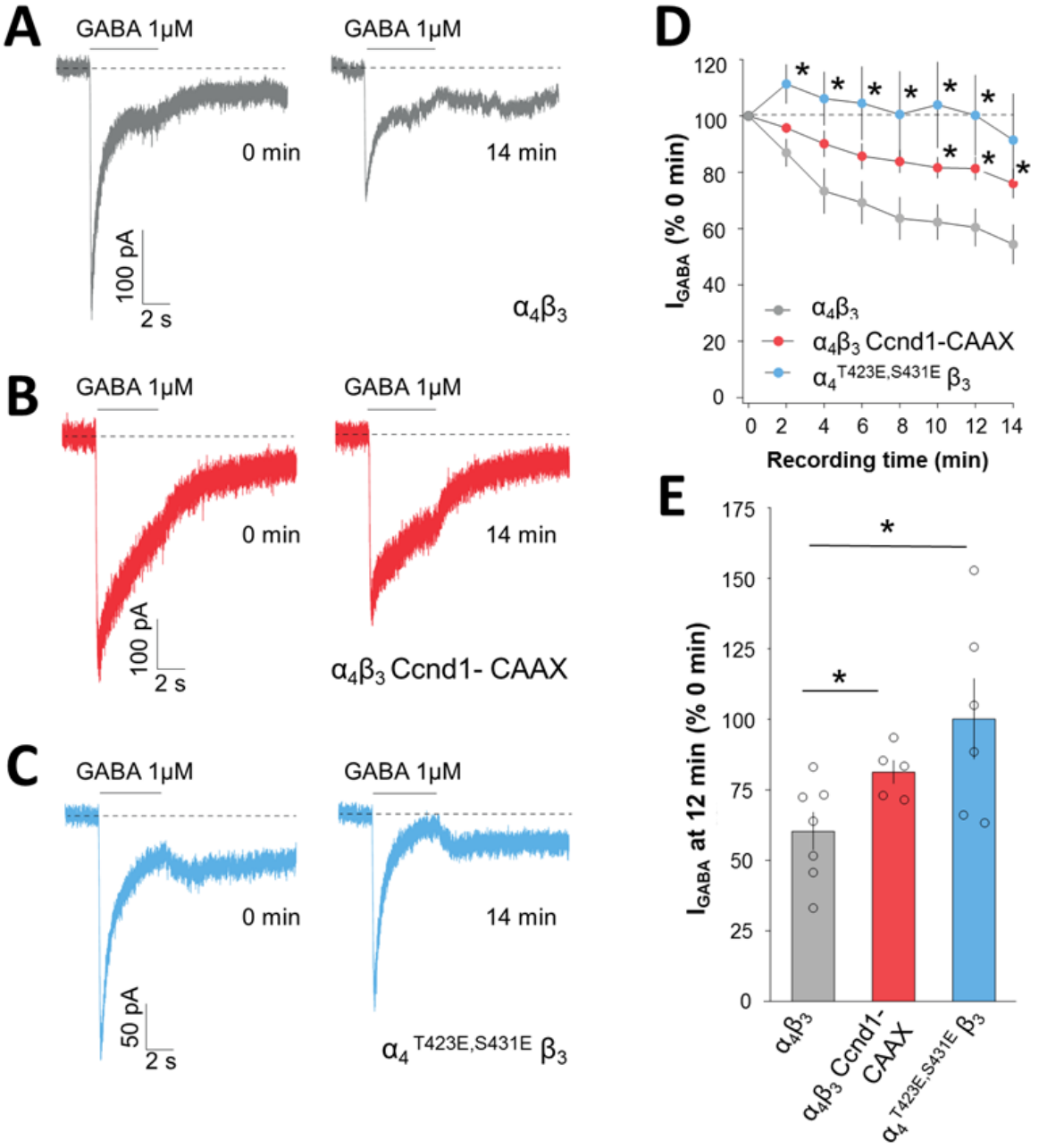

Figure 28: Cytoplasmic cyclin D1 or mimicking phosphorylation of the alpha 4 subunit of $GABA_A$ receptor prevent GABA receptor's run-down. A) Representative examples of whole-cell currents evoked by rapid application of 1 μM GABA (solid line above the trace) to tsA201 cells expressing WT α4β3 $GABA_AR$ plus a control vector. The GABA evoked current at the beginning of the recording (time 0 min) is shown on the left and the response after 14 min is shown on the right. Dashed line denotes the zero current. Holding potential is held at -60 mV. **B)** Same as A, but co-expressing WT α4β3 $GABA_AR$ plus Ccnd1-CAAX. **C)** Same as A, but co-expressing phosphomimetic $GABA_A$ receptor $\alpha4^{T423E,\ S431E}$ β3 plus a control vector. **D)** Time dependence relationship for $GABA_AR$-mediated currents for WT receptor alone (grey circles), together with Ccnd1 (red circles) or for phosphomimetic $GABA_AR$ (blue circles). *p<0.05, α4β3 vs. α4β3 + Ccnd1-CAAX and $\alpha^{4T423E,\ S431E}$ β3. **E)** Bar graph showing the mean ± S.E.M of the relative current at t=12 minutes compared with current at time=0 for cells expressing wild type α4β3 (n=7), α4β3 + Ccnd1-CAAX (n=5) or for $\alpha4^{T423E,\ S431E}$ β3 $GABA_ARs$ (n=6). Open circles denote single experiment values.

To study the physiological effects of cytoplasmic Ccnd1 on $GABA_AR$, HEK tsA201 cells are transfected with α4 and β3 subunits of the receptor together with Ccnd1-CAAX or a control plasmid. The transient expression of α4β3 receptors resulted in functional channels that generated GABA-evoked currents (Figure 28A and *Abramian et al. 2010*). When α4β3 receptors are expressed together with the control vector, GABA-mediated current amplitude decreased over time after 12 min of repetitive GABA stimulation (Figure 28A). By comparison, when α4β3 receptors are co-expressed with Ccnd1-CAAX, the response intensity after 12 min of $GABA_AR$ stimulation with its agonist was closer to the initial response (Figure 28B). Hence, the loss of function of the α4β3 receptors measured as a diminution in their responses after 10 to 14 min of stimulation is significantly prevented by the overexpression of Ccnd1-CAAX.

Besides, the heterologous expression of a phosphomimetic mutant of the alpha4 subunit ($\alpha4^{T423E, S431E}$) together with the β3 subunit prevents the run-down observed in the WT α4β3 $GABA_AR$ (Figure 28C). In fact, the overexpression of this phosphomimetic mutant averts the receptor run-down more efficiently than the overexpression of Ccnd1-CAAX (Figure 28D, E).

Therefore, cytoplasmic Ccnd1 or the phosphomimetic allele of α4 subunit maintains efficacy of α4β3 receptors.

4.3.4. Cyclin D-Cdk4/6 complex effect on the functionality of $GABA_A$ receptors in rat hippocampal slices.

Next, we wanted to study the effects of Ccnd1-Cdk4 complex on $GABA_AR$ in a physiological context. As mentioned before and according to *in situ* hybridization data available on the brain atlas (Allen institute for brain science) mRNA of both Ccnd1 and α4 are expressed at the hippocampus of adult mice (Figure 22). For this reason, we used rat hippocampal slices (P5-7) to measure GABA tonic currents and mIPSC. To evaluate the influence of α4 phosphorylation by Ccnd1-Cdk4, we inhibited Ccnd-Cdk4/6 complex by the addition of 2.5 μM Palbociclib. The following results were obtained in collaboration with Dr. José Antonio Esteban (CBMSO-UAM).

4.3.5. Cyclin D1-Cdk4/6 complex inhibition with Palbociclib

The inhibition of Ccnd1-Cdk4/6 is achieved by means of 2.5 μM Palbociclib for 2 h. The specificity of this drug at this dose has been described previously (*Fry et al. 2004*). However, we wanted to confirm the effect of Palbociclib in 400 μm hippocampal slices obtained from postnatal rats (P5-7).

For that, hippocampal slices are treated with either 2.5 μM Palbociclib or DMSO for 2 h, samples are collected and the activity of the complex is analyzed by measuring the levels of phosphorylation of the known Ccnd1-Cdk4 substrate Pxn in a WB (Figure 29).

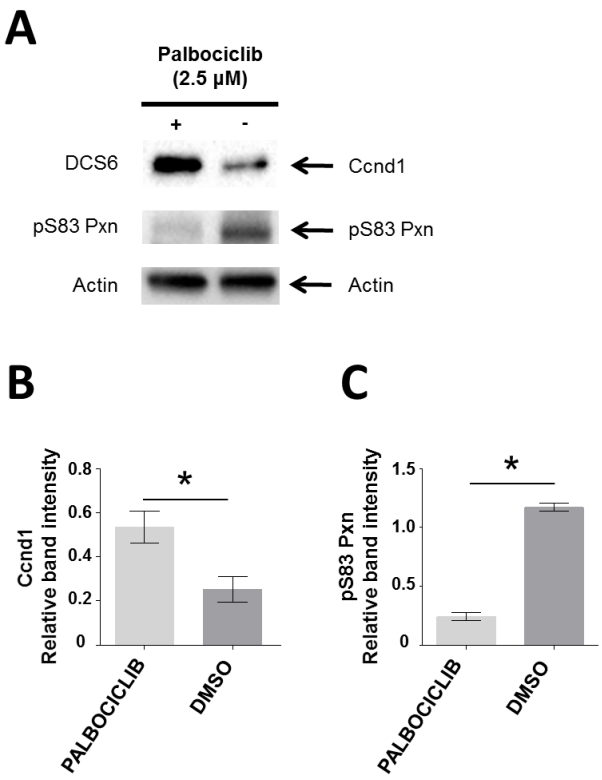

Figure 29: Inhibition of Cyclin D-Cdk4/6 complexes by 2.5 μM Palbociclib significantly reduces the phosphorylation state of paxillin at serine 83 in hippocampal slices. A). Phosphorylation of Pxn S83 is measured in 400 μm hippocampal slices previously treated with either 2.5 μM Palbociclib or DMSO during 2h. Immunoblot using a specific Pxn S83 antibody. Ccnd1 (Dcs6 antibody) levels are assessed and actin is used as a loading control. Lane 1: Palbociclib treated slices. Lane 2: DMSO treated slices are used as a control. **B)** Quantification of Ccnd1 normalized to actin levels. **C)** Quantification of P-Pxn S83 normalized to actin levels. Values are expressed as mean ± SEM (n=3). Statistical significance is determined by t-test (*$p<0.05$).

Since Pxn S83 is a phosphorylation target for Ccnd1-Cdk4 complex (*Fusté et al. 2016*), we tested the phosphorylation status of PaxS83 in both Palbociclib and DMSO treated samples. As it is seen, the treatment of hippocampal slices for 2 hours with Palbociclib, significantly reduces the Pxn phosphorylation at S83. Furthermore, the inactivation of the Ccnd-Cdk4/6 complex leads to an increment of Ccnd1. This is likely due to Ccnd1-Cdk4/6 inhibition by preventing its autophosphorylation and subsequent degradation.

4.3.6. Cdk4/6 role in GABA tonic currents

Once we have shown that 2.5 μM treatment with Palbociclib is capable of inhibiting Ccnd-Cdk4/6 complex in hippocampal slices, we aimed to study the effect of this inhibitor on $GABA_AR$-mediated tonic currents. Inhibitory tonic currents are usually measured applying a saturating specific $GABA_AR$ antagonist, such as picrotoxin. This drug causes a shift in the holding current related to a decrease in the operative $GABA_A$ channels (*Bright and Smart 2013b*). Briefly, rat hippocampal slices are treated with either 2.5 μM Palbociclib or DMSO for 2 h and placed into the patch clamp set-up with continuous perfusion of an external solution containing in addition to DMSO or 2,5 μM Palbociclib, AMPA receptor blocker (CNQX), NMDA receptor blocker (AP-V), glycine receptor antagonist (Strychnine) and 2-chloroadenosine. Cells are held at – 60mV during the recording. To measure inhibitory events at this voltage, high chloride concentrations in the internal solutions are used. Then CA3 to CA1 synapses are evoked by Schaffer collateral stimulation (Figure 30A). Once both the holding current and the peak amplitude of the synaptic response are stabilized (baseline), picrotoxin 100 μM is added (t= 0 min). Picrotoxin, an antagonist of synaptic $GABA_AR$, takes about 2 min to inhibit the synaptic response. For each cell, GABA tonic current is defined by the outward shift of the base-line current after the application of the antagonist picrotoxin (100 μM), once the synaptic response is mostly abolished (average of the holding current during one minute). Figure 30B shows the shift in the holding current produced by the picrotoxin addition. Each point represents the mean values of holding current at a specific time for 10 cells. While the holding current in DMSO treated cells diminishes 21.39 ± 3.81 pA, the holding current in Palbociclib treated cells diminishes 9.11 ± 2.92 pA (Figure 30C). Therefore, cyclin D-Cdk4/6 inhibition by acute Palbociclib application causes a significant diminution in the $GABA_AR$ tonic current.

4.3.7. Cdk4/6 role in GABA mIPSC

Because Ccnd-Cdk4/6 inhibition with 2.5 μM Palbociclib significantly reduced GABA tonic currents in hippocampal slices, we decided to test whether this acute Ccnd inhibition may in turn affect synaptic function given that α4 subunit can form synaptic receptors when clustered together with βxγ2 subunits. To this end, organotypic cultures are treated with either DMSO or 2.5 μM Palbociclib for 2 h and placed at the electrophysiology set-up with continuous perfusion of external solution containing aCSF supplemented with either DMSO or 2.5 μM Palbociclib, plus pharmacological inhibitors of the excitatory neurotransmitters' receptors (CNQX and AP-V) and the glycine receptor antagonist (Strychnine). When measuring mIPSCs the addition of TTX to inhibit the generation of spontaneous action potentials is also necessary. mIPSCs are recorded at -60 mV using whole-cell configuration in the gap-free mode.

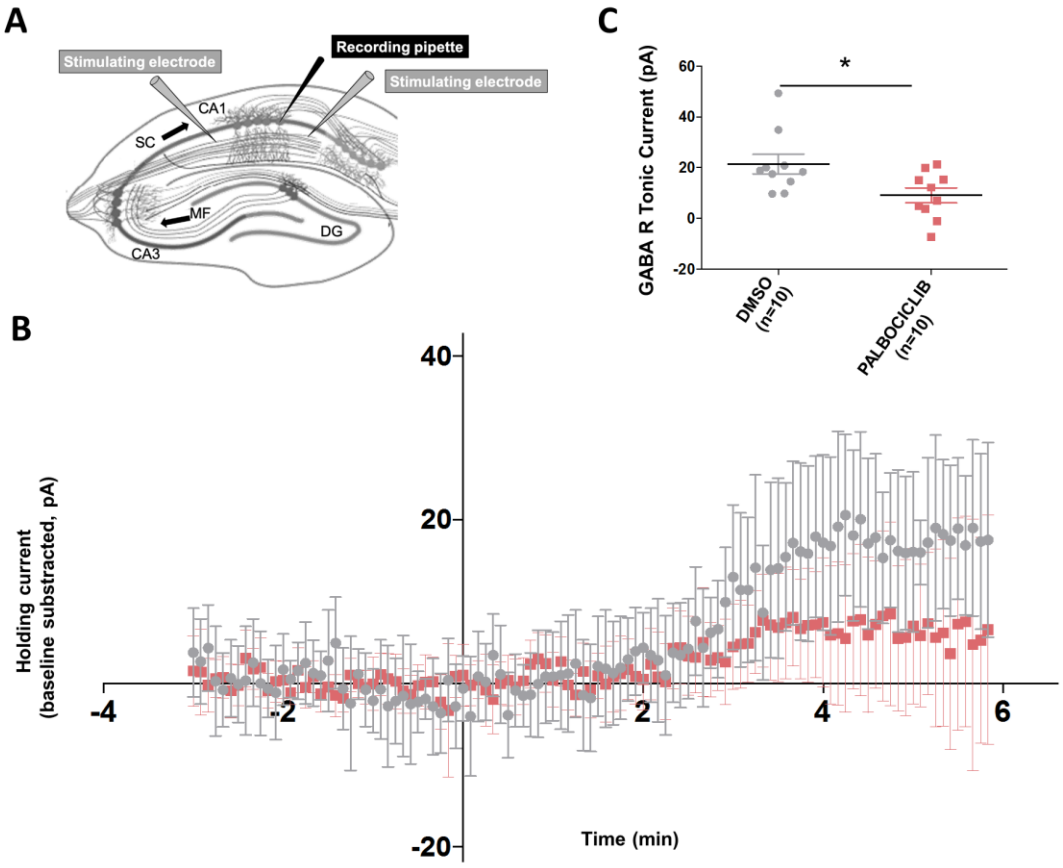

Figure 30: Cyclin D-Cdk4/6 inhibition with Palbociclib significantly reduces GABA tonic currents in hippocampal slices. A) Schematic representation of the experimental configuration for GABA tonic currents recordings in CA1 neurons. **B)** Effects of picrotoxin (100 μM) on holding currents recorded in DMSO (grey rounds) or Palbociclib (red squares) (2,5 μM, 2 hours) treated hippocampal slices. Tonic currents are reduced in Palbociclib treated slices compared to vehicle (n=10 for each). Recordings are aligned by the time of drug addition (t=0). **C)** Quantification of results in A represented in a scatter dot plot shows mean values ± S.E.M (*p<0.05, Wilcoxon-Mann-Whitney test).

To measure inhibitory events at this voltage, high chloride concentrations in the internal solutions are used. Thus, by inhibiting the generation of action potentials and not evoking GABA responses, one is able to measure the spontaneous release of GABA vesicles and the consequent response generated at postsynaptic $GABA_AR$, that is the mIPSC. Under these conditions, we observed that both the amplitude and frequency of the spontaneous response are reduced after Ccnd-Cdk4/6 inhibitor treatment (Figure 31). Specifically, the addition of Palbociclib to the cells significantly reduces mIPSC amplitude (-105.87 ± 20.30 pA for DMSO vs -50.78 ± 5.08 pA for Palbociclib). Besides, the frequency of mIPSC in Palbociclib-treated slices is lower than for controls (0.9 ± 0.51 Hz vs 0.48 ± 0.17 Hz respectively) although the difference is not statistically significant.

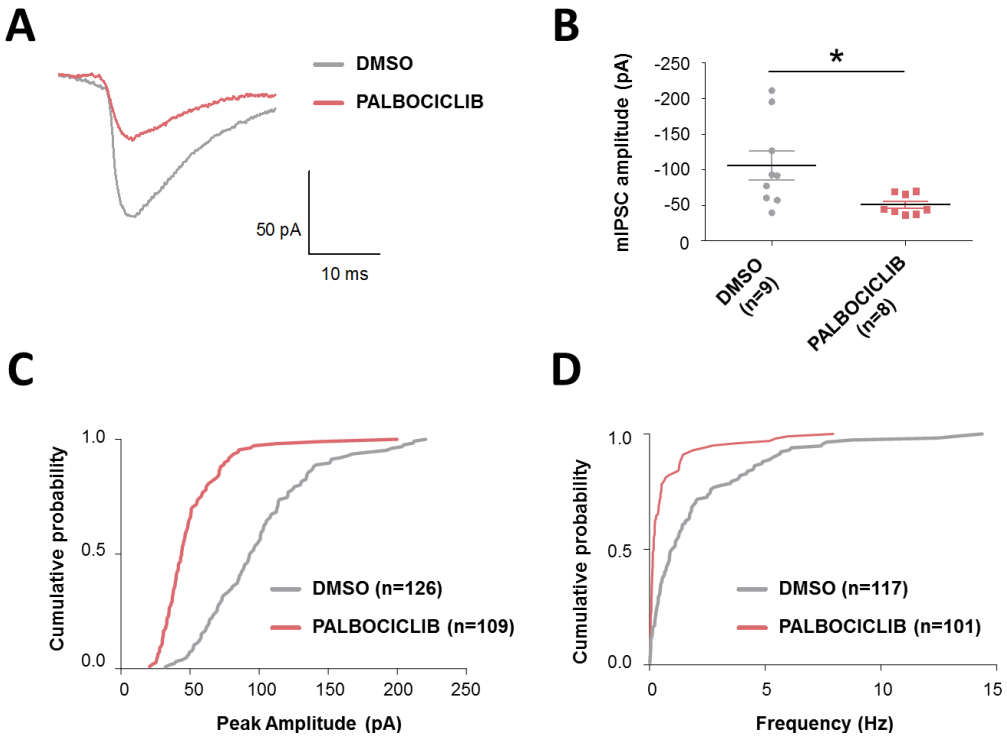

Figure 31: Palbociclib treatment decreases both mIPSC amplitude and frequency in organotypic hippocampal slices. A) Representative traces of miniature inhibitory post-synaptic currents of DMSO or 2.5 μM Palbociclib treated cells. Bars: (horizontal) 10 ms; (vertical) 50 pA. **B)** Scatter dot plot showing mIPSC amplitude quantifications of DMSO (n=9) and Palbociclib (2.5 μM, 2 hours) treated cells (n=8). Bars show mean values ± S.E.M. *p<0.05, Wilcoxon-Mann-Whitney test. **C)** Cumulative distribution of mIPSC amplitude from CA1 pyramidal neurons treated with either Palbociclib or control vehicle, as indicated. "n" represents number of miniature responses recorded from nine (DMSO) and eight (Palbociclib) cells. **D)** Similar to C for mIPSC frequencies. "n" represents number of miniature frequencies recorded from eight (DMSO) and five (Palbociclib) cells. The frequency of the two groups is compared using Wilcoxon-Mann-Whitney test.

Put together, all electrophysiological experiments show that Ccnd1 enhances $GABA_ARs$ function presumably through α4 phosphorylation.

4.4 Cytoplasmic cyclin D1 role in the assembly of α4β3 containing $GABA_A$ receptors.

4.4.1. Cyclin D1 interaction with β3 subunit of the $GABA_A$ receptor

Once we had characterized the interaction of Ccnd1 and α4 subunit, we wondered whether Ccnd1 was also interacting directly with the β3 subunit. For this, a pull-down assay was performed using GST-β3 and flag-tagged Ccnd1 as described before for α4 (Figure 18). Under these conditions, we also detect a directed and specific interaction between β3 and Ccnd1 (Figure 32).

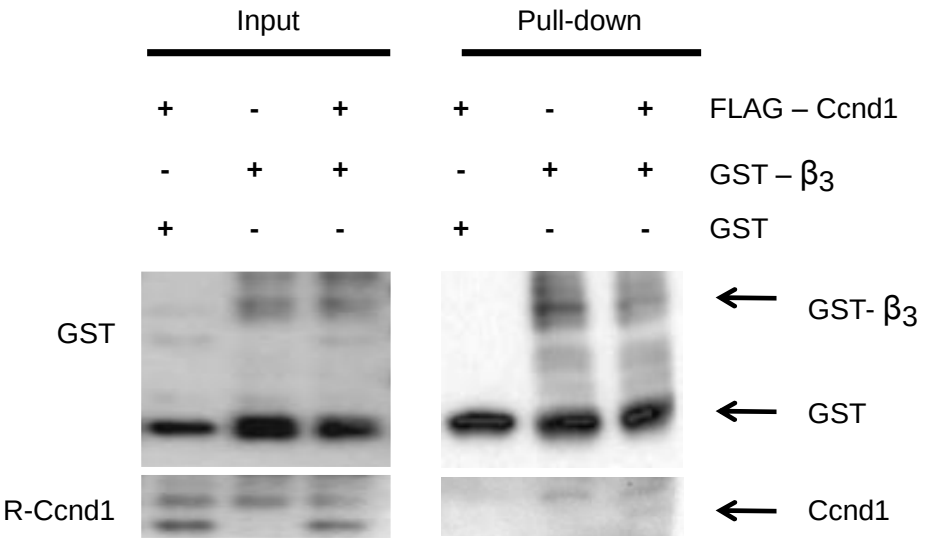

Figure 32: Cyclin D1 interacts with β3 *in vitro*. In vitro GST pull-down assay showing a direct interaction between β3 and Ccnd1. GST or GST-β3 purified from *E. coli* are immobilized on glutathione beads, followed by incubation with FLAG-tagged Ccnd1 obtained by *in vitro* transcription and translation in reticulocyte lysate system (Promega). WB showing the input and pull-down samples. GST and GST-β3 were detected with an anti-GST antibody; Ccnd1 was detected with a rabbit anti-Ccnd1 antibody.

Further, this interaction is tested in HEK293 cells by heterologous co-expression of flag-tagged β3 and HA-Ccnd1-CAAX, and then immunoprecipitating β3-FLAG. As Figure 33 shows, HA-Ccnd1-CAAX co-immunoprecipitates with β3-FLAG in this assay. Hence, not only can Ccnd1 interact with α4 but also with the β3 subunit of $GABA_A$Rs *in vitro* and *in vivo*.

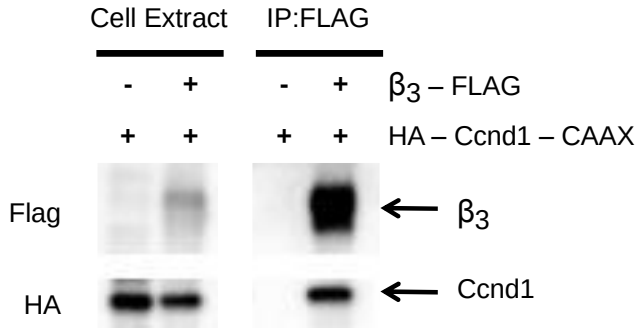

Figure 33: Heterologous HA-Ccnd1-CAAX interacts with β3-FLAG. HEK 293 cells are co-transfected with HA-Ccnd 1-CAAX and either β3-FLAG or a control vector. After 24 hours in culture, cells are collected for IP with M2-FLAG beads. WB of the cell extract and immunoprecipitation (IP) is shown. Antibodies used for protein detection are indicated on the left of the blot.

As for other subunits, β3 sequence contains a large cys-loop extracellular domain at the N-terminal, four helical TM and two cytoplasmic domains (Figure 34). Although the large intracellular loop between TM3-4 is phosphorylated by other kinases, β3 does not have any putative CDK phosphorylation site (serine-proline; threonine-proline).

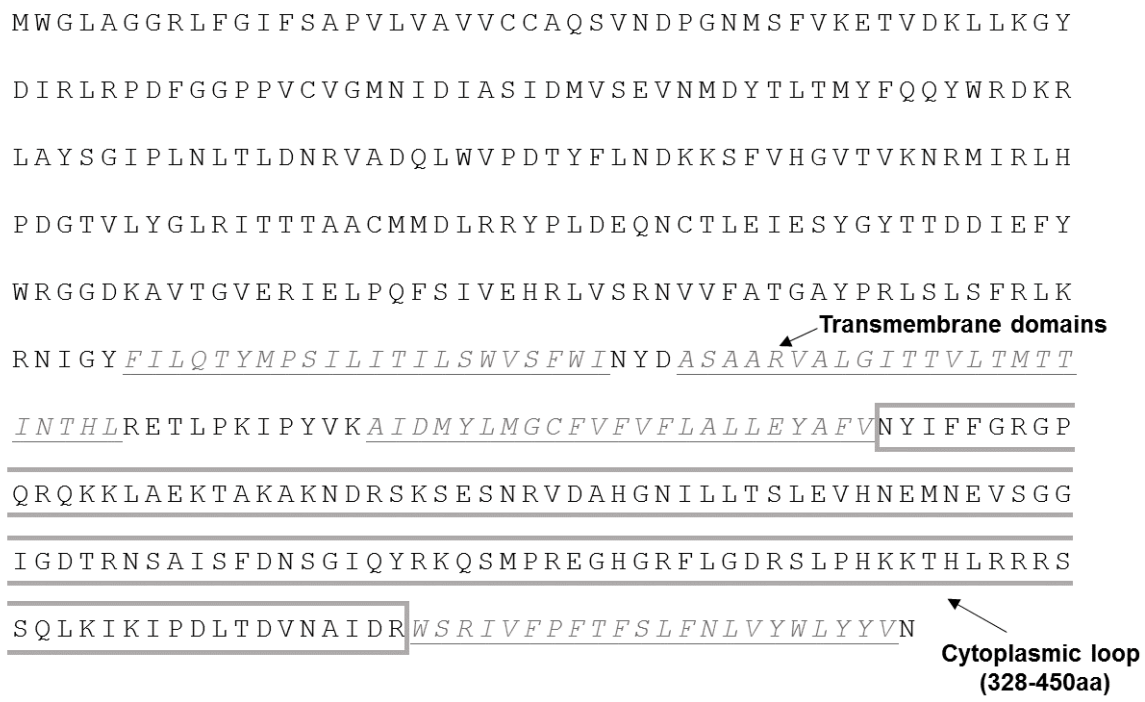

Figure 34: Human $GABA_A$ receptor β3 subunit amino acidic sequence. Underlined and in italics, four TM domains; framed, intracellular loop between TM3 and TM4. Note that nor S-P neither T-P putative phosphorylation sites for CDKs are found.

Although β3 does not have any putative Cdk phosphorylation site, we tested the capacity of the Ccnd1-Cdk4 complex to phosphorylate β3 in an *in vitro* assay. As expected, Ccnd1-Cdk4 purified from insect cells (Sigma) does not phosphorylate GST-β3 recovered from heterologous expression in *E. coli* (Figure 35).

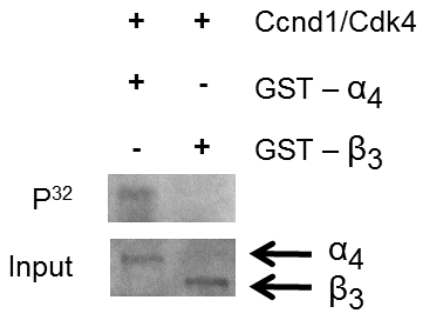

Figure 35: β3 is not an *in vitro* substrate of Cyclin D1-Cdk4 complex. Ccnd1-Cdk4 complex (Sigma) is used in a kinase assay in the presence of γ-^{32}P-ATP to test the phosphorylation of GST-β3 purified from E. coli. Coomassie staining of the gel is shown in the lower stripe (input) as a loading control.

4.4.2. Cytoplasmic cyclin D1 effect on α4 and β3 surface levels

Abramian and collaborators have shown that α4 phosphorylation at the intracellular loop (S443) by PKC enhances α4 subunit levels at the cell surface of HEK293 cells expressing heterologous α4β3 receptors (*Abramian et al. 2010*). Moreover, this increment in α4 levels at the cell surface prevents $GABA_AR$ run-down. Because Ccnd1-Cdk4 phosphorylates α4 *in vitro* and cytoplasmic Ccnd1 affects $GABA_AR$ run-down in tsA201 cells, we wanted to investigate whether Ccnd1 is modulating the surface levels of α4 and β3 subunits.

For this reason, HEK293 were co-transfected with β3-FLAG and α4 plus either a control vector, HA-Ccnd1-CAAX, or HA-$Ccnd1^{K112E}$-CAAX, and a surface biotinylation assay was carried out. Briefly, 24 h after transfection, cells were labeled with sulfo-NHS-SS-biotin which forms covalent bonds with primary amines on surface proteins. After washing, cells were lysed and biotin-labeled proteins were isolated with Streptavidin-agarose beads (Figure 36A). The expression levels of both α4 (Figure 36B) and β3 (Figure 36C) were normalized to transferrin receptor protein (TFRC) levels. As shown in Figure 36, neither cytoplasmic Ccnd1-CAAX nor $Ccnd1^{K112E}$-CAAX alter the surface levels of the α4 subunit significantly. However, α4 surface levels tend to increase when Ccnd1-CAAX is present (19 ± 12 %) but not with $Ccnd1^{K112E}$-CAAX. Contrary, β3 subunit surface levels are decreased due to the presence of Ccnd1-CAAX (29 ± 5 %) and, to a less extend, of $Ccnd1^{K112E}$-CAAX (12 ± 8 %). Hence, cytoplasmic Ccnd1 presence lightly increases the amount of α4 and significantly reduces β3 subunits at the cell surface.

Moreover, and in order to understand the mechanism by which cytoplasmic Ccnd1 is affecting α4 and β3 surface levels, further studies are done. We also designed an experiment to test whether the receptor endocytosis during its turnover was specifically affected by Ccnd1. The approach is similar to the one described above but with certain modifications.

Transfected HEK293 are labelled with biotin, washed and incubated for 15 min at 37 ºC with medium to allow endocytosis of labelled proteins. After this, cells are incubated with a cleavage buffer containing glutathione, which breaks the disulfide bond between biotin and surface proteins, to eliminate the biotin labeling of remaining surface proteins. Subsequently, cells are collected and biotin-labelled proteins, which correspond to endocyted proteins, are pulled down with Streptavidin-agarose beads and analyzed by WB (Figure 37A). Quantifications are calculated as the fraction of protein endocyted (labeled 15') compared to the surface levels at time 0 (0h). For α4 subunit, 41% and 40% of the initial protein at the cell surface was internalized in control conditions (pNBM470) or in the presence of cytoplasmic Ccnd1, respectively (Figure 37B).

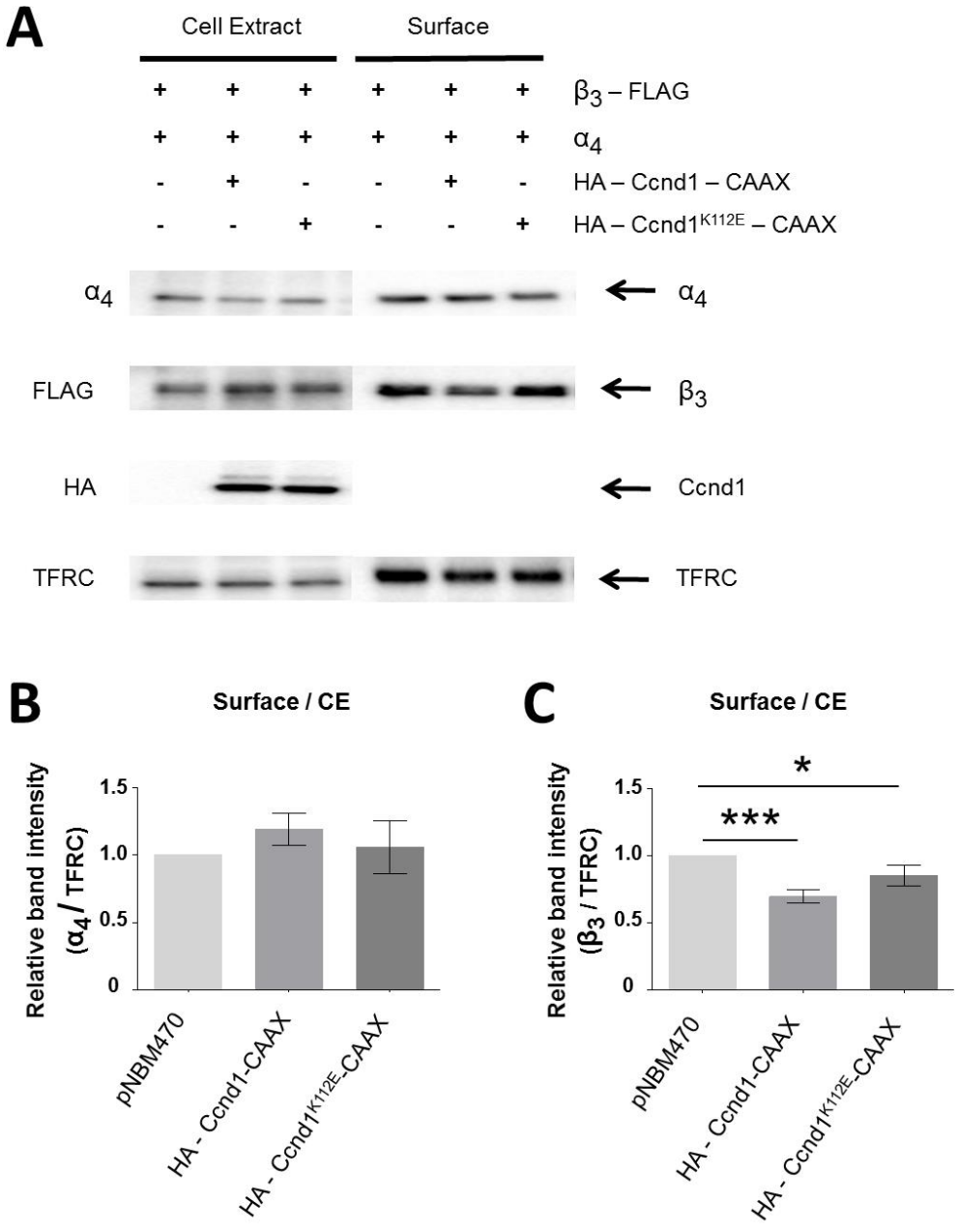

Figure 36: Cyclin D1-CAAX presence diminishes surface levels of β3, but not α4, subunit. A) HEK293 are co-transfected with β3-FLAG and α4 plus either HA-Ccnd1-CAAX or HA-Ccnd1^{K112E}-CAAX or a control vector. A biotinylation assay is used to purify cell surface proteins. TFRC is used to normalize α4 and β3 levels. WB shows cell extract and surface proteins. Antibodies used for protein detection are indicated on the left of the blot. **B** and **C)** Quantifications of the experiment in A as a ratio surface:CE. Bars show mean values ± S.E.M (n=4 independent experiments) of the ratio surface vs total protein levels. *p<0.05; ***p<0.001 (t-test, compared to control).

For the β3 subunit, these values were 34% and 39%, respectively (Figure 37C). Hence, overexpression of HA-Ccnd1-CAAX does not result in any significant change in the endocytosis process of neither α4 nor β3 subunits.

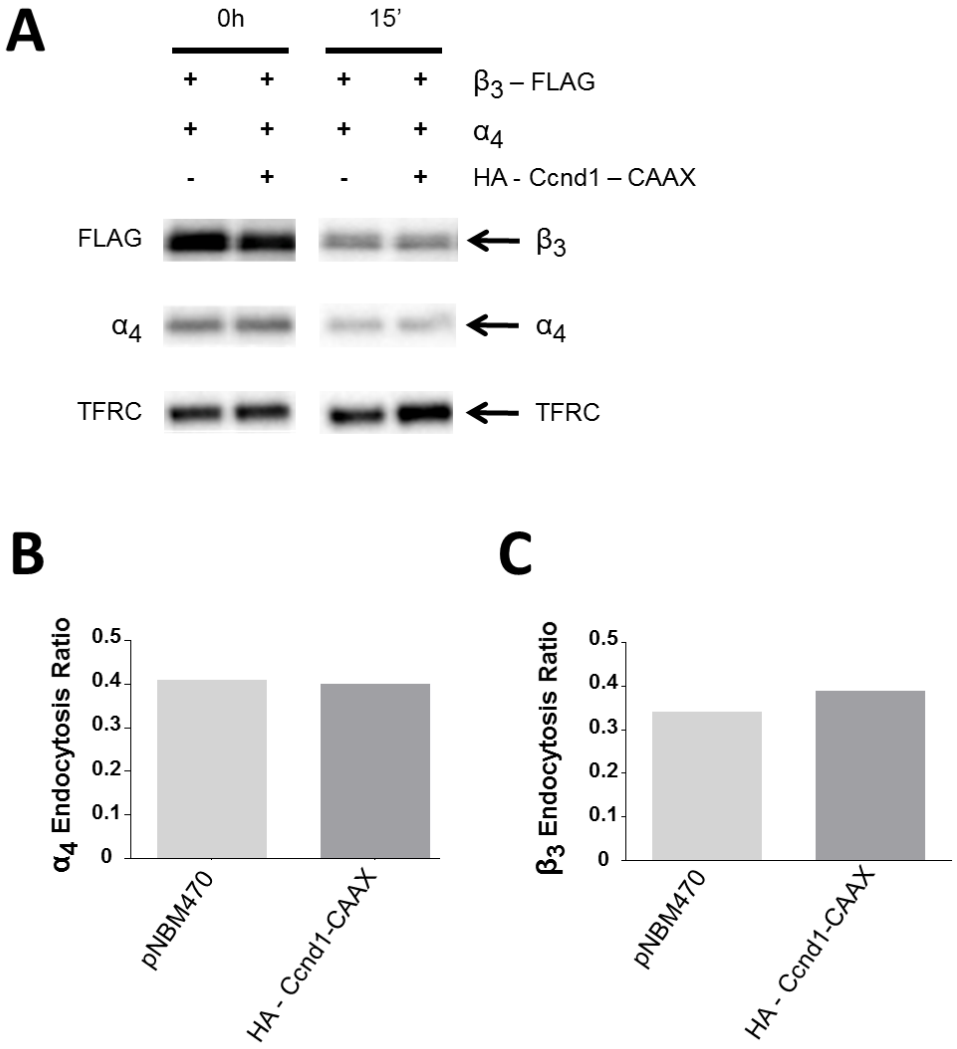

Figure 37: Endocytosis process of the α4 and β3 subunits is not affected by cytoplasmic cyclin D1 in HEK293 cells. Heterologous α4 and β3-FLAG with or without HA-Ccnd1-CAAX are expressed in HEK293 cells. Endocytosis is assessed by biotin labelling of surface proteins followed by 15 min DMEM incubation to allow endocytosis, and cleavage of the biotin bound to the remaining surface proteins. Biotin-labelled fractions are purified with streptavidin-agarose beads. **A)** Western blot analysis of samples taken at time 0h (total surface proteins) and after 15' of endocytosis. Antibodies are indicated on the left of the blots. **B)** Quantification of α4 levels. Results are shown as a ratio of the amount of protein endocyted for 15 min compared to the initial levels (0h). **C)** Quantification of β3 levels as just mentioned for α4.

Next, we tested whether the receptor insertion into the membrane is affected by the presence of cytoplasmic Ccnd1. Again, HEK293 are transfected with α4 and β3 subunits together with HA-Ccnd1-CAAX or pNBM470 as a control vector. Cell surface proteins are labelled with biotin and further cleaved with cleavage buffer containing glutathione, as described above, and cells are collected at this point (t=0h) or incubated with medium for 2 h at 37 ºC, so that new receptors are inserted into the membrane, and can be subjected to a new round of biotin labelling (t=2h) (Figure 38).

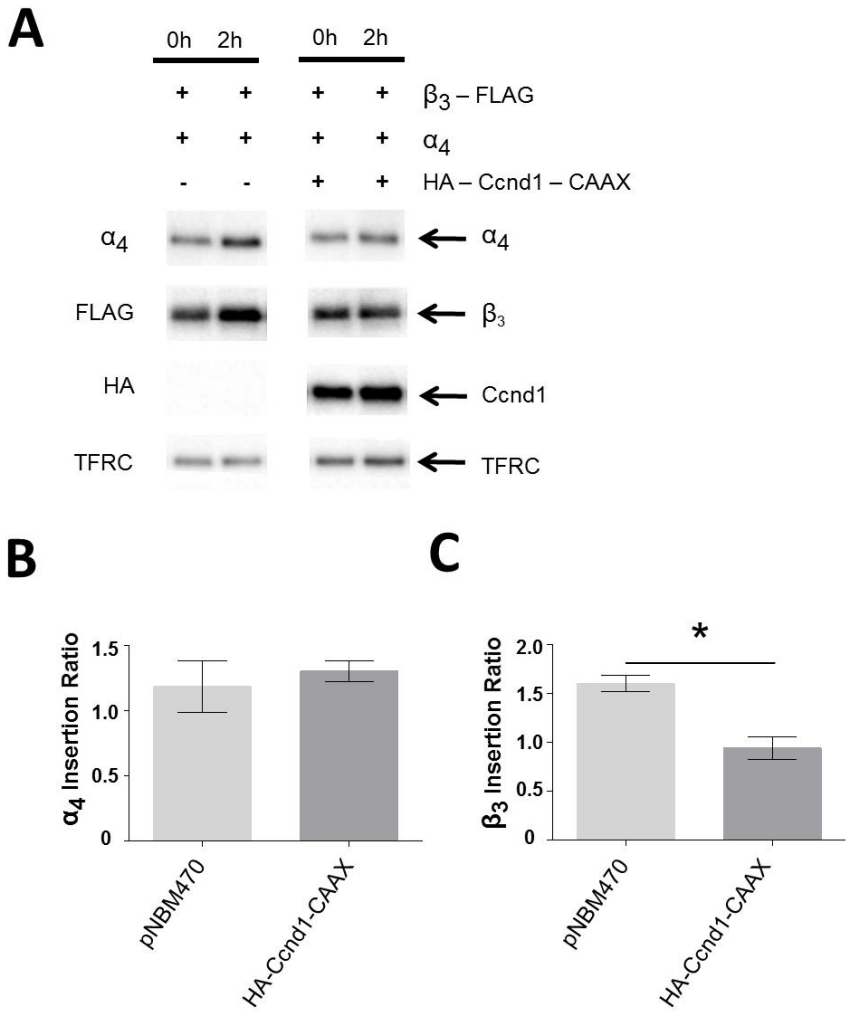

Figure 38: Cytoplasmic cyclin D1 decreases the insertion of β3 to the cell surface in HEK293. A) Heterologous α4 and β3-FLAG subunits are expressed in HEK293 cells in the presence (lanes 3 and 4) or not (lanes 1 and 2) of HA-Ccnd1-CAAX. Cells are subjected to biotinylation, cleavage and 2 hours of incubation with medium at 37 ºC followed by biotin labelling. Cell surface fractions are purified with streptadivin-agarose beads. WBs are immunoblotted with the antibodies indicated on the left of the blot. The insertion rate for each α4 and β3 is measured by comparing the labelling at time 0h and time 2h. **B** and **C)** Quantification of α4 and β3 levels normalized to TFRC. Results are shown as a ratio of the amount of protein at 2h compared to the initial levels (0h). *p<0.05 (t-test).

As it is seen in Figure 38B, in control conditions, after the cleavage and the incubation with DMEM for 2 hours, there are slightly higher levels of α4/TFRC at the cell surface (1.2 times). This same effect is seen when Ccnd1 is present with an increment of 1.3 times of α4/TFRC at the cell surface. On the other hand, Figure 38C shows the effects observed for β3. There is a significant increase in the amount of β3/TFRC at the cell surface (1.6 times) in control conditions. Contrary, the presence of cytoplasmic Ccnd1 avoids the insertion of the β3 subunit at the cell surface after 2 hours of incubation. Hence, the co-transfection of HA-Ccnd1-CAAX with the α4

and β3 subunits in HEK293 cells results in a lowering of the insertion rate of the β3, but not α4, subunit at the cell surface. Henceforth, cytoplasmic Ccnd1 diminishes β3 subunit levels at the cell surface by hindering its insertion to the membrane, but not its endocytosis.

Finally, since β3 stability and levels at the cell surface are affected by its ubiquitination (*Saliba et al. 2007, 2008*), the role of Ccnd1 on β3 in this process is tested. The ubiquitination assay is performed in HEK293 co-transfected with α4 and β3-FLAG together with pNBM470 (control plasmid), HA-Ccnd1-CAAX or the kinase inactive allele HA-Ccnd ^{K112E}-CAAX. We then carried out an IP of β3-FLAG with FLAG antibody and used a ubiquitin antibody to detect ubiquitinated forms of β3 by WB (Figure 39A).

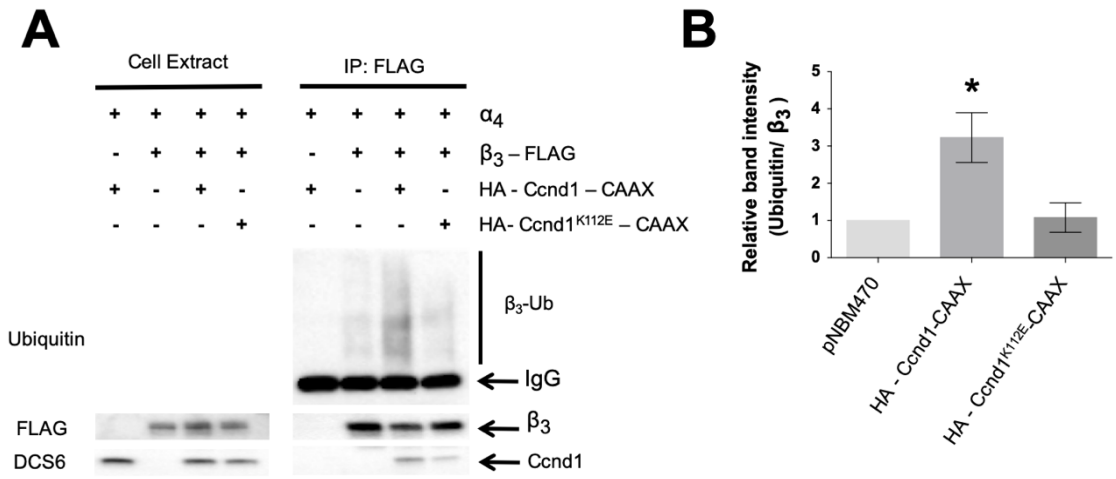

Figure 39: Cyclin D1-CAAX promotes ubiquitination of β3 in HEK293. A) Heterologous β3-FLAG is immunoprecipitated with FLAG antibody-conjugated beads. The levels of ubiquitination are evaluated in samples containing control vector (Lane 2), HA-Ccnd1-CAAX (Lane 3) or the kinase mutant HA-Ccnd1^{K112E}-CAAX (Lane 4). The specificity of the immunoprecipitation is checked in lane 1 (no β3-FLAG present). Antibodies used are indicated on the left of the blot. **B)** Quantification of β3 ubiquitination levels normalized to total β3. *p<0.05 (t-test compared to control).

Overexpression of HA-Ccnd1-CAAX significantly increases β3 ubiquitination (3.23 ± 0.67 fold increase) compared to control (pNBM470 vector). Moreover, this effect is kinase- dependent since the overexpression of HA-Ccnd ^{K112E}-CAAX does not increase the ubiquitination of β3 (1.08 ± 0.39 fold increase). All together these results suggest that Ccnd1 is decreasing the surface levels of the β3 subunit by hindering its insertion into the membrane and increasing β3 ubiquitination in a kinase-dependent manner.

DISCUSSION

5. DISCUSSION

5.1 Cytoplasmic cyclin D1-Cdk4/6 complexes induce neuritogenesis in cortical neurons

Pointed up by previous observations (*Sicinski et al. 1995; Sumrejkanchanakij et al. 2003; Marampon et al. 2008*), in this thesis we have studied whether Ccnd1 plays a role in neuritogenesis. Overexpression of Ccnd1 in cortical neurons led to apoptotic cell death, presumably by its nuclear accumulation in agreement with a previous report (*Sumrejkanchanakij et al. 2003*). To circumvent this problem, we have used a Ccnd1 version with a CAAX motif at its C-terminus, which seemingly becomes farnesylated and targets the protein to cell membranes avoiding its nuclear entry *(Fusté et al. 2016).* Overexpression of this cytoplasmic Ccnd1 in cortical neurons *in vitro* results in roughly 50% increase in both axon and neurite length. Furthermore, this effect is dependent on the kinase activity of Ccnd1-Cdk4 because when we use a kinase-dead mutant ($Ccnd1^{K112E}$) that forms an inactive complex with CDKs *(Baker et al. 2005)* no difference in length is obtained. Similar to Ccnd1, overexpressing a membrane-targeted version of Cdk4 (Cdk4-CAAX) also produces an increase in axon and neurite lengths. This effect is seen after four days of *in vitro* differentiation when the levels of the endogenous CCND1 mRNA are very low. We propose several alternatives to account for this apparent contradiction. One possibility is that Ccnd1-Cdk4 complexes operate earlier in the differentiation process but we observe their effects with some delay. Alternatively, cyclins other than Ccnd1 may partner with Cdk4 and contribute to the observed effects.

To study a putative role of the endogenous Ccnd1 in neuritogenesis we have followed two approaches. First, we downregulated the levels of Ccnd1 by RNA interference in cortical neurons *in vitro*. In agreement with a previous study in PC12 cells *(Marampon et al. 2008)*, we have observed a significant (20-25%) reduction in the lengths of both axons and neurites as well as a decrease in the number of neurites per cell. Second, we have compared neurite outgrowth in cortical neurons isolated from wild type and CCND1 KO animals. Similarly, cells lacking Ccnd1 developed shorter axons and neurites and reduced number of neurites per cell than their WT counterparts. This difference was more obvious just after one day of *in vitro* differentiation in consonance with the progressive decline in CCND1 mRNA levels, and suggests that Ccnd1 plays a role in the early stages of neuritogenesis. These findings agree with the fact that E13.5 mouse brains electroporated with Ccnd1 presents higher percentage of multipolar cells at high cortical plate than control or $Ccnd1^{K112E}$ electroporated brains (*Rocandio 2018*). Marampon and co-workers have proposed that this effect of Ccnd1 on neuritogenesis could be due to the regulation

of several transcription factors by Ccnd1 (*Marampon et al. 2008*). By contrast, our results with Ccnd1-CAAX point toward of a cytoplasmic function of Ccnd1. Hence, we propose that cytoplasmic sequestration of Ccnd1 in postmitotic neurons not only avoids apoptotic neuronal death as previously suggested (*Sumrejkanchanakij et al. 2003*), but also plays a role in neuritogenesis.

5.2 Paxillin phosphorylation at S83, S178 and S244 promotes neurite outgrowth

Differentiating neurons assemble the nervous system by projecting axons and dendrites. FA proteins facilitate the signaling across the membrane to facilitate cell migration and axon pathfinding. Pxn, together with other FA proteins, localizes to the neuronal growth cone. Because cytoplasmic Ccnd1-Cdk4 complex controls cell spreading, invasion and metastasis through the phosphorylation of Pxn at S83 and S178 (*Fusté et al. 2016*), we have studied Pxn as a target of Ccnd1 in the control of neuritogenesis. Pxn phosphorylation at S83 and S178 was assessed at different time points during differentiation, and as we expected, Pxn phosphorylation at both serines decreases at 4 DIV in comparison to 1 DIV coinciding with the decrease of CCND1 mRNA levels. As Ccnd1-Cdk4 is able to phosphorylate S83, S178 and S244 *in vitro* (*Fusté et al. 2016*), we studied neurite outgrowth in the presence of a non-phosphorylatable mutant of Pxn (Pxn^{TM}; S83A, S178A and S244A). As compared to WT Pxn, overexpression of the Pxn^{TM} in cortical neurons promotes a shortening in both axon (18%) and neurite (16%) length and also in neurite number (4.05 average vs 3.21 average) at 1 DIV. Hence, Pxn phosphorylation at S83, S178 and S244 is important for the neurite extension in E15.5 cortical neurons at 1 DIV, when Ccnd1 is regulating neuritogenesis. This result concurs with other studies that involved Pxn phosphorylation in neurite formation and outgrowth implicating different kinases and phosphorylation sites. In particular, p38MAPK at S85 (S83 in rats) (*Huang et al. 2004*), JNK at S178 (*Yamauchi et al. 2006*), GSK3β at S126 and ERK at S130 (*Cai et al. 2006*), and Nemo-like kinase at S126 (*Ishitani et al. 2009*). Because some kinases can phosphorylate Pxn at the same residues phosphorylated by Ccnd1-Cdk4, further studies should be done in order to confirm that the effect observed in mouse cortical neurons overexpressing the Pax^{TM} mutant is actually due to a decreased phosphorylation by Ccnd1-Cdk4 complex and not by other kinases. For instance, we could test Pxn phosphorylation levels at WT and CCND1 KO cortical neurons and the overexpression of a triple phosphomimetic mutant of Pxn ($Pxn^{S83E,\ S178E,\ S244E}$) should be able to rescue the defect in neurite outgrowth observed in cortical neurons from CCND1 KO mice.

On the whole, we can propose a model in which cytoplasmic Ccnd1-Cdk4/6 complexes regulate neuronal morphology and neurite outgrowth through the phosphorylation of Pxn (Figure 40).

In vivo studies connect Pxn phosphorylation state not only with neuritogenesis but also with migration (*Chen et al. 2009*; *Rashid et al. 2017*), complementary studies should be done to assess the role of the Ccnd1-Cdk4/6 complex in collaboration with Pxn in brain development and function. For example, studies concerning the ability of Ccnd1-Cdk4/6 complex through Pxn phosphorylation to promote axon outgrowth in regenerating systems could reveal a potential therapeutic target after neuronal injury or disease (*Kuboyama et al. 2013*). Furthermore, we could perform *in utero* electroporations with Pxn or Pxn^{TM} and analyze the organization of cortical layers and the lengths of leading processes.

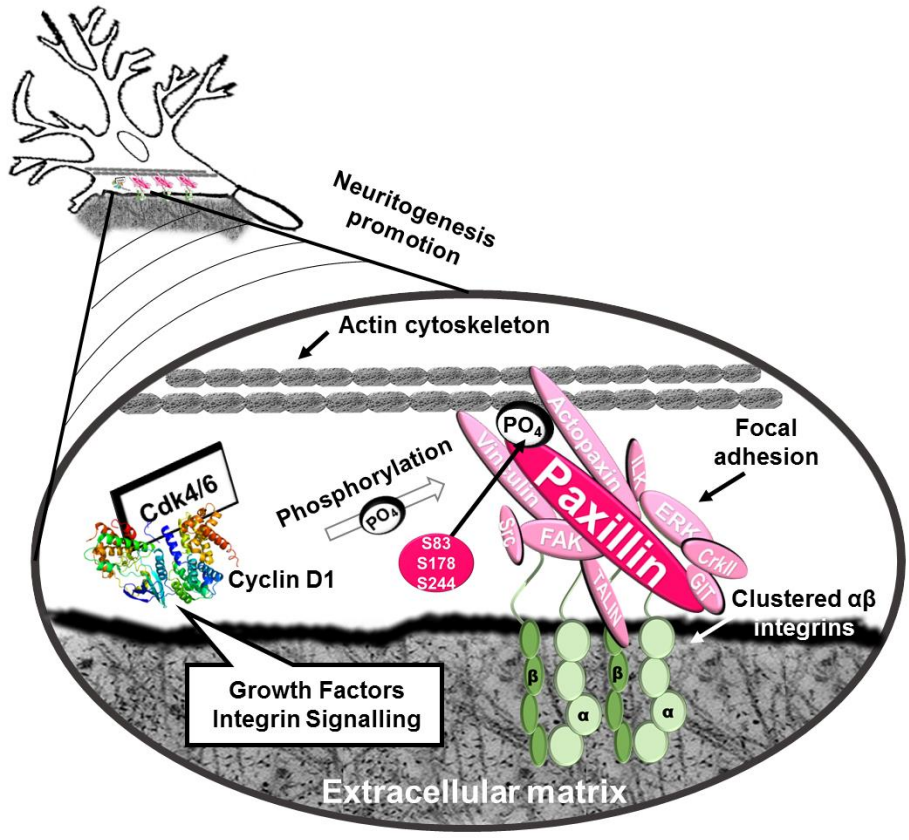

Figure 40: Proposed model whereby Ccnd1 promotes neurite outgrowth at early stages of development. Pxn, together with other FA proteins, localizes to the neuronal growth cone. Cytoplasmic Ccnd1-Cdk4/6 complex phosphorylates Pxn at S83, S178 and S244 thus promoting neuritogenesis.

5.3 Cytoplasmic cyclin D1 interacts with and phosphorylates the α4 subunit of $GABA_A$ receptors preventing their run-down

A previous yeast two hybrid screen performed in our lab had detected an interaction between Ccnd1 and the α4 subunit of $GABA_AR$. Specifically, Ccnd1 interacted with 3 independent clones of the C-terminus of the protein, containing the intracellular loop between TM3 and TM4. Here we have demonstrated this interaction between Ccnd1 and the intracellular loop of the α4 subunit *in vitro*. Moreover, we have also detected the interaction with overexpressed Ccnd1-CAAX and α4 in HEK293 cells, as well as colocalization by immunofluorescence in HEK293 cells and cortical neurons. Inspection of mRNA expression patterns in the mouse brain at the brain Atlas database (Allen brain atlas), shows that both Ccnd1 and α4 subunit are found at the hippocampus of adult mice. Curiously, both proteins share a common pattern of expression that is lower at CA3 and increases in CA1. Notably, we have observed endogenous interaction of Ccnd1 and α4 in the hippocampus of adult mice. Besides, among several CDK putative phosphorylation sites present in the intracellular loop, we have shown that the Ccnd1-Cdk4 complex phosphorylates *in vitro* the. α4 subunit at T423 and S431. As phosphorylation by PKC of another residue (S443) in the same intracellular region is known to regulate the $GABA_A$ receptor activity (*Abramian et al. 2010*, *2014*) we have explored the effect of T423 and S431 phosphorylation in $GABA_AR$ function.

In collaboration with Dr. Soto from Hospital Clinic at the University of Barcelona, we have first studied the functional effects of cytoplasmic Ccnd1 overexpression in heterologous α4β3 WT receptors in tsA201 cells. Whole-cell recordings revealed that the presence of Ccnd1-CAAX, but not $Ccnd1^{K112E}$-CAAX, significantly prevents $GABA_AR$ run-down. Besides, we have studied the consequences of α4 phosphorylation at T423 and S431 by the heterologous expression of receptors containing WT β3 subunits plus a phosphomimetic ($\alpha4^{T423E,S431E}$) mutant in tsA201 cells. In this case, the mimicking of the α4 subunit into a "persistently phosphorylated" state results in a nearly zero loss of $GABA_AR$ function. Hence, our results suggest that the Ccnd1-Cdk4/6 complex phosphorylation of α4 at T423 and S431 reduces the $GABA_AR$ run-down and that this phosphorylation can be performed *in vivo* by the Ccnd1-Cdk4 complex. The fact that $\alpha4^{T423E,S431E}$ mutant is more effective in preventing $GABA_AR$ run-down than Ccnd1-CAAX overexpression, could be explained by incomplete phosphorylation of all $GABA_ARs$, even under increased levels of Ccnd1. These may not be enough or there may be phosphatases at play. Consistently, PKC phosphorylation of α4 at another site in the intracellular loop, S443, also prevented GABA current run-down increasing the activity of the α4β3 WT receptor in HEK293 cells (*Abramian et al. 2010*). Other kinases like PKA are also able to regulate $GABA_AR$ function

by phosphorylation. In particular, PKA phosphorylates β3 subunit at residues S408 and S409 thereby enhancing receptor function *(McDonald et al. 1998*). Hence, we wondered whether the effects observed of Ccnd1 on $GABA_A$Rs might also be via β3 phosphorylation. Nevertheless, β3 subunit does not contain any Cdk phosphorylation site (SP or TP) and we have been unable to detect phosphorylation of the β3 subunit by Ccnd1-Cdk4 *in vitro*. Therefore, we propose that Ccnd1 enchances $GABA_A$Rs function through α4 phosphorylation on residues T423 and S431.

Epilepsy is caused by the abnormal regulation of the neuronal excitability by $GABA_A$Rs. $GABA_A$R run-down is more pronounced in epileptogenic tissue, in part because $GABA_A$Rs in TLE tissue present decreased affinity for GABA compared to control tissue (*Ragozzino et al. 2005*) or because the replacement of α1 for α4 subunit (*Mazzuferi et al. 2010*). The phosphorylation status of the $GABA_A$R subunits is important for receptor function, both physiologically and in disease. This is consistent with experiments that use phosphatase inhibitors to attenuate the run-down of $GABA_A$Rs (*Palma et al. 2004*) and other that prevent the run-down of the GABA response by the addition of Mg-ATP or Mg-ATPγS (*Chen et al. 1990*). We have observed that cytoplasmic Ccnd1-Cdk4 as well as the phosphomimetic α4 when expressed in HEK tsA201 cells prevent α4β3 $GABA_A$R run-down. Hence, it would be interesting to compare Ccnd1 levels in brain slices from epileptic patients and control individuals. Similarly, using an antibody that recognizes α4 (T423, S431) phosphosites, we could test if in epileptic patients' samples or in an epileptic mouse model there is a reduction in the phosphorylation levels of α4 at these residues. Also, in animal models of induced epileptogenesis, we could compare if there are changes in Ccnd1 expression levels before and after the induction of epilepsy. Besides, it would be relevant to know whether CCND1 KO mice are more vulnerable to develop epilepsy than their WT littermates. Finally, since α4 KO mice have impaired adult hippocampal neurogenesis and reduced dendritic growth and complexity (*Duveau et al. 2011*), we should test adult hippocampal neurogenesis in CCND1 KO mice as well as in an $\alpha4^{S423AT431A}$ knockin mouse.

In this work, we have not explored the possible interaction between Ccnd1 and other $GABA_A$Rs subunits. However, by sequence alignment, we have observed that the most variable region between α (α1-6) subunits is actually the intracellular domain which is susceptible to phosphorylation. Although other α subunits also contain putative Cdk phosphorylation sites (SP or TP), there is not any conserved region in the intracellular loop that contains these SP or TP sites among α subunits. In fact, α4 is the subunit with the larger intracellular loop and interacts with Ccnd1 through it. When comparing human and mouse α4 sequences, we can observe that SP and TP sites are conserved even though there are variations in the nearby amino acids. Interestingly, α4 and β3 present less homology than for other α subunits. The intracellular loop of

β3 subunit is shorter and does not contain any Cdk phosphorylation site. Hence, it could be interesting to further test the interaction of Ccnd1 with other $GABA_A$Rs subunits and reveal new targets for Ccnd1 in the control of the CNS function.

5.4 Cyclin D-Cdk4/6 complex modulates GABA tonic currents and mIPSCs in hippocampal slices

Since the α4 subunit is mainly localized extrasynaptically contributing to tonic inhibition, we have intended to study the effect of Ccnd-Cdk4/6 complexes in the modulation of GABA tonic currents in collaboration with Dr. Esteban from the Centro de Biología Molecular Severo Ochoa in Madrid. To that aim, we have inhibited the Ccnd-Cdk4/6 complex with Palbociclib, a specific Cdk4/6 inhibitor (*Fry et al. 2004*), in rat (P5-7) hippocampal slices, and measured GABA tonic currents in CA1 pyramidal neurons. Whole-cell recordings show that the inhibition of the Ccnd-Cdk4/6 complex significantly reduces GABA tonic currents in this model, suggesting that Cdk4/6 activity promotes the extrasynaptic $GABA_A$R function through the phosphorylation of the α4 subunit. This result is in accordance with the diminished $GABA_A$R run-down produced by Ccnd1-CAAX and the phosphomimetic version of α4 that we have observe in tsA201 cells and with the fact that neurosteroids promote GABA tonic currents via PKC phosphorylation of α4 subunit at S443 in hippocampal neurons (*Abramian et al. 2010, 2014*). Nonetheless, whether the effect on tonic currents we observe with Palbociclib is via phosphorylation of α4 at T423 and S431 or not remains to be investigated with future experiments. Recordings should be done in hippocampal slices infected with viruses to express Ccnd1-CAAX, $Ccnd1^{K112E}$-CAAX and α4 mutants (phosphomimetic and non-phosphorylatable). We would expect that Ccnd1-CAAX enhances GABA tonic currents while the kinase-inactive mutant $Ccnd1^{K112E}$-CAAX does not. Similarly, the expression of the non-phosphorylatable mutant of α4 should behave as $Ccnd1^{K112E}$-CAAX or Palbociclib-treated cells. On the contrary, the expression of the phosphomimetic mutant of α4 should be able to revert the effects of Palbociclib treatment on GABA tonic currents.

Phosphorylation of $GABA_A$R subunits often promotes GABA tonic currents, and the imbalance between neuronal excitation and inhibition can lead to epilepsy; specifically the α4 subunit has been related to this disease. Since Ccnd1-Cdk4 phosphorylates α4 at T423 and S431 *in vitro* and Ccnd1-Cdk4/6 inhibition decreases GABA tonic currents in hippocampal slices, further studies should be carried out in order to explore the potential relationship of this phosphorylation with epilepsy. First, if we had a specific antibody against phosphorylated T423 and S431 residues, we could compare the phosphorylation state of the α4 subunit in both CCND1 KO and WT mice.

Second, it would be interesting to compare GABA tonic currents in a CCND1 KO vs a WT animal. In such experiments, one would expect that mice lacking Ccnd1 present diminished tonic inhibition. If this is the case, the expression by *in utero* electroporation or slice infection of either cytoplasmic Ccnd1 or the phosphomimetic α4 mutant ($\alpha4^{T423E,S431E}$) in CCND1 KO mice should be able to rescue the defect in GABA tonic currents. Also, we should test whether the CCND1 KO mice present more susceptibility to develop epilepsy under convulsant kainate or pilocarpine injection.

Even though α4 is mostly extrasynaptical, it can also form synaptic $GABA_A$Rs when assembled with γ2. For this reason, we have assessed the effect of Palbociclib on mIPSC of hippocampal neurons using mIPSCs of CA1 pyramidal neurons as functional indicators of the inhibitory synapse's efficacy. We have observed that the inhibition of Ccnd-Cdk4/6 complexes causes a decrease in both the amplitude and the frequency of mIPSCs. Thus, not only the tonic currents are affected by Ccnd1-Cdk4/6 inhibition, but also the mIPSCs. These results imply that Ccnd-Cdk4/6 complex is somehow modulating the spontaneous release of GABA neurotransmitter (decreased mIPSC frequency) and also affecting the activation of the postsynaptic $GABA_A$R (decreased mIPSC amplitude). Regarding a putative role of Ccnd1 in the release of GABA vesicles, we can speculate that Ccnd-Cdk4/6 might exert its action through the small GTPases Ral A/B to regulate the exocyst complex. Indeed, Ccnd1 interacts with exocyst components (Sec6) and RalA and B small GTPases, which regulate the exocyst (*Fernández et al. 2011*; *Fernández-Hernández et al. 2013*). In neurons, the exocyst (also known as Sec6/8 complex) is highly expressed in regions undergoing neurite outgrowth, vesicle targeting and synapse formation (*Vega and Hsu 2001*). Hence, it seems pausible that blocking Ccnd-Cdk4/6 activity also affects the formation and/or the release of new GABA vesicles through exocyst alteration.

Concerning mIPSC amplitude, it is feasible that phosphorylation of α4 by Ccnd-Cdk4/6 complexes is still promoting its activity also when the α4 subunit is forming α4βxγ2 receptors at the synapse (*Wafford et al. 1996*). This would mean that α4 phosphorylation by Ccnd-Cdk4/6 has the same effect irrespective of whether the receptor localizes synaptically or extrasynaptically. By contrast, α4-containing synaptic and extrasynaptic receptors show different modulation by PKA and PKC phosphorylation. PKA activation decreases synaptic α4 expression while decreases extrasynaptic α4. Activation of PKC instead promotes α4 expression at the synapse and has no effect extrasynaptically (*Bohnsack et al. 2016*).

The α4βδ containing receptors have been involved in synaptic plasticity (*Shen et al. 2010*). Synaptic plasticity refers to the ability of individual synapses to modify their response to different

stimuli or environmental cues. When there is a persistent increase of the efficacy of synaptic transmission, it is called Long-Term Potentiation (LTP) whereas if the synaptic transmission efficacy is persistently decreased, it is called Long-Term Depression (LTD). A potential regulation system of synaptic plasticity is the balance between the phosphorylation and dephosphorylation of specific substrates (*Soderling and Derkach 2000*). Thus, the Ccnd-Cdk4/6 complex might also induce inhibitory LTP (iLTP) by phosphorylating the α4 subunit of the $GABA_A$Rs. This would not be a far-fetched idea since other similar cases have been reported such as the dephosphorylation of the γ2 subunit by Calcineurin leading to inhibitory LTD (iLTD) (*Wang et al. 2003*) or the β3 phosphorylation by CaMKII promoting iLTP (*Petrini et al. 2014*). Nevertheless, future studies on this issue should be performed. For instance, it should be assessed whether there is a change in the number of α4-containing $GABA_A$Rs at the cell surface in hippocampal organotypic slices in the presence or absence of Ccnd1. Moreover, specific experiments of iLTP should be carried out and possibly some memory and behavioral studies with both WT and CCND1 KO mice could reveal a role of Ccnd1 in synaptic plasticity.

Synaptic pruning is the process of synapse removal that takes place naturally in the brain at puberty and early young adulthood. This is concurrent with the increase in the expression of the α4 subunit of the $GABA_A$Rs, and extrasynaptic α4βδ $GABA_A$Rs play an important role in synaptic pruning at puberty through the impairment of NMDA receptor activation (*Shen et al. 2010*; *Afroz et al. 2016*). Also, synaptic pruning of CA1 hippocampus is prevented in α4 KO adolescent female mice. Because of its effects on α4, we may expect Ccnd1 to have a role in synaptic pruning. Thus, it will be interesting to test spine density both pre- and post-puberty in the CCND1 KO mice, expecting that the lack of Ccnd1 leads to decreased α4βδ $GABA_A$Rs activity and thus, decreased pruning.

5.5 Cytoplasmic cyclin D1 regulates α4β3-containing $GABA_A$R expression at the cell surface

To understand the mechanism underlying the electrophysiological effects of cytoplasmic Ccnd1 on α4β3 receptors, we have studied whether Ccnd1-CAAX affects the number and recycling of α4 and β3 subunits at the cell surface. First of all, we tested if Ccnd1 also interacts with β3. We have observed co-immunoprecipitation of Ccnd1 and β3 in HEK293 cells and they directly interact *in vitro*. Nevertheless, β3 does not seem to be a phosphorylation target of the Ccnd1-Cdk4 complex: it does not contain any putative CDK phosphorylation site and we did not observe phosphorylation of β3 in an *in vitro* kinase assay in which α4 was readily phosphorylated.

Expression of $GABA_AR$s at the cell surface is regulated by the phosphorylation of their subunits (see page 27). Thus, we have assessed the effect of Ccnd1-CAAX on α4 and β3 levels at the cell surface in HEK293 cells by biotin-labelling of surface proteins followed by precipitation with streptadivin. The presence of cytoplasmic Ccnd1 causes a small not-statistically-significant increase in the surface levels of α4. By contrast, PKC phosphorylation of α4 at S443 has been shown to enhance α4 expression at the cell surface in HEK293 (*Abramian et al. 2010*). Alike, THDOC induced phosphorylation via PKC of α4 leads to increased α4-containing receptors at the cell surface and this effect was prevented when the non-phosphorylatable mutant was overexpressed (*Abramian et al. 2014*). This increase in the surface levels of α4-containing $GABA_AR$s is connected with the decrease in loss of function of the $GABA_AR$s observed when α4 is phosphorylated. Hence, it is possible that the decrease in the $GABA_AR$ run-down and the enhancement of both the GABA-tonic currents and mIPSCs adhered to cytoplasmic Ccnd1-Cdk4/6 complex activity is due to the stabilization or expression triggering of α4 through phosphorylation. Conversely, surface levels of β3 are diminished in a kinase-dependent manner by Ccnd1. These reduced β3 surface levels may alter the α4/β3 stoichiometry and lead to the generation of more α4β3 receptors instead of β3 homopentamers, which could increase $GABA_AR$ function.

Further, to reveal the mechanism by which cytoplasmic Ccnd1 affects both α4 and β3 surface levels, we have studied the endocytosis process. However, neither the endocytosis of α4 nor β3 is altered by the presence of Ccnd1-CAAX. By contrast, the phosphorylation of residues in the intracellular loop of β3 and γ2 subunits maintains the surface levels of $GABA_AR$ while dephosphorylation leads to the internalization of the receptor since this phosphorylation avoids the binding to AP2 protein, an adaptor protein involved in clathrin-mediated endocytosis (*Kittler et al. 2005, 2008*). Next, we measured the insertion rate of α4 and β3 subunits at the cell surface in HEK293 cells. In these experiments, the co-expression of Ccnd1-CAAX together with α4 and β3 affected the insertion of the β3 subunit to the cell surface. Hence, cytoplasmic Ccnd1 seems to be diminishing β3 at the cell surface by hindering its insertion into the membrane.

Because β3 is susceptible to activity-dependent ubiquitination (*Saliba et al. 2012*) and its interaction with Plic-1 stabilizes and increases β3-containing $GABA_AR$s into the neuronal cell surface (*Saliba et al. 2008*), it is conceivable that the reduction in the insertion rate of β3 observed in our experiments is due to an increased subunit degradation. We then tested β3 ubiquitination levels in HEK293 cells co-transfected with heterologous α4β3 receptors plus Ccnd1-CAAX or the $Ccnd1^{K112E}$-CAAX mutant. Our results reflect that when cytoplasmic Ccnd1 is present, there is

an increase (3.23 fold) in the amount of β3 ubiquitination, and this effect is prevented by co-expression of the $Ccnd1^{K112E}$ mutant. Therefore, we conclude that Ccnd1 is decreasing β3 expression at the cell surface by altering its insertion to the membrane, increasing its ubiquitination and, perhaps, its proteasomal degradation in a kinase-dependent manner. All in all, we propose a model in which cytoplasmic Ccnd1-Cdk4/6 complexes modulate not only the number but also the function of α4β3 $GABA_A$Rs (Figure 41).

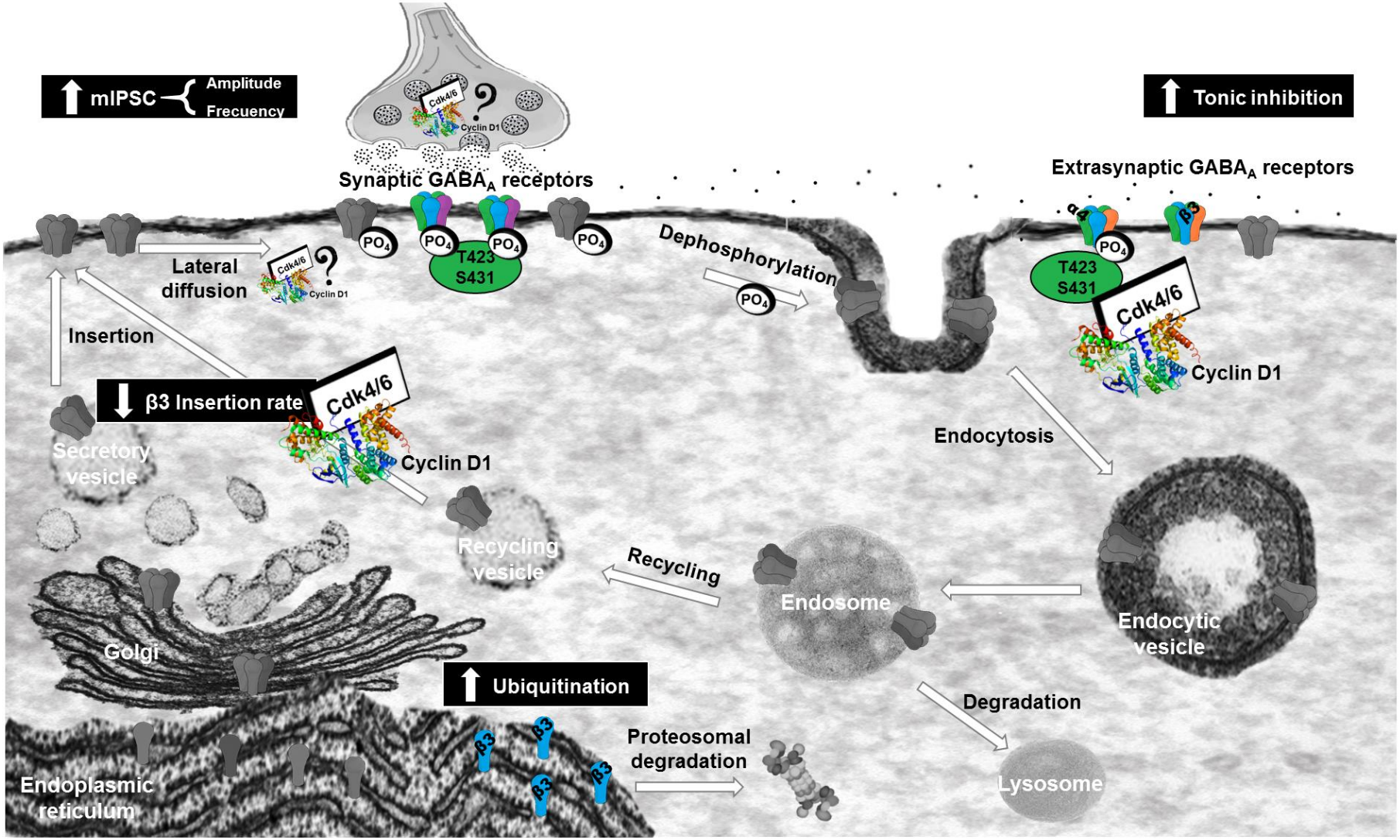

Figure 41: Model of the mechanism whereby Ccnd1 controls GABA$_A$ receptor expression and function proposed based on the results obtained in this thesis. Cytoplasmic Ccnd1 phosphorylates α4 at T423 and S431 promoting both phasic and tonic inhibition. Increased mIPSC frequency and amplitude suggest that Ccnd1 affect GABA vesicles release and postsynaptic GABAARs, respectively**.** Besides, cytoplasmic Ccnd1 promotes β3 ubiquitination and diminishes β3 insertion rate.

CONCLUSIONS

6. CONCLUSIONS

First. Cyclin D1-Cdk4 promotes early neuritogenesis in cultured cortical neurons in a manner that depends on the kinase activity of the complex.

Second. Paxillin is likely a downstream target of cyclin D1-Cdk4 in neuritogenesis.

Third. Cyclin D1 directly interacts with the α4 and β3 subunits of $GABA_A$ receptors *in vitro* and endogenously with the α4 subunit at the hippocampus of adult mice.

Fourth. Cyclin D1-Cdk4 complex phosphorylates α4 subunit at residues T423 and S431 *in vitro*.

Fifth. Cyclin D1 or a phosphomimetic allele of α4 prevent $GABA_A$ receptor run-down. *In vivo,* cyclin D-Cdk4/6 complexes increase the efficacy of $GABA_A$ receptors.

BIBLIOGRAPHY

7. BIBLIOGRAPHY

~A~

Abramian AM, Comenencia-Ortiz E, Modgil A, et al (2014) Neurosteroids promote phosphorylation and membrane insertion of extrasynaptic GABAA receptors. Proc Natl Acad Sci 111:7132–7137. doi: 10.1073/pnas.1403285111

Abramian AM, Comenencia-Ortiz E, Vithlani M, et al (2010) Protein kinase C phosphorylation regulates membrane insertion of GABA A receptor subtypes that mediate tonic inhibition. J Biol Chem. doi: 10.1074/jbc.M110.149229

Afroz S, Parato J, Shen H, Smith SS (2016) Synaptic pruning in the female hippocampus is triggered at puberty by extrasynaptic GABAA receptors on dendritic spines. Elife. doi: 10.7554/eLife.15106

Alam S, Laughton DL, Walding A, Wolstenholme AJ (2006) Human peripheral blood mononuclear cells express GABAA receptor subunits. Mol Immunol. doi: 10.1016/j.molimm.2005.07.025

Albrecht BE, Darlison MG (1995) Localization of the ρ1- and ρ2-subunit messenger RNAs in chick retina by in situ hybridization predicts the existence of γ-aminobutyric acid type C receptor subtypes. Neurosci Lett. doi: 10.1016/0304-3940(95)11479-G

Alhaja E, Adan J, Pagan R, et al (2004) Anti-migratory and anti-angiogenic effect of p16: A novel localization at membrane ruffles and lamellipodia in endothelial cells. Angiogenesis. doi: 10.1007/s10456-005-0368-9

Alt JR, Cleveland JL, Hannink M, Diehl JA (2000) Phosphorylation-dependent regulation of cyclin D1 nuclear export and cyclin D1-dependent cellular transformation. Genes Dev. doi: 10.1101/gad.854900

Andäng M, Lendahl U (2008) Ion fluxes and neurotransmitters signaling in neural development. Curr. Opin. Neurobiol.

Arancibia-Cárcamo IL, Yuen EY, Muir J, et al (2009) Ubiquitin-dependent lysosomal targeting of GABAA receptors regulates neuronal inhibition. Proc Natl Acad Sci U S A.

Assoian RK, Klein EA (2008) Growth control by intracellular tension and extracellular stiffness. Trends Cell Biol.

~B~

Bai D, Zhu G, Pennefather P, et al (2001) Distinct Functional and Pharmacological Properties of Tonic and Quantal Inhibitory Postsynaptic Currents Mediated by γ-Aminobutyric Acid A Receptors in Hippocampal Neurons. Mol Pharmacol. doi: 10.1124/mol.59.4.814

Baker GL, Landis MW, Hinds PW (2005) Multiple functions of D-type cyclins can antagonize pRb-mediated suppression of proliferation. Cell Cycle

Barker JL, Nicoll RA, Padjen A (1975) Studies on convulsants in the isolated frog spinal cord. I. Antagonism of amino acid responses. J Physiol. doi: 10.1113/jphysiol.1975.sp010859

Barnard EA, Skolnick P, Olsen RW, et al (1998) International Union of Pharmacology. XV. Subtypes of gamma-aminobutyric acidA receptors: classification on the basis of subunit structure and receptor function. Pharmacol Rev

Bedford FK, Kittler JT, Muller E, et al (2001) GABAA receptor cell surface number and subunit stability are regulated by the ubiquitin-like protein Plic-1. Nat Neurosci. doi: 10.1038/nn0901-908

Bencsits E, Ebert V, Tretter V, Sieghart W (1999) A significant part of native γ-aminobutyric acid(A) receptors containing α4 subunits do not contain γ/or δ subunits. J Biol Chem. doi: 10.1074/jbc.274.28.19613

Bendris N, Lemmers B, Blanchard JM (2015) Cell cycle, cytoskeleton dynamics and beyond: the many functions of cyclins and CDK inhibitors. Cell Cycle

Benzeno S, Lu F, Guo M, et al (2006) Identification of mutations that disrupt phosphorylation-dependent nuclear export of cyclin D1. Oncogene. doi: 10.1038/sj.onc.1209644

Beroukhim R, Mermel CH, Porter D, et al (2010) The landscape of somatic copy-number alteration across human cancers. Nature. doi: 10.1038/nature08822

Bjurstöm H, Wang JY, Ericsson I, et al (2008) GABA, a natural immunomodulator of T lymphocytes. J Neuroimmunol. doi: 10.1016/j.jneuroim.2008.08.017

Boal F, Stephens DJ (2010) Specific functions of BIG1 and BIG2 in endomembrane organization. PLoS One. doi: 10.1371/journal.pone.0009898

Bogdanov Y, Michels G, Armstrong-Gold C, et al (2006) Synaptic GABAA receptors are directly recruited from their extrasynaptic counterparts. EMBO J. doi: 10.1038/sj.emboj.7601309

Bohnsack JP, Carlson SL, Morrow AL (2016) Differential regulation of synaptic and extrasynaptic α4 GABA(A) receptor populations by protein kinase A and protein kinase C in cultured cortical neurons. Neuropharmacology 105:. doi: 10.1016/j.neuropharm.2016.01.009

Bollan K, Robertson LA, Tang H, Connolly CN (2003) Multiple assembly signals in γ-aminobutyric acid (type A) receptor subunits combine to drive receptor construction and composition. In: Biochemical Society Transactions

Bortone D, Polleux F (2009) KCC2 Expression Promotes the Termination of Cortical Interneuron Migration in a Voltage-Sensitive Calcium-Dependent Manner. Neuron. doi: 10.1016/j.neuron.2009.01.034

Boussif O, Lezoualc'h F, Zanta MA, et al (1995) A versatile vector for gene and oligonucleotide transfer into cells in culture and in vivo: polyethylenimine. Proc Natl Acad Sci U S A 92:7297–301. doi: 10.1073/pnas.92.16.7297

Bowery NG, Smart TG (2006) GABA and glycine as neurotransmitters: A brief history. Br. J. Pharmacol.

Bradley CA, Taghibiglou C, Collingridge GL, Yu TW (2008) Mechanisms involved in the reduction of GABAA receptor α1-subunit expression caused by the epilepsy mutation A322D in the trafficking-competent receptor. J Biol Chem. doi: 10.1074/jbc.M801708200

Brandon NJ, Jovanovic JN, Colledge M, et al (2003) A-kinase anchoring protein 79/150 facilitates the phosphorylation of GABAA receptors by cAMP-dependent protein kinase via selective interaction with receptor β subunits. Mol Cell Neurosci. doi: 10.1016/S1044-7431(02)00017-9

Breitinger HG, Becker CM (2002) The inhibitory glycine receptor - Simple views of a complicated channel. ChemBioChem

Brickley SG, SG C-C, of Neuroscience F-M (1999) Single-channel properties of synaptic and extrasynaptic {GABAA} receptors suggest differential targeting of receptor subtypes. J Neurosci. doi: 10.1523/JNEUROSCI.19-08-02960.1999

Bright DP, Smart TG (2013a) Protein kinase C regulates tonic GABAA receptor-mediated inhibition in the hippocampus and thalamus. Eur J Neurosci. doi: 10.1111/ejn.12352

Bright DP, Smart TG (2013b) Methods for recording and measuring tonic GABAA receptor-mediated inhibition. Front Neural Circuits 7:. doi: 10.3389/fncir.2013.00193

Brooks-Kayal a R, Shumate MD, Jin H, et al (1998) Selective changes in single cell GABA(A) receptor subunit expression and function in temporal lobe epilepsy. Nat Med. doi: 10.1038/2661

Brown MC, Perrotta JA, Turner CE (1996) Identification of LIM3 as the principal determinant of paxillin focal adhesion localization and characterization of a novel motif on paxillin directing vinculin and focal adhesion kinase binding. J Cell Biol. doi: 10.1083/jcb.135.4.1109

Brown MC, Turner CE (2004) Paxillin: Adapting to Change. Physiol Rev. doi: 10.1152/physrev.00002.2004

Burbelo P, Wellstein A, Pestell RG (2004) Altered Rho GTPase signaling pathways in breast cancer cells. Breast Cancer Res. Treat.

Burridge K, Turner CE, Romer LH (1992) Tyrosine phosphorylation of paxillin and pp125FAK accompanies cell adhesion to extracellular matrix: A role in cytoskeletal assembly. J Cell Biol. doi: 10.1083/jcb.119.4.893

Byrnes KR, Stoica BA, Fricke S, et al (2007) Cell cycle activation contributes to post-mitotic cell death and secondary damage after spinal cord injury. Brain. doi: 10.1093/brain/awm179

~C~

Cai X, Li M, Vrana J, Schaller MD (2006) Glycogen Synthase Kinase 3- and Extracellular Signal-Regulated Kinase-Dependent Phosphorylation of Paxillin Regulates Cytoskeletal Rearrangement. Mol Cell Biol. doi: 10.1128/mcb.26.7.2857-2868.2006

Cancedda L, Fiumelli H, Chen K, Poo M -m. (2007) Excitatory GABA Action Is Essential for Morphological Maturation of Cortical Neurons In Vivo. J Neurosci. doi: 10.1523/jneurosci.5169-06.2007

Chandra D, Halonen LM, Linden AM, et al (2010) Prototypic GABAA receptor agonist muscimol acts preferentially through forebrain high-affinity binding sites. Neuropsychopharmacology. doi: 10.1038/npp.2009.203

Chandra D, Jia F, Liang J, et al (2006) GABAA receptor 4 subunits mediate extrasynaptic inhibition in thalamus and dentate gyrus and the action of gaboxadol. Proc Natl Acad Sci. doi: 10.1073/pnas.0604304103

Charles J. Sherr (1995) D-type Cyclins. Trends Biochem Sci. doi: 10.1016/s0968-0004(00)89005-2

Charych EI, Yu W, Miralles CP, et al (2004) The brefeldin A-inhibited GDP/GTP exchange factor 2, a protein involved in vesicular trafficking, interacts with the β subunits of the GABA A receptors. J Neurochem. doi: 10.1111/j.1471-4159.2004.02481.x

Chen D liang, Wang Z qiang, Ren C, et al (2013) Abnormal expression of paxillin correlates with tumor progression and poor survival in patients with gastric cancer. J Transl Med. doi: 10.1186/1479-5876-11-277

Chen NH, Reith MEA, Quick MW (2004) Synaptic uptake and beyond: The sodium- and chloride-dependent neurotransmitter transporter family SLC6. Pflugers Arch. Eur. J. Physiol.

Chen QX, Stelzer A, Kay AR, Wong RK (1990) GABAA receptor function is regulated by phosphorylation in acutely dissociated guinea- pig hippocampal neurones. J Physiol. doi: 10.1113/jphysiol.1990.sp017908

Chen ZL, Haegeli V, Yu H, Strickland S (2009) Cortical deficiency of laminin γ1 impairs the AKT/GSK-3β signaling pathway and leads to defects in neurite outgrowth and neuronal migration. Dev Biol. doi: 10.1016/j.ydbio.2008.12.006

Choquet D, Triller A (2013) The dynamic synapse. Neuron

Chuang SH, Reddy DS (2018) Genetic and molecular regulation of extrasynaptic GABA-A receptors in the brain: Therapeutic insights for epilepsy. J. Pharmacol. Exp. Ther.

Collins AL, Ma D, Whitehead PL, et al (2006) Investigation of autism and GABA receptor subunit genes in multiple ethnic groups. Neurogenetics. doi: 10.1007/s10048-006-0045-1

Connelly WM, Errington AC, Di Giovanni G, Crunelli V (2013) Metabotropic regulation of extrasynaptic GABA A receptors. Front. Neural Circuits

Connolly CN, Kittler JT, Thomas P, et al (1999) Cell surface stability of γ-aminobutyric acid type A receptors. Dependence on protein kinase C activity and subunit composition. J Biol Chem. doi: 10.1074/jbc.274.51.36565

Connolly CN, Krishek BJ, McDonald BJ, et al (1996) Assembly and cell surface expression of heteromeric and homomeric γ-aminobutyric acid type A receptors. J Biol Chem. doi: 10.1074/jbc.271.1.89

Corringer P-J, Novère N Le, Changeux J-P (2000) Nicotinic Receptors at the Amino Acid Level. Annu Rev Pharmacol Toxicol. doi: 10.1146/annurev.pharmtox.40.1.431

Craig AM, Blackstone CD, Huganir RL, Banker G (1994) Selective clustering of glutamate and gamma-aminobutyric acid receptors opposite terminals releasing the corresponding neurotransmitters. Proc Natl Acad Sci U S A

Cross DAE, Alessi DR, Cohen P, et al (1995) Inhibition of glycogen synthase kinase-3 by insulin mediated by protein kinase B. Nature. doi: 10.1038/378785a0

~D~

Da Silva JS, Dotti CG (2002) Breaking the neuronal sphere: Regulation of the actin cytoskeleton in neuritogenesis. Nat. Rev. Neurosci.

Darlison MG, Pahal I, Thode C (2005) Consequences of the evolution of the GABAA receptor gene family. Cell. Mol. Neurobiol.

Davies M (2003) The role of GABAA receptors in mediating the effects of alcohol in the central nervous system. J. Psychiatry Neurosci.

Davies PA, Wang W, Hales TG, Kirkness EF (2003) A novel class of ligand-gated ion channel is activated by Zn2+. J Biol Chem. doi: 10.1074/jbc.M208814200

de Luca E, Ravasenga T, Petrini EM, et al (2017) Inter-Synaptic Lateral Diffusion of GABAA Receptors Shapes Inhibitory Synaptic Currents. Neuron 95:. doi: 10.1016/j.neuron.2017.06.022

Deakin NO, Turner CE (2008) Paxillin comes of age. J Cell Sci. doi: 10.1242/jcs.018044

Dehay C, Kennedy H (2007) Cell-cycle control and cortical development. Nat. Rev. Neurosci.

Di Giovanni S, Movsesyan V, Ahmed F, et al (2005) Cell cycle inhibition provides neuroprotection and reduces glial proliferation and scar formation after traumatic brain injury. Proc Natl Acad Sci U S A. doi: 10.1073/pnas.0500989102

Dibbens LM, Harkin LA, Richards M, et al (2009) The role of neuronal GABAA receptor subunit mutations in idiopathic generalized epilepsies. Neurosci Lett. doi: 10.1016/j.neulet.2009.02.038

Diefenbach TJ, Latham VM, Yimlamai D, et al (2002) Myosin 1c and myosin IIB serve opposing roles in lamellipodial dynamics of the neuronal growth cone. J Cell Biol. doi: 10.1083/jcb.200202028

Diehl JA, Cheng M, Roussel MF, Sherr CJ (1998) Glycogen synthase kinase-3β regulates cyclin D1 proteolysis and subcellular localization. Genes Dev. doi: 10.1101/gad.12.22.3499

Diehl JA, Zindy F, Sherr CJ (1997) Inhibition of cyclin D1 phosphorylation on threonine-286 prevents its rapid degradation via the ubiquitin-proteasome pathway. Genes Dev. doi: 10.1101/gad.11.8.957

Dong J-M, Lau L-S, Ng Y-W, et al (2009) Paxillin nuclear-cytoplasmic localization is regulated by phosphorylation of the LD4 motif: evidence that nuclear paxillin promotes cell proliferation. Biochem J. doi: 10.1042/BJ20080170

Dudek H, Datta SR, Franke TF, et al (1997) Regulation of neuronal survival by the serine-threonine protein kinase Akt. Science (80-). doi: 10.1126/science.275.5300.661

Dulić V, Lees E, Reed SI (1992) Association of human cyclin e with a periodic G1-S phase protein kinase. Science (80-). doi: 10.1126/science.1329201

Duveau V, Laustela S, Barth L, et al (2011) Spatiotemporal specificity of GABA A receptor-mediated regulation of adult hippocampal neurogenesis. 34:362–373. doi: 10.1111/j.1460-9568.2011.07782.x

Dzhala VI, Talos DM, Sdrulla DA, et al (2005) NKCC1 transporter facilitates seizures in the developing brain. Nat Med. doi: 10.1038/nm1301

~E~

Edwards FA, Konnerth A, Sakmann B (1990) Quantal analysis of inhibitory synaptic transmission in the dentate gyrus of rat hippocampal slices: a patch- clamp study. J Physiol. doi: 10.1113/jphysiol.1990.sp018289

Erlitzki R, Gong Y, Zhang M, Minuk G (2000) Identification of γ-aminobutyric acid receptor subunit types in human and rat liver. Am J Physiol - Gastrointest Liver Physiol

~F~

Fang C, Deng L, Keller CA, et al (2006) GODZ-mediated palmitoylation of GABAA receptors is required for normal assembly and function of GABAergic inhibitory synapses. J Neurosci. doi: 10.1523/JNEUROSCI.4214-06.2006

Fantl V, Stamp G, Andrews A, et al (1995) Mice lacking cyclin D1 are small and show defects in eye and mammary gland development. Genes Dev. doi: 10.1101/gad.9.19.2364

Farrant M, Kaila K (2007) The cellular, molecular and ionic basis of GABAA receptor signalling. Prog. Brain Res.

Farrant M, Nusser Z (2005) Variations on an inhibitory theme: Phasic and tonic activation of GABAAreceptors. Nat. Rev. Neurosci.

Fernández-Hernández R, Rafel M, Fusté NP, et al (2013) Cyclin D1 localizes in the cytoplasm of keratinocytes during skin differentiation and regulates cell-matrix adhesion. Cell Cycle 12:2510–7. doi: 10.4161/cc.25590

Fernández RMH, Ruiz-Miró M, Dolcet X, et al (2011) Cyclin D1 interacts and collaborates with Ral GTPases enhancing cell detachment and motility. Oncogene 30:1936–1946. doi: 10.1038/onc.2010.577

Feucht M, Fuchs K, Pichlbauer E, et al (1999) Possible association between childhood absence epilepsy and the gene encoding GABRB3. Biol Psychiatry. doi: 10.1016/S0006-3223(99)00039-6

Fritschy J - M, Mohler H (1995) GABAA- receptor heterogeneity in the adult rat brain: Differential regional and cellular distribution of seven major subunits. J Comp Neurol. doi: 10.1002/cne.903590111

Fritschy JM, Brünig I (2003) Formation and plasticity of GABAergic synapses: Physiological mechanisms and pathophysiological implications. Pharmacol. Ther.

Fritschy JM, Kiener T, Bouilleret V, Loup F (1999) GABAergic neurons and GABA(A)-receptors in temporal lobe epilepsy. In: Neurochemistry International

Fritschy JM, Panzanelli P (2014) GABAA receptors and plasticity of inhibitory neurotransmission in the central nervous system. Eur J Neurosci. doi: 10.1111/ejn.12534

Fritschy JM, Panzanelli P, Tyagarajan SK (2012) Molecular and functional heterogeneity of GABAergic synapses. Cell. Mol. Life Sci.

Froestl W (2011) An historical perspective on GABAergic drugs. Future Med Chem. doi: 10.4155/fmc.10.285

Fry DW, Harvey PJ, Keller PR, et al (2004) Specific inhibition of cyclin-dependent kinase 4 / 6 by PD 0332991 and associated antitumor activity in human tumor xenografts. 3:1427–1438

Fusté NP (2016) Mecanismes de regulació de l'adhesió i la invasió cel·lulars pel complex ciclina D1-CDK4 citoplasmàtic

Fusté NP, Fernández-hernández R, Cemeli T, et al (2016) Cytoplasmic cyclin D1 regulates cell spreading , invasion and metastasis through the phosphorylation of paxillin . doi: 10.1038/ncomms11581

~G~

Galanopoulou AS (2010) Mutations affecting GABAergic signaling in seizures and epilepsy. Pflugers Arch 460:505–23. doi: 10.1007/s00424-010-0816-2

Ge S, Goh ELK, Sailor KA, et al (2006) GABA regulates synaptic integration of newly generated neurons in the adult brain. Nature. doi: 10.1038/nature04404

Geiger B, Bershadsky A, Pankov R, Yamada KM (2001) Transmembrane extracellular matrix-cytoskeleton crosstalk. Nat Rev Mol Cell Biol. doi: 10.1038/35099066

Glykys J, Mody I (2007a) Activation of GABAA Receptors: Views from Outside the Synaptic Cleft. Neuron

Glykys J, Mody I (2007b) The main source of ambient GABA responsible for tonic inhibition in the mouse hippocampus. J Physiol. doi: 10.1113/jphysiol.2007.134460

Goodkin HP, Sun C, Yeh JL, et al (2007) GABAA receptor internalization during seizures. In: Epilepsia

Grabenstatter HL, Cogswell M, Cruz Del Angel Y, et al (2014) Effect of spontaneous seizures on GABA A receptor a4 subunit expression in an animal model of temporal lobe epilepsy. Epilepsia 55:1826–1833. doi: 10.1111/epi.12771

Gumbiner BM (1996) Cell adhesion: The molecular basis of tissue architecture and morphogenesis. Cell

Gunther U, Benson J, Benke D, et al (1995) Benzodiazepine-insensitive mice generated by targeted disruption of the γ2 subunit gene of γ-aminobutyric acid type A receptors. Proc Natl Acad Sci U S A. doi: 10.1073/pnas.92.17.7749

Gurba KN, Hernandez CC, Hu N, Macdonald RL (2012) GABRB3 mutation, G32R, associated with childhood absence epilepsy alters α1β3γ2L γ-aminobutyric acid type A (GABA A) receptor expression and channel gating. J Biol Chem. doi: 10.1074/jbc.M111.332528

~H~

Hagel M, George EL, Kim A, et al (2002) The adaptor protein paxillin is essential for normal development in the mouse and is a critical transducer of fibronectin signaling. Mol Cell Biol

Halterman MW, Giuliano R, DeJesus C, Schor NF (2009) In-tube transfection improves the efficiency of gene transfer in primary neuronal cultures. J Neurosci Methods 177:348–354. doi: 10.1016/j.jneumeth.2008.10.023

Hanchar HJ, Dodson PD, Olsen RW, et al (2005) Alcohol-induced motor impairment caused by increased extrasynaptic GABAA receptor activity. Nat Neurosci. doi: 10.1038/nn1398

Hatten ME (2002) CENTRAL NERVOUS SYSTEM NEURONAL MIGRATION. Annu Rev Neurosci. doi: 10.1146/annurev.neuro.22.1.511

Hausrat TJ, Muhia M, Gerrow K, et al (2015) Radixin regulates synaptic GABA A receptor density and is essential for reversal learning and short-term memory. Nat Commun. doi: 10.1038/ncomms7872

Hesdorffer DC, Beck V, Begley CE, et al (2013) Research implications of the Institute of medicine report, epilepsy across the Spectrum: Promoting health and understanding. Epilepsia

Hinds PW, Dowdy SF, Eaton EN, et al (1994) Function of a human cyclin gene as an oncogene. Proc Natl Acad Sci U S A

Hochegger H, Takeda S, Hunt T (2008) Cyclin-dependent kinases and cell-cycle transitions: Does one fit all? Nat. Rev. Mol. Cell Biol.

Hoffman GR, Cerione RA (2002) Signaling to the Rho GTPases: Networking with the DH domain. FEBS Lett.

Horenstein J, Wagner DA, Czajkowski C, Akabas MH (2001) Protein mobility and GABA-induced conformational changes in GABAA receptor pore-lining M2 segment. Nat Neurosci. doi: 10.1038/87425

Hörtnagl H, Tasan RO, Wieselthaler A, et al (2013) Patterns of mRNA and protein expression for 12 GABAA receptor subunits in the mouse brain. Neuroscience.

Houston CM, Lee HHC, Hosie AM, et al (2007) Identification of the sites for CaMK-II-dependent phosphorylation of GABAA receptors. J Biol Chem. doi: 10.1074/jbc.M611533200

Huang C-C, Wu D-W, Lin P-L, Lee H (2015) Paxillin promotes colorectal tumor invasion and poor patient outcomes via ERK-mediated stabilization of Bcl-2 protein by phosphorylation at Serine 87. Oncotarget. doi: 10.18632/oncotarget.3537

Huang C, Borchers CH, Schaller MD, Jacobson K (2004) Phosphorylation of paxillin by p38MAPK is involved in the neurite extension of PC-12 cells. J Cell Biol. doi: 10.1083/jcb.200307081

Huang Z, Yan DP, Ge BX (2008) JNK regulates cell migration through promotion of tyrosine phosphorylation of paxillin. Cell Signal. doi: 10.1016/j.cellsig.2008.07.014

Huard JM, Forster CC, Carter ML, et al (1999) Cerebellar histogenesis is disturbed in mice lacking cyclin D2. Development

Hydbring P, Malumbres M, Sicinski P (2016) Non-canonical functions of cell cycle cyclins and cyclin-dependent kinases. Nat Rev Mol Cell Biol 17:280–292. doi: 10.1038/nrm.2016.27

Hynes RO (2002) Integrins: bidirectional, allosteric signaling machines. Cell

~I~

Ishitani T, Ishitani S, Matsumoto K, Itoh M (2009) Nemo-like kinase is involved in NGF-induced neurite outgrowth via phosphorylating MAP1B and paxillin. J Neurochem.

Ivankovic-Dikic I, Grönroos E, Blaukat A, et al (2000) Pyk2 and FAK regulate neurite outgrowth induced by growth factors and integrins. Nat Cell Biol 2:574–581. doi: 10.1038/35023515

~J~

Jagadeeswaran R, Surawska H, Krishnaswamy S, et al (2008) Paxillin is a target for somatic mutations in lung cancer: Implications for cell growth and invasion. Cancer Res. doi: 10.1158/0008-5472.CAN-07-1998

Jiang YH, Pan Y, Zhu L, et al (2010) Altered ultrasonic vocalization and impaired learning and memory in Angelman syndrome mouse model with a large maternal deletion from Ube3a to Gabrb3. PLoS One. doi: 10.1371/journal.pone.0012278

Jones M V., Westbrook GL (1996) The impact of receptor desensitization on fast synaptic transmission. Trends Neurosci. doi: 10.1016/S0166-2236(96)80037-3

~K~

Kaila K (1994) Ionic basis of GABAA receptor channel function in the nervous system. Prog. Neurobiol.

Kaila K, Price TJ, Payne JA, et al (2014) Cation-chloride cotransporters in neuronal development, plasticity and disease. Nat. Rev. Neurosci.

Kato J, Matsushime H, Hiebert SW, et al (1993) Direct binding of cyclin D to the retinoblastoma gene product (pRb) and pRb phosphorylation by the cyclin D-dependent kinase CDK4. Genes Dev 7:331–342. doi: 10.1101/gad.7.3.331

Keating N, Zeak N, Smith SS (2019) Pubertal hormones increase hippocampal expression of α4βδ GABA A receptors. Neurosci Lett. doi: 10.1016/j.neulet.2019.02.005

Keller CA, Yuan X, Panzanelli P, et al (2004) The γ2 subunit of GABAA receptors is a substrate for palmitoylation by GODZ. J Neurosci. doi: 10.1523/JNEUROSCI.1037-04.2004

Kim G, Davidson B, Henning R, et al (2012) Adhesion molecule protein signature in ovarian cancer effusions is prognostic of patient outcome. Cancer. doi: 10.1002/cncr.26449

Kittler JT, Chen G, Honing S, et al (2005) Phospho-dependent binding of the clathrin AP2 adaptor complex to GABAA receptors regulates the efficacy of inhibitory synaptic transmission. Proc Natl Acad Sci. doi: 10.1073/pnas.0506653102

Kittler JT, Chen G, Kukhtina V, et al (2008) Regulation of synaptic inhibition by phospho-dependent binding of the AP2 complex to a YECL motif in the GABAA receptor 2 subunit. Proc Natl Acad Sci. doi: 10.1073/pnas.0707920105

Kittler JT, Delmas P, Jovanovic JN, et al (2000) Constitutive endocytosis of GABA(A) receptors by an association with the adaptin AP2 complex modulates inhibitory synaptic currents in hippocampal neurons. J Neurosci

Kittler JT, Moss SJ (2003) Modulation of GABAA receptor activity by phosphorylation and receptor trafficking: implications for the efficacy of synaptic inhibition. Curr Opin Neurobiol 13:341–7

Kittler JT, Thomas P, Tretter V, et al (2004) Huntingtin-associated protein 1 regulates inhibitory synaptic transmission by modulating γ-aminobutyric acid type A receptor membrane trafficking. Proc Natl Acad Sci U S A. doi: 10.1073/pnas.0401860101

Klein EA, Assoian RK (2008) Transcriptional regulation of the cyclin D1 gene at a glance. J Cell Sci. doi: 10.1242/jcs.039131

Klempan TA, Sequeira A, Canetti L, et al (2009) Altered expression of genes involved in ATP biosynthesis and GABAergic neurotransmission in the ventral prefrontal cortex of suicides with and without major depression. Mol Psychiatry. doi: 10.1038/sj.mp.4002110

Knoblich JA (2008) Mechanisms of Asymmetric Stem Cell Division. Cell

Knudsen KE (2006) The cyclin D1b splice variant: An old oncogene learns new tricks. Cell Div.

Koeller HB, Ross ME, Glickstein SB (2008) Cyclin D1 in excitatory neurons of the adult brain enhances kainate-induced neurotoxicity. Neurobiol Dis. doi: 10.1016/j.nbd.2008.04.010

Korpi ER, Kuner T, Kristo P, et al (1994) Small N- Terminal Deletion by Splicing in Cerebellar α6 Subunit Abolishes GABAA Receptor Function. J Neurochem. doi: 10.1046/j.1471-4159.1994.63031167.x

Kozar K, Ciemerych MA, Rebel VI, et al (2004) Mouse development and cell proliferation in the absence of D-cyclins. Cell. doi: 10.1016/j.cell.2004.07.025

Kuboyama T, Luo X, Park K, et al (2013) Paxillin phosphorylation counteracts proteoglycan-mediated inhibition of axon regeneration. Exp Neurol. doi: 10.1016/j.expneurol.2013.06.011

Kullmann DM (2000) Spillover and synaptic cross talk mediated by glutamate and GABA in the mammalian brain. In: Progress in Brain Research

~L~

Lachance-Touchette P, Martin C, Poulin C, et al (2010) Screening of GABRB3 in French-Canadian families with idiopathic generalized epilepsy. Epilepsia. doi: 10.1111/j.1528-1167.2010.02642.x

Lagrange AH, Botzolakis EJ, Macdonald RL (2007) Enhanced macroscopic desensitization shapes the response of α4 subtype-containing GABAA receptors to synaptic and extrasynaptic GABA. J Physiol. doi: 10.1113/jphysiol.2006.122135

Lam EWF, Glassford J, Banerji L, et al (2000) Cyclin D3 compensates for loss of cyclin D2 in mouse D-lymphocytes activated via the antigen receptor and CD40. J Biol Chem. doi: 10.1074/jbc.275.5.3479

Lange C, Huttner WB, Calegari F (2009) Cdk4/CyclinD1 Overexpression in Neural Stem Cells Shortens G1, Delays Neurogenesis, and Promotes the Generation and Expansion of Basal Progenitors. Cell Stem Cell. doi: 10.1016/j.stem.2009.05.026

Laurie DJ, Seeburg PH, Wisden W (1992) The distribution of 13 GABA(A) receptor subunit mRNAs in the rat brain. II. Olfactory bulb and cerebellum. J Neurosci

Leil TA (2004) GABAA Receptor-Associated Protein Traffics GABAA Receptors to the Plasma Membrane in Neurons. J Neurosci. doi: 10.1523/jneurosci.3355-04.2004

Leventhal PS, Feldman EL (1996) Tyrosine phosphorylation and enhanced expression of paxillin during neuronal differentiation in vitro. J Biol Chem. doi: 10.1074/jbc.271.11.5957

Li L, Wang J, Gao L, Gong L (2015) Expression of paxillin in laryngeal squamous cell carcinoma and its prognostic value. Int J Clin Exp Pathol

Li S, Guan J-L, Chien S (2005) Biochemistry and Biomechanics of Cell Motility. Annu Rev Biomed Eng. doi: 10.1146/annurev.bioeng.7.060804.100340

Li Z, Chen K, Jiao X, et al (2014) Cyclin D1 integrates estrogen-mediated DNA damage repair signaling. Cancer Res. doi: 10.1158/0008-5472.CAN-13-3137

Li Z, Jiao X, Wang C, et al (2006a) Cyclin D1 induction of cellular migration requires p27 KIP1. Cancer Res. doi: 10.1158/0008-5472.CAN-06-1596

Li Z, Wang C, Jiao X, et al (2006b) Cyclin D1 Regulates Cellular Migration through the Inhibition of Thrombospondin 1 and ROCK Signaling. Mol Cell Biol.

Liang J, Zhang N, Cagetti E, et al (2006) Chronic intermittent ethanol-induced switch of ethanol actions from extrasynaptic to synaptic hippocampal GABAA receptors. J Neurosci. doi: 10.1523/JNEUROSCI.4702-05.2006

Liu QY, Schaffner AE, Chang YH, et al (2000) Persistent activation of GABA(A) receptor/Cl(-) channels by astrocyte-derived GABA in cultured embryonic rat hippocampal neurons. J Neurophysiol. doi: 10.1152/jn.2000.84.3.1392

Loebrich S, Bähring R, Katsuno T, et al (2006) Activated radixin is essential for GABAA receptor α5 subunit anchoring at the actin cytoskeleton. EMBO J. doi: 10.1038/sj.emboj.7600995

Loup F, Wieser HG, Yonekawa Y, et al (2000) Selective alterations in GABAA receptor subtypes in human temporal lobe epilepsy. J Neurosci 20:5401–19

Lummis SCR (2012) 5-HT3 receptors. J. Biol. Chem.

Lund I V, Hu Y, Raol YH, et al (2008) BDNF selectively regulates GABAA receptor transcription by activation of the JAK/STAT pathway. Sci Signal 1:ra9. doi: 10.1126/scisignal.1162396

Luo B-H, Carman C V., Springer TA (2007) Structural Basis of Integrin Regulation and Signaling. Annu Rev Immunol. doi: 10.1146/annurev.immunol.25.022106.141618

Luscher B, Shen Q, Sahir N (2011) The GABAergic deficit hypothesis of major depressive disorder. Mol Psychiatry. doi: 10.1038/mp.2010.120

~M~

Ma DQ, Whitehead PL, Menold MM, et al (2005) Identification of significant association and gene-gene interaction of GABA receptor subunit genes in autism. Am J Hum Genet. doi: 10.1086/433195

Ma X, Hammes SR (2018) Paxillin actions in the nucleus. Steroids. doi: 10.1016/j.steroids.2017.10.012

MacDonald RL, Twyman RE (1992) Kinetic properties and regulation of GABAA receptor channels. Ion Channels

Madsen KK, Larsson OM, Schousboe A (2007) Regulation of excitation by GABA neurotransmission: Focus on metabolism and transport. Results Probl. Cell Differ.

Malumbres M (2011) Physiological Relevance of Cell Cycle Kinases. Physiol Rev. doi: 10.1152/physrev.00025.2010

Malumbres M, Sotillo R, Santamaría D, et al (2004) Mammalian cells cycle without the D-type cyclin-dependent kinases Cdk4 and Cdk6. Cell. doi: 10.1016/j.cell.2004.08.002

Marampon F, Casimiro MC, Fu M, et al (2008) Nerve Growth factor regulation of cyclin D1 in PC12 cells through a p21RAS extracellular signal-regulated kinase pathway requires cooperative interactions between Sp1 and nuclear factor-kappaB. Mol Biol Cell 19:2566–2578. doi: E06-12-1110 [pii]\r10.1091/mbc.E06-12-1110

Marin O, Rubenstein JLR (2003) Cell migration in the forebrain. Annu Rev Neurosci. doi: 10.1146/annurev.neuro.26.041002.131058

Marsden KC, Beattie JB, Friedenthal J, Carroll RC (2007) NMDA receptor activation potentiates inhibitory transmission through GABA receptor-associated protein-dependent exocytosis of GABAA receptors. J Neurosci. doi: 10.1523/JNEUROSCI.4433-07.2007

Martin DL, Rimvall K (1993) Regulation of γ- Aminobutyric Acid Synthesis in the Brain. J. Neurochem.

Matsumoto RR (1989) GABA receptors: are cellular differences reflected in function? Brain Res. Rev.

Matsushime H, Roussel MF, Ashmun RA, Sherr CJ (1991) Colony-stimulating factor 1 regulates novel cyclins during the G1 phase of the cell cycle. Cell. doi: 10.1016/0092-8674(91)90101-4

Mazzuferi M, Palma E, Martinello K, et al (2010) Enhancement of GABAA-current run-down in the hippocampus occurs at the first spontaneous seizure in a model of temporal lobe epilepsy. Proc Natl Acad Sci U S A. doi: 10.1073/pnas.0914710107

McDonald BJ, Amato A, Connolly CN, et al (1998) Adjacent phosphorylation sites on GABAA receptor β subunits determine regulation by cAMP-dependent protein kinase. Nat Neurosci. doi: 10.1038/223

Meng H, Tian L, Zhou J, et al (2011) PACSIN 2 represses cellular migration through direct association with cyclin D1 but not its alternate splice form cyclin D1b. Cell Cycle. doi: 10.4161/cc.10.1.14243

Mihalek RM, Banerjee PK, Korpi ER, et al (1999) Attenuated sensitivity to neuroactive steroids in γ-aminobutyrate type A receptor delta subunit knockout mice. Proc Natl Acad Sci U S A. doi: 10.1073/pnas.96.22.12905

Miller PS, Aricescu AR (2014) Crystal structure of a human GABAA receptor. Nature. doi: 10.1038/nature13293

Milner R, Campbell IL (2002) The integrin family of cell adhesion molecules has multiple functions within the CNS. J. Neurosci. Res.

Minier F, Sigel E (2004) Positioning of the -subunit isoforms confers a functional signature to -aminobutyric acid type A receptors. Proc Natl Acad Sci. doi: 10.1073/pnas.0400220101

Minuk GY, Zhang M, Gong Y, et al (2007) Decreased hepatocyte membrane potential differences and GABA A-β3 expression in human hepatocellular carcinoma. Hepatology. doi: 10.1002/hep.21562

Miyamoto Y, Torii T, Yamamori N, et al (2012) Paxillin is the target of c-Jun N-terminal kinase in Schwann cells and regulates migration. Cell Signal. doi: 10.1016/j.cellsig.2012.06.013

Miyamoto Y, Yamauchi J, Chan JR, et al (2007) Cdk5 regulates differentiation of oligodendrocyte precursor cells through the direct phosphorylation of paxillin. J Cell Sci. doi: 10.1242/jcs.018218

Mizuta K, Xu D, Pan Y, et al (2008) GABA A receptors are expressed and facilitate relaxation in airway smooth muscle . Am J Physiol Cell Mol Physiol. doi: 10.1152/ajplung.00287.2007

Modgil A, Parakala ML, Ackley MA, et al (2017) Endogenous and synthetic neuroactive steroids evoke sustained increases in the efficacy of GABAergic inhibition via a protein kinase C-dependent mechanism. Neuropharmacology. doi: 10.1016/j.neuropharm.2016.10.010

Mody I, De Koninck Y, Otis TS, Soltesz I (1994) Bridging the cleft at GABA synapses in the brain. Trends Neurosci

Mody I, Pearce RA (2004) Diversity of inhibitory neurotransmission through GABA A receptors. Trends Neurosci.

Moreno-Bueno G, Rodríguez-Perales S, Sánchez-Estévez C, et al (2003) Cyclin D1 gene (CCND1) mutations in endometrial cancer. Oncogene. doi: 10.1038/sj.onc.1206868

~N~

Nadler LS, Guirguis ER, Siegel RE (1994) GABAA receptor subunit polypeptides increase in parallel but exhibit distinct distributions in the developing rat cerebellum. J Neurobiol. doi: 10.1002/neu.480251206

Najas S, Arranz J, Lochhead PA, et al (2015) DYRK1A-mediated Cyclin D1 Degradation in Neural Stem Cells Contributes to the Neurogenic Cortical Defects in Down Syndrome. EBioMedicine. doi: 10.1016/j.ebiom.2015.01.010

Nakamura Y, Darnieder LM, Deeb TZ, Moss SJ (2015) Regulation of GABAARs by phosphorylation. In: Advances in Pharmacology

Narasimha AM, Kaulich M, Shapiro GS, et al (2014) Cyclin D activates the Rb tumor suppressor by mono-phosphorylation. Elife. doi: 10.7554/eLife.02872.001

Negis Y, Karabay A (2016) Expression of cell cycle proteins in cortical neurons—Correlation with glutamate-induced neurotoxicity. BioFactors. doi: 10.1002/biof.1282

Neumeister P (2003) Cyclin D1 Governs Adhesion and Motility of Macrophages. Mol Biol Cell. doi: 10.1091/mbc.02-07-0102

Nusser Z, Cull-Candy S, Farrant M (1997) Differences in synaptic GABA(A) receptor number underlie variation in GABA mini amplitude. Neuron. doi: 10.1016/S0896-6273(00)80382-7

Nusser Z, Mody I (2002) Selective modulation of tonic and phasic inhibitions in dentate gyrus granule cells. J Neurophysiol. doi: 10.1152/jn.2002.87.5.2624

Nusser Z, Roberts J, Baude A, et al (1995) Relative densities of synaptic and extrasynaptic GABAA receptors on cerebellar granule cells as determined by a quantitative immunogold method. J Neurosci. doi: 10.1523/jneurosci.15-04-02948.1995

Nusser Z, Sieghart W, Benke D, et al (1996) Differential synaptic localization of two major gamma-aminobutyric acid type A receptor alpha subunits on hippocampal pyramidal cells. Proc Natl Acad Sci U S A

Nusser Z, Sieghart W, Somogyi P (1998) Segregation of different GABAA receptors to synaptic and extrasynaptic membranes of cerebellar granule cells. J Neurosci

~O~

Obata K, Oide M, Tanaka H (1978) Excitatory and inhibitory actions of GABA and glycine on embryonic chick spinal neurons in culture. Brain Res. doi: 10.1016/0006-8993(78)90447-X

Olsen RW, Sieghart W (2008) International Union of Pharmacology. LXX. Subtypes of γ-aminobutyric acidA receptors: Classification on the basis of subunit composition, pharmacology, and function. Update. Pharmacol. Rev.

Osuga H, Osuga S, Wang F, et al (2000) Cyclin-dependent kinases as a therapeutic target for stroke. Proc Natl Acad Sci U S A. doi: 10.1073/pnas.170144197

~P~

Palma E, Ragozzino D, Angelantonio S Di, et al (2007) The antiepileptic drug levetiracetam stabilizes the human epileptic GABAA receptors upon repetitive activation. Epilepsia. doi: 10.1111/j.1528-1167.2007.01131.x

Palma E, Ragozzino DA, Di Angelantonio S, et al (2004) Phosphatase inhibitors remove the run-down of -aminobutyric acid type A receptors in the human epileptic brain. Proc Natl Acad Sci. doi: 10.1073/pnas.0403683101

Palma E, Torchia G, Limatola C, et al (2005) BDNF modulates GABAA receptors microtransplanted from the human epileptic brain to Xenopus oocytes. Proc Natl Acad Sci U S A. doi: 10.1073/pnas.0409442102

Parsons JT, Horwitz AR, Schwartz MA (2010) Cell adhesion: integrating cytoskeletal dynamics and cellular tension. Nat Rev Mol Cell Biol. doi: 10.1038/nrm2957

Paternot S, Arsenijevic T, Coulonval K, et al (2006) Distinct specificities of pRb phosphorylation by CDK4 activated by cyclin D1 or cyclin D3: Differential involvement in the distinct mitogenic modes of thyroid epithelial cells. Cell Cycle. doi: 10.4161/cc.5.1.2265

Peng Z, Huang CS, Stell BM, et al (2004) Altered expression of the delta subunit of the GABAA receptor in a mouse model of temporal lobe epilepsy. J Neurosci 24:8629–39. doi: 10.1523/JNEUROSCI.2877-04.2004

Pestell RG (2013) New roles of cyclin D1. Am. J. Pathol.

Petrini EM, Ravasenga T, Hausrat TJ, et al (2014) Synaptic recruitment of gephyrin regulates surface GABA A receptor dynamics for the expression of inhibitory LTP. Nat Commun.

Pilaz LJ, Patti D, Marcy G, et al (2009) Forced G1-phase reduction alters mode of division, neuron number, and laminar phenotype in the cerebral cortex. Proc Natl Acad Sci U S A. doi: 10.1073/pnas.0909894106

Pirker S, Schwarzer C, Wieselthaler A, et al (2000) GABA(A) receptors: Immunocytochemical distribution of 13 subunits in the adult rat brain. Neuroscience. doi: 10.1016/S0306-4522(00)00442-5

Porcello DM, Huntsman MM, Mihalek RM, et al (2006) Intact Synaptic GABAergic Inhibition and Altered Neurosteroid Modulation of Thalamic Relay Neurons in Mice Lacking δ Subunit. J Neurophysiol. doi: 10.1152/jn.00899.2002

Porcello DM, Huntsman MM, Mihalek RM, et al (2003) Intact synaptic GABAergic inhibition and altered neurosteroid modulation of thalamic relay neurons in mice lacking δ subunit. J Neurophysiol. doi: 10.1152/jn.00899.2002

~R~

Raftopoulou M, Hall A (2004) Cell migration: Rho GTPases lead the way. Dev. Biol.

Ragozzino D, Palma E, Di Angelantonio S, et al (2005) Rundown of GABA type A receptors is a dysfunction associated with human drug-resistant mesial temporal lobe epilepsy. Proc Natl Acad Sci U S A. doi: 10.1073/pnas.0507339102

Rajasekaran K, Joshi S, Sun C, et al (2010) Receptors with low affinity for neurosteroids and GABA contribute to tonic inhibition of granule cells in epileptic animals. Neurobiol Dis 40:490–501. doi: 10.1016/j.nbd.2010.07.016

Rashid M, Belmont J, Carpenter D, et al (2017) Neural-specific deletion of the focal adhesion adaptor protein paxillin slows migration speed and delays cortical layer formation. Development. doi: 10.1242/dev.147934

Rhee S, Lee KH, Kim D, et al (2000) Sustained formation of focal adhesions with paxillin in morphological differentiation of PC12 cells. Mol Cells. doi: 10.1007/s10059-000-0169-3

Ridley AJ (2001a) Rho GTPases and cell migration. J Cell Sci

Ridley AJ (2015) Rho GTPase signalling in cell migration. Curr. Opin. Cell Biol.

Ridley AJ (2001b) Rho family proteins: Coordinating cell responses. Trends Cell Biol.

Roberts DS, Raol YH, Bandyopadhyay S, et al (2005) Erg3 stimulation of GABRA4 promoter activity as a mechanism for seizure-induced up-regulation of GABRA4 expression. pnas 102:

Rocandio D (2018) Role of cytoplasmic cyclin D1 in radial migration of cortical neurons during brain development. Universitat de Lleida

~S~

Sakamaki T, Casimiro MC, Ju X, et al (2006) Cyclin D1 Determines Mitochondrial Function In Vivo. Mol Cell Biol. doi: 10.1128/MCB.02074-05

Sakmann B, Fassberg A (1987) Mechanism of Anion Permeation Through Channels Gated. J Physiol

Saliba RS, Gu Z, Yan Z, Moss SJ (2009) Blocking L-type voltage-gated Ca2+ channels with dihydropyridines reduces γ-aminobutyric acid type A receptor expression and synaptic inhibition. J Biol Chem. doi: 10.1074/jbc.M109.040071

Saliba RS, Kretschmannova K, Moss SJ (2012) Activity-dependent phosphorylation of GABAA receptors regulates receptor insertion and tonic current. EMBO J. d 10.1038/emboj.

Saliba RS, Michels G, Jacob TC, et al (2007) Activity-Dependent Ubiquitination of GABAA Receptors Regulates Their Accumulation at Synaptic Sites. J Neurosci. doi: 10.1523/jneurosci.3277-07.2007

Saliba RS, Pangalos M, Moss SJ (2008) The ubiquitin-like protein plic-1 enhances the membrane insertion of GABAA receptors by increasing their stability within the endoplasmic reticulum. J Biol Chem. doi: 10.1074/jbc.M802077200

Sanidas I, Morris R, Fella KA, et al (2019) A Code of Mono-phosphorylation Modulates the Function of RB. Mol Cell. doi: 10.1016/j.molcel.2019.01.004

Sanna E, Mostallino MC, Murru L, et al (2009) Changes in Expression and Function of Extrasynaptic GABAA Receptors in the Rat Hippocampus during Pregnancy and after Delivery. J Neurosci. doi: 10.1523/jneurosci.3684-08.2009

Schaefer AW, Schoonderwoert VTG, Ji L, et al (2008) Coordination of Actin Filament and Microtubule Dynamics during Neurite Outgrowth. Dev Cell. doi: 10.1016/j.devcel.2008.05.003

Schaller MD (2001) Paxillin: A focal adhesion-associated adaptor protein. Oncogene

Schwarzer C, Tsunashima K, Wanzenböck C, et al (1997) GABA(A) receptor subunits in the rat hippocampus II: Altered distribution in kainic acid-induced temporal lobe epilepsy. Neuroscience. doi: 10.1016/S0306-4522(97)00145-0

Sciarretta C, Minichiello L (2010) The preparation of primary cortical neuron cultures and a practical application using immunofluorescent cytochemistry. Methods Mol Biol 633:221–231. doi: 10.1007/978-1-59745-019-5_16

Scimemi A (2005) Multiple and Plastic Receptors Mediate Tonic GABAA Receptor Currents in the Hippocampus. J Neurosci. doi: 10.1523/JNEUROSCI.2520-05.2005

Sen A, De Castro I, DeFranco DB, et al (2012) Paxillin mediates extranuclear and intranuclear signaling in prostate cancer proliferation. J Clin Invest. doi: 10.1172/JCI62044

Sequeira A, Mamdani F, Ernst C, et al (2009) Global brain gene expression analysis links Glutamatergic and GABAergic alterations to suicide and major depression. PLoS One. doi: 10.1371/journal.pone.0006585

Shen H, Gong Q, Aoki C, et al (2007) Reversal of neurosteroid effects at alpha4beta2delta GABAA receptors triggers anxiety at puberty. Nat Neurosci.

Shen H, Sabaliauskas N, Sherpa A, et al (2010) A critical role for α4βδ GABAA receptors in shaping learning deficits at puberty in mice. Science (80-). doi: 10.1126/science.1184245

Sherr CJ (1996) Cancer cell cycles. Science (80-.).

Sherr CJ, Roberts JM (1999) CDK inhibitors: Positive and negative regulators of G1-phase progression. Genes Dev. 13:1501–1512

Sherr CJ, Roberts JM, Sherr CJ, Roberts JM (2004) Living with or without cyclins and cyclin-dependent kinases Living with or without cyclins and cyclin-dependent kinases. 2699–2711. doi: 10.1101/gad.1256504

Shumate MD, Lin DD, Gibbs JW, et al (1998) GABA(A) receptor function in epileptic human dentate granule cells: comparison to epileptic and control rat. Epilepsy Res 32:114–28

Sicinska E, Aifantis I, Le Cam L, et al (2003) Requirement for cyclin D3 in lymphocyte development and T cell leukemias. Cancer Cell. doi: 10.1016/S1535-6108(03)00301-5

Sicinski P, Donaher JL, Geng Y, et al (1996) Cyclin D2 is an FSH-responsive gene involved in gonadal cell proliferation and oncogenesis. Nature. doi: 10.1038/384470a0

Sicinski P, Donaher JL, Parker SB, et al (1995) Cyclin D1 provides a link between development and oncogenesis in the retina and breast. Cell 82:621–630. doi: 10.1016/0092-8674(95)90034-9

Sieghart W, Sperk G (2002) Subunit Composition, Distribution and Function of GABA-A Receptor Subtypes. Curr Top Med Chem. doi: 10.2174/1568026023393507

Sigel E, Baur R, Trube G, et al (1990) The effect of subunit composition of rat brain GABAAreceptors on channel function. Neuron. doi: 10.1016/0896-6273(90)90224-4

Sigel E, Steinmann ME (2012) Structure, function, and modulation of GABAA receptors. J. Biol. Chem.

Sine SM, Engel AG (2006) Recent advances in Cys-loop receptor structure and function. Nature

Soderling TR, Derkach VA (2000) Postsynaptic protein phosphorylation and LTP. Trends Neurosci.

Solecki DJ, Govek EE, Tomoda T, Hatten ME (2006) Neuronal polarity in CNS development. Genes Dev.

Spigelman I, Li Z, Banerjee PK, et al (2002) Behavior and physiology of mice lacking the GABAA-receptor δ subunit. In: Epilepsia

Sullivan H (1992) Ionic Channels of Excitable Membranes, 2nd Ed. Neurology. doi: 10.1212/wnl.42.7.1439-a

Sumrejkanchanakij P, Tamamori-Adachi M, Matsunaga Y, et al (2003) Role of cyclin D1 cytoplasmic sequestration in the survival of postmitotic neurons. Oncogene 22:8723–8730. doi: 10.1038/sj.onc.1206870

Sundstrom-Poromaa I, Smith DH, Gong QH, et al (2002) Hormonally regulated α4β2λ GABAA receptors are a target for alcohol. Nat Neurosci. doi: 10.1038/nn888

~T~

Tan HO, Reid CA, Single FN, et al (2007) Reduced cortical inhibition in a mouse model of familial childhood absence epilepsy. Proc Natl Acad Sci U S A. doi: 10.1073/pnas.0708440104

Tanaka M, Olsen RW, Medina MT, et al (2008) Hyperglycosylation and Reduced GABA Currents of Mutated GABRB3 Polypeptide in Remitting Childhood Absence Epilepsy. Am J Hum Genet. doi: 10.1016/j.ajhg.2008.04.020

Tang X, Hernandez CC, Macdonald RL (2010) Modulation of Spontaneous and GABA-Evoked Tonic alpha 4 beta 3 delta and alpha 4 beta 3 gamma 2L GABA(A) Receptor Currents by Protein Kinase A. J Neurophysiol. doi: 10.1152/jn.00801.2009

Terunuma M, Jang IS, Ha SH, et al (2004) GABAA receptor phospho-dependent modulation is regulated by phospholipase C-related inactive protein type 1, a novel protein phosphatase 1 anchoring protein. J Neurosci. doi: 10.1523/JNEUROSCI.1323-04.2004

Terunuma M, Xu J, Vithlani M, et al (2008) Deficits in phosphorylation of GABAA receptors by intimately associated protein kinase C activity underlie compromised synaptic inhibition during status epilepticus. J Neurosci. doi: 10.1523/JNEUROSCI.4346-07.2008

Thomas P, Mortensen M, Hosie AM, Smart TG (2005) Dynamic mobility of functional GABAA receptors at inhibitory synapses. Nat Neurosci. doi: 10.1038/nn1483

Thoumine O (2008) Interplay between adhesion turnover and cytoskeleton dynamics in the control of growth cone migration. Cell Adh Migr. doi: 10.4161/cam.2.4.7274

Tozuka Y, Fukuda S, Namba T, et al (2005) GABAergic excitation promotes neuronal differentiation in adult hippocampal progenitor cells. Neuron. doi: 10.1016/j.neuron.2005.08.023

Tretter V, Hauer B, Nusser Z, et al (2001) Targeted Disruption of the GABAA Receptor δ Subunit Gene Leads to an Up-regulation of γ2 Subunit-containing Receptors in Cerebellar Granule Cells. J Biol Chem. doi: 10.1074/jbc.M011054200

Tretter V, Mukherjee J, Maric H-M, et al (2012) Gephyrin, the enigmatic organizer at GABAergic synapses. Front Cell Neurosci. doi: 10.3389/fncel.2012.00023

Turner CE (2000) Paxillin interactions. J Cell Sci

Twelvetrees AE, Yuen EY, Arancibia-Carcamo IL, et al (2010) Delivery of GABAARs to Synapses Is Mediated by HAP1-KIF5 and Disrupted by Mutant Huntingtin. Neuron. doi: 10.1016/j.neuron.2009.12.007

~U~

Urak L, Feucht M, Fathi N, et al (2006) A GABRB3 promoter haplotype associated with childhood absence epilepsy impairs transcriptional activity. Hum Mol Genet. doi: 10.1093/hmg/ddl174

Urbánek P, Wang ZQ, Fetka I, et al (1994) Complete block of early B cell differentiation and altered patterning of the posterior midbrain in mice lacking Pax5 BSAP. Cell. doi: 10.1016/0092-8674(94)90079-5

~V~

Van der Flier A, Sonnenberg A (2001) Function and interactions of integrins. Cell Tissue Res.

Vega IE, Hsu SC (2001) The Exocyst complex associates with microtubules to mediate vesicle targeting and neurite outgrowth. J Neurosci

~W~

Wafford KA, Thompson SA, Thomas D, et al (1996) Functional characterization of human γ-aminobutyric acid(A) receptors containing the α4 subunit. Mol Pharmacol

Wallner M, Hanchar HJ, Olsen RW (2003) Ethanol enhances α4β3δ and α6β3δ γ-aminobutyric acid type A receptors at low concentrations known to affect humans. Proc Natl Acad Sci U S

Wang C, Li Z, Lu Y, et al (2006) Cyclin D1 repression of nuclear respiratory factor 1 integrates nuclear DNA synthesis and mitochondrial function. Proc Natl Acad Sci. doi: 10.1073/pnas.0603363103

Wang J, Liu SH, Haditsch U, et al (2003) Interaction of calcineurin and type-A GABA receptor γ2 subunits produces long-term depression at CA1 inhibitory synapses. J Neurosci

Webb DJ, Donais K, Whitmore LA, et al (2004) FAK-Src signalling through paxillin, ERK and MLCK regulates adhesion disassembly. Nat Cell Biol. doi: 10.1038/ncb1094

Wei W, Faria LC, Mody I (2004) Low ethanol concentrations selectively augment the tonic inhibition mediated by δ subunit-containing GABAA receptors in hippocampal neurons. J Neurosci. doi: 10.1523/JNEUROSCI.2040-04.2004

Wei W, Zhang N, Peng Z, et al (2003) Perisynaptic localization of delta subunit-containing GABA(A) receptors and their activation by GABA spillover in the mouse dentate gyrus. J Neurosci

Weiner MP, Costa GL, Schoettlin W, et al (1994) Site-directed mutagenesis of double-stranded DNA by the polymerase chain reaction. Gene 151:119–23

Whiting PJ (1999) The GABA-A receptor gene family: New targets for therapeutic intervention. Neurochem. Int.

Whiting PJ, McKernan RM, Wafford KA (1995) Structure and Pharmacology of Vertebrate GABAA Receptor Subtypes. Int Rev Neurobiol. doi: 10.1016/S0074-7742(08)60525-5

Wisden W, Cope D, Klausberger T, et al (2002) Ectopic expression of the GABAA receptor α6 subunit in hippocampal pyramidal neurons produces extrasynaptic receptors and an increased tonic inhibition. Neuropharmacology. doi: 10.1016/S0028-3908(02)00151-X

Wisden W, Laurie DJ, Monyer H, Seeburg PH (1992) The distribution of 13 GABAA receptor subunit mRNAs in the rat brain. I. Telencephalon, diencephalon, mesencephalon. J Neurosci

Wong CGT, Bottiglieri T, Snead OC (2003) GABA, γ-hydroxybutyric acid, and neurological disease. In: Annals of Neurology

Woodrow MA, Woods D, Cherwinski HM, et al (2003) Ras-induced serine phosphorylation of the focal adhesion protein paxillin is mediated by the Raf→MEK→ERK pathway. Exp Cell Res. doi: 10.1016/S0014-4827(03)00122-8

Wooltorton JRA (1997) Pharmacological and Physiological Characterization of Murine Homomeric β3 GABAa Receptors. Eur J Neurosci. doi: 10.1111/j.1460-9568.1997.tb01641.x

Wozniak MA, Modzelewska K, Kwong L, Keely PJ (2004) Focal adhesion regulation of cell behavior. Biochim. Biophys. Acta - Mol. Cell Res.

Wu DW, Chuang CY, Lin WL, et al (2014) Paxillin promotes tumor progression and predicts survival and relapse in oral cavity squamous cell carcinoma by microRNA-218 targeting. Carcinogenesis. doi: 10.1093/carcin/bgu102

~Y~

Yamada J, Furukawa T, Ueno S, et al (2007) Molecular basis for the GABAA receptor-mediated tonic inhibition in rat somatosensory cortex. Cereb Cortex. doi: 10.1093/cercor/bhl087

Yamauchi J, Miyamoto Y, Sanbe A, Tanoue A (2006) JNK phosphorylation of paxillin, acting through the Rac1 and Cdc42 signaling cascade, mediates neurite extension in N1E-115 cells. Exp Cell Res 312:2954–2961. doi: 10.1016/j.yexcr.2006.05.016

~Z~

Zaidel-Bar R, Itzkovitz S, Ma'ayan A, et al (2007) Functional atlas of the integrin adhesome. Nat Cell Biol. doi: 10.1038/ncb0807-858

Zaidel-Bar R, Milo R, Kam Z, Geiger B (2006) A paxillin tyrosine phosphorylation switch regulates the assembly and form of cell-matrix adhesions. J Cell Sci. doi: 10.1242/jcs.03314

Zeid NA, Vallés AM, Boyer B (2006) Serine phosphorylation regulates paxillin turnover during cell migration. Cell Commun Signal. doi: 10.1186/1478-811X-4-8

Zhang N, Wei W, Mody I, Houser CR (2007) Altered localization of GABA(A) receptor subunits on dentate granule cell dendrites influences tonic and phasic inhibition in a mouse model of epilepsy. J Neurosci 27:7520–31. doi: 10.1523/JNEUROSCI.1555-07.2007

Zhong Z, Yeow WS, Zou C, et al (2010) Cyclin D1/cyclin-dependent kinase 4 interacts with filamin A and affects the migration and invasion potential of breast cancer cells. Cancer Res. doi: 10.1158/0008-5472.CAN-08-1108